

Università degli Studi di Salerno
DIPARTIMENTO DI CHIMICA E BIOLOGIA “A. ZAMBELLI”
DOTTORATO DI RICERCA IN CHIMICA
XXXI CICLO



*“CO₂ fixation in cyclic carbonates
and polycarbonates by salen-like
based metal complexes”*

Mariachiara Cozzolino

TUTOR

Prof. Marina Lamberti

CO-TUTOR

Prof. Mina Mazzeo

COORDINATOR

Prof. Gaetano Guerra

***A mio Padre,
la mia ricchezza più grande,
che mi ha trasmesso la
passione per la chimica e la
voglia di raggiungere questo
traguardo.***

*"The best scientist is open to
experience and begins with
romance - the idea that
anything is possible."*

Ray Bradbury

Index

Summary	1
List of abbreviations.....	4
General Introduction	7
1.1. Carbon dioxide: from problem to resource.....	8
1.2. Reaction of CO ₂ with Epoxides.....	12
1.2.1. Cyclic carbonates	12
1.2.2. Polycarbonates	14
1.3. Catalytic systems for the CO ₂ /epoxide reaction...	17
1.3.1. General mechanism.....	18
1.3.2. Catalytic systems for the synthesis of cyclic carbonates	21
1.3.3. Catalytic systems for the synthesis of polycarbonates	34
1.4. Aims of the thesis.....	41
References.....	49
CHAPTER 2	54
CO ₂ Fixation in Cyclic Carbonates by Salalen Aluminum Complexes and Mechanistic studies	54
2.1. Introduction	55
2.2. Results and Discussion	56
2.2.1. Characterization of Salalen ligands	56
2.2.2. Synthesis and characterization of Salalen Aluminum complexes.....	57
2.2.3. Single-crystal structure analysis	59
2.2.4. Cycloaddition of carbon dioxide with epoxides	60

2.2.5. NMR mechanistic studies of the CO ₂ /CHO reaction promoted by complex 1.....	69
2.3. Conclusions.....	79
2.4. Experimental Section	81
2.4.1 General considerations	81
2.4.2. Synthesis of Salalen Ligands	81
2.4.3. Synthesis and Characterization of Salalen Aluminum Complexes (1-5).....	82
2.4.4. Synthesis of Salen and Salan Aluminum Complexes (6-8).....	88
2.4.5. CO ₂ /CHO reaction procedure.....	89
2.4.6. NMR mechanistic studies of the CO ₂ /CHO reaction promoted by complex 1.....	93
References.....	98
CHAPTER 3.....	100
“Salen like” Iron (III) Complexes as Catalysts for CO ₂ /Epoxides Reactions and ROP of Cyclic Esters .	100
3.1. Introduction	101
3.1.1. Iron-based catalysts for CO ₂ /epoxide reactions and ROP of cyclic esters	101
3.1.2. Ring-Opening Polymerization of Cyclic esters.....	103
3.2.1. Synthesis and characterization of ligands H ₂ L ₁₋₄ .	107
3.2.2. Synthesis of Complexes 1-4	107
3.2.3. Characterization of Complexes 1-4	108
3.2.4. Catalytic cycloaddition of carbon dioxide with epoxides.....	118
3.2.5. Study of the reactivity of Fe complexes in the polymerization of lactide and ε-caprolactone	125

3.3. Conclusions	136
3.4. Experimental Section	138
3.4.1 General considerations	138
3.4.2. Synthesis and Characterization of Complexes 1-4	140
CHAPTER 4	157
Synthesis of a New Zinc Complex as Catalyst for ROCOP of CO ₂ and Cyclohexeneoxide	157
4.1. Introduction	158
4.2. Results and Discussion	161
4.2.1. Synthesis and characterization of salalen Zinc complexes.....	161
4.2.2. Cycloaddition of carbon dioxide with propylene oxide	164
4.2.3. Synthesis of new hexadentate dianionic ligands.	165
4.2.4. Synthesis of the bimetallic zinc complex.....	169
4.2.5. Ring-opening copolymerization of carbon dioxide with cyclohexene-oxide.....	171
4.3. Conclusions	173
4.4. Experimental Section	175
4.4.1 General considerations	175
4.4.2. Synthesis of Salalen ligands	175
4.4.3. Synthesis and characterization of complex 1.....	175
4.4.4. Synthesis and characterization of complex 2.....	179
4.4.5. Synthesis and characterization of the OSNNSO ligand.....	182
4.4.6. Synthesis and characterization of complex 3.....	186
References	188

CHAPTER 5.....	189
Organocatalyzed Domino [3+2] Cycloaddition/Payne-Type Rearrangement using Carbon Dioxide and Epoxy Alcohols.....	189
5.1. Introduction	190
5.1.1. Synthesis of cyclic carbonates promoted by metal catalysis and organocatalysis	190
5.1.2. Mechanisms proposed for organocatalysts	192
5.1.3. The importance of highly substituted carbonates.....	193
5.2. Results and discussion	196
5.2.1 Monosubstituted epoxides	196
5.2.1. Disubstituted epoxides	202
5.2.3. Trisubstituted epoxides	203
5.2.4. Selective protection of the primary alcohol.....	206
5.2.5. One pot synthetic protocol	208
5.2.6. Substrate scope	209
5.2.7. Control experiments to support the mechanism proposal	212
5.3. Conclusions.....	215
5.4. Experimental Section	217
5.4.1 General considerations	217
5.4.2. General procedure for the catalytic experiments	217
5.4.3. Spectroscopic data for all compounds	218
References.....	229

Summary

At the current rate of consumption of petroleum resources, they are predicted to be exhausted within the next century. For this reason, the development of new chemical processes using biorenewable resources is attracting an increasing interest. One of such resource is carbon dioxide: an abundant, nonflammable, non-toxic and renewable carbon source, the only feedstock readily and cheaply available. However, CO₂ has a high thermodynamic stability and many scientists have been and are searching catalysts which overcome the low CO₂ reactivity. In industrially practicable processes, carbon dioxide has to be reacted with energy-rich strained rings. In particular, the transformation of epoxides and carbon dioxide into either cyclic carbonates or aliphatic polycarbonates is one of the most attractive and commercially important process.

Since the discovery of catalysts for the coupling of CO₂ and epoxides in the late 1960-s, a significant amount of research has been directed towards the development of catalysts with improved activity and selectivity. In the first chapter, well-defined catalysts for CO₂/ epoxide reactions are described, with particular emphasis to catalysts deriving from inexpensive, earth-crust abundant metals, such as aluminum, zinc and iron.

In the second chapter, the synthesis of monometallic salalen aluminium complexes and their use as catalysts in the reactions of CO₂ with different epoxides is described. In particular, the reaction of cyclohexene oxide and CO₂ was

thoroughly investigated. The effect of the reaction conditions (nature and equivalents of the cocatalyst, CO₂ pressure and temperature) and of the ligand structures (substituents on the ancillary ligand, nature of the labile ligand and nature of the nitrogen donor atoms) on activity and selectivity of the catalysts was studied. Moreover, the cycloaddition reaction of the CO₂ with terminal epoxides, bearing different functional groups, was realized. Finally, NMR mechanistic studies have been carried out to shed light on the catalytic cycle active with this class of catalysts. Interestingly, the characterization of an intermediate species in the mechanism of the reaction of cyclohexene oxide with CO₂, catalyzed by one of the salalen–aluminum complexes, was accomplished.

In the third chapter, the synthesis of an iron complex with one of the salalan ligands used for aluminium complexes and its counterparts, salen and salan ligands, is described. The ligands bear the same substituents on the phenolate rings and differ only for the nature of the nitrogen donor atoms. The paramagnetic iron complexes were characterized by UV-Vis and IR-spectroscopy, MALDI-ToF mass spectrometry and measurement of magnetic moments by the NMR Evans method. The catalytic behaviour of these systems in the reaction of CO₂ with benchmark epoxides, such as propylene-oxide (PO), styrene-oxide (SO) and cyclohexene-oxide (CHO) and subsequently in the ring-opening polymerization of L-lactide and ϵ -caprolactone was investigated.

In the fourth chapter the synthetic strategy conceived for the preparation of a new class of hexadentate ligands is described. These ligands present two additional sulphur donors between the phenolate moieties and the imino atoms of the classic salen ligands, thus creating a coordinative environment able to allocate two metal centers. The first ligand of this class has been synthesized and then used for the preparation of the corresponding bimetallic Zn (II) complex. The zinc complex has been tested in the reaction of CO₂ with cyclohexene oxide. The effect of the reaction conditions (such as, temperature, CO₂ pressure and time) on the activity and the selectivity of the catalyst was evaluated.

In the fifth chapter of this thesis, an organocatalytic approach towards the synthesis of highly substituted cyclic carbonates from tri- and tetra-substituted epoxides and carbon dioxide is described. The developed protocol involves the use of a simple base under mild conditions towards the initial formation of a less substituted carbonate product. The latter equilibrates to a tri- or even tetra-substituted cyclic carbonate under thermodynamic control and can be easily trapped *in situ* providing overall a new domino process for the preparation of synthetically elusive heterocyclic scaffolds.

List of abbreviations

AP: 2-Aminopyridine

BDI: β -diiminate

CCS: Carbon Capture and Storage

CCU: Carbon Capture and Utilization

CHDO: 1,2-epoxy-4-cyclohexene

CHO: cyclohexene-oxide

cis-CHC: *cis*-cyclohexene carbonate

CL: caprolactone

DBU: 1,8-Diazabicyclo(5.4.0)undec-7-ene

DPEA: N,N-Diisopropylethylamine

DMAP: 4-Dimethylaminopyridine

DMF: N,N-dimethylformamide

DMSO: Dimethyl sulfoxide

DPG: 1,3-Diphenylguanidine

HMPA: Hexamethylphosphoramide

LA: lactide

mCPBA: meta-Chloroperbenzoic acid

NMIM: N-methylimidazole

NMP: N-Methyl-2-pyrrolidone

MM: Melamine Monomer

MTBD: Triazabicyclo[4.4.0]dec-5-ene

OTG: 1-(o-Tolyl)biguanide

PC: propylene carbonate

PCHC: polycyclohexene carbonate

PCL: polycaprolactone

PLA: polylactide

PO: propylene-oxide

PPC: polypropylene carbonate

PPNCl: bis(triphenylphosphoranylidene)ammonium chloride

ROCOP: ring-opening copolymerization

ROP: ring-opening polymerization

SC: styrene carbonate

scCO₂: supercritical CO₂

SO: styrene oxide

SQ: Squaramide

TBAOAc: tetrabutylammonium acetate

TBAB: tetrabutylammonium bromide

TBAI: tetrabutylammonium iodide

TBD: 1,5,7-Triazabicyclo[4.4.0]dec-5-ene

TEA: Triethylamine

TMG: 1,1,3,3-Tetramethylguanidine

TOF: turnover frequencies

TON: turnover numbers

TPP: tetraphenylporphyrin

trans-CHC: *trans*-cyclohexene carbonate

CHAPTER 1

General Introduction

The use of carbon dioxide as a renewable raw reagent for the production of chemicals and materials is a topic of high interest. CO₂ is a highly abundant, inexpensive and non-toxic one-carbon source. The drawback is its high thermodynamic and kinetic stability that leads to low reactivity. To overcome this issue, reactions with highly energetic molecules have been taken into consideration. In particular, the transformation of epoxides and carbon dioxide into either cyclic carbonates or aliphatic polycarbonates is one of the most attractive and commercially important process.

In chapter 1 we will focus on the CO₂/epoxide reactions, in particular on the development of catalytic systems able to promote these reactions. An excursus on some of the most important catalytic systems based on aluminum, zinc and iron will be done.



1.1. Carbon dioxide: from problem to resource

Carbon dioxide is an inert, odorless and colorless gas, not toxic and not harmful and it is naturally present in the atmosphere. In low concentrations, it contributes positively to the natural thermoregulation of the earth, allowing suitable thermal conditions for the development of living organisms; thanks to a complex thermal balance, indeed, a homogeneous and constant temperature throughout the earth's crust is maintained. Since pre-industrial times, the concentration of carbon dioxide in the atmosphere has been steadily increasing to reach a value of 400 ppm (compared to 280 ppm, of the pre-industrial times). The high concentration of CO₂ may influence natural phenomena such as global temperature and the acidity of oceans, and thus affect the environment.^{1,2}

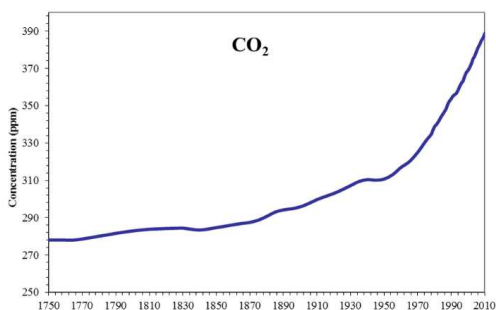


Figure 1.1. Evolution of the concentration of carbon dioxide present in the atmosphere.

To limit the emissions of CO₂ into the atmosphere, several strategies are being evaluated such as, for example, the use of renewable energy sources, better building insulation and greater efficiency in production processes. Furthermore, a further remedy is represented by the use of natural gas, as fuel coal, in fact, coal emits 950 g of CO₂ per KWh electricity produced, compared to 497g / KWh from natural gas. Recently, particular interest has been shown in the capture and storage of carbon dioxide, (CCS technologies, Carbon Capture and Storage) in natural depleted deposits of oil and gases, and in groundwater.^{3,4} Main problem of this technology, however, consists in the huge investments it requires, as well as the many doubts regarding the residence time of CO₂ in the places where it is stored. For these reasons the approval and application of CCS technologies did not take place in several countries, including Germany, Austria and Denmark. An intense research activity in the chemical industry is directed towards the development of new synthetic strategies that use carbon dioxide as a reagent for the production of chemicals, (CCU, Carbon Capture and Utilization). However the high thermodynamic stability of CO₂ ($\Delta G_f^\circ = -396 \text{ KJ / mol}$) constitutes a drawback of this strategy.⁵ One way to overcome this limitation is to combine carbon dioxide with highly reactive species, such as molecular hydrogen, unsaturated compounds, or tensioned compounds, thus making the energy balance of these reactions less unfavorable.⁶

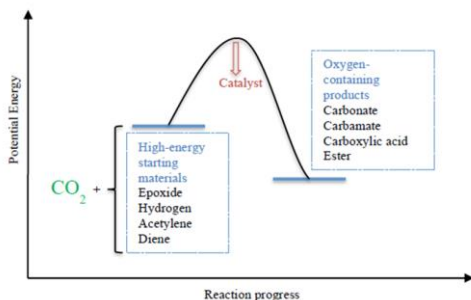


Figure 1.2. Organic synthesis using CO₂.⁶

There are many processes that see the use of CO₂ as a reagent and some of these are particularly interesting from an industrial point of view, such as, for example, the reaction with ammonia for the production of urea, the reaction with molecular hydrogen for the obtainment of methanol or formic acid, and the coupling reaction of carbon dioxide with epoxides to give cyclic carbonates and polycarbonates (Figure 1.3).⁷

In order to expand the synthetic potential of converting CO₂ into useful compounds, in processes with a low energy demand, the election of an adequate catalyst is crucial. In fact, many reactions involving carbon dioxide have high activation energies and so require a catalyst to lower the kinetic barrier and to allow the reaction to occur under reasonable reaction conditions. For this reason, in recent years, intensive research focused on the development of effective catalytic systems able to promote such reactions under mild reaction conditions.

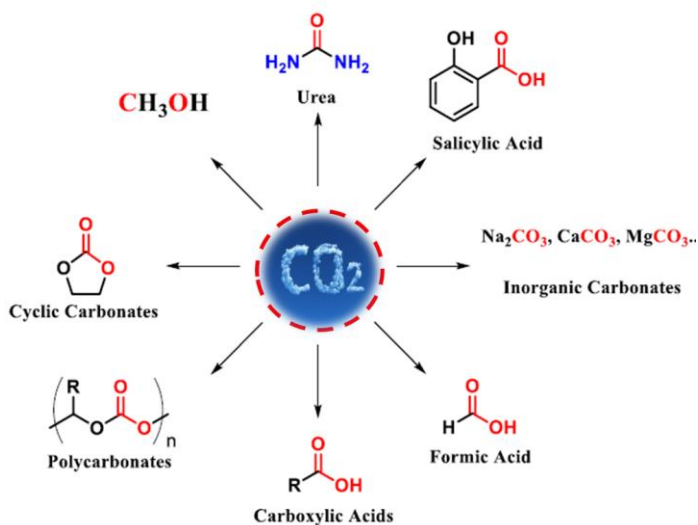


Figure 1.3. Example of products derived from carbon dioxide and manufactured at industrial scale.

Another point of reflection for the reaction involving CO_2 , concerns the life cycle of the compounds in which CO_2 is fixed, in fact, the less quickly the organic derivatives will degrade, the more effective it will be the incorporation of carbon dioxide inside them. Therefore in recent years, great attention has been paid to the process that leads to the production of species stable for years, such as polycarbonates and cyclic carbonates, starting from CO_2 and epoxides.^{8,2}

1.2. Reaction of CO₂ with Epoxides

The use of carbon dioxide may represent an interesting alternative to conventional reactants used so far in the chemical industry. The CO₂/epoxide reaction has the peculiarity of using carbon dioxide as one-carbon source, in addition, this process offers many advantages to reduce the environmental impact: it is not necessary to use solvents to conduct the reaction, there is a complete conversion of the reagents into products, it is possible to operate in mild conditions through the use of suitable catalysts, the transformation of dangerous and difficult to handle compounds, such as epoxides, into more harmless and stable products is accomplished. The reaction of CO₂ with epoxides can generate either polycarbonates or cyclic carbonates as possible products (Figure 1.4).

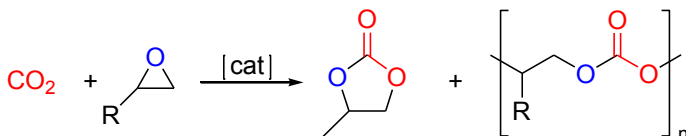


Figure 1.4. Coupling reaction of CO₂ with epoxides

1.2.1. Cyclic carbonates

Cyclic carbonates are usually synthesized by reaction of 1,2-diols with a molecule containing only one carbon atom, generally phosgene (Figure 1.5). Phosgene is an extremely toxic and dangerous substance both for humans and for the environment. Its use in the production of cyclic carbonates releases large amounts of hydrochloric acid, which must then

be disposed off. Thus, much efforts have been devoted to find valid alternatives to this reagent, and CO₂ constitutes an excellent candidate as a substitute for phosgene.⁹

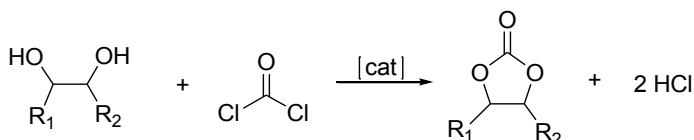


Figure 1.5. Conventional synthesis of cyclic carbonates.

For these reasons, the production of the cyclic carbonates through the coupling reactions of the epoxides with the carbon dioxide, using suitable catalysts, is particularly interesting (Figure 1.6). This reaction is also efficient from an atomic point of view since the complete conversion of the reagents into the products is achieved and there is no formation of by-products that would require the subsequent disposal.

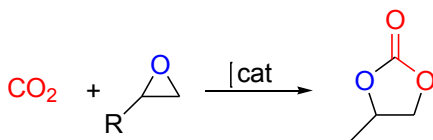


Figure 1.6. Synthesis of cyclic carbonates by coupling reaction of CO₂ with epoxides.

Cyclic carbonates have a general structure of the type shown in Figure 1.7 (a), the most interesting are undoubtedly those which have a five-term ring (Figure 1.7 (b)) that are thermodynamically more stable than linear analogs. They

have good dielectric constants and good specific conductivities.⁹

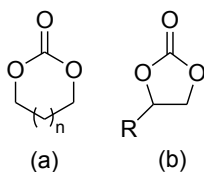


Figure 1.7. (a) general structure of cyclic carbonates (b) five-term cyclic carbonate structure.

Thanks to these properties, cyclic carbonates have numerous and interesting applications since they can be used as polar aprotic solvents¹⁰ capable of replacing traditional solvents such as DMF, DMSO, NMP, HMPA and acetonitrile (which generate NO_x or SO_x when incinerated), electrolytes in lithium ion batteries,¹¹ precursors for polymeric materials,¹² fine chemical intermediates, fuel additives. Moreover, they are also found in natural products¹³ and potential pharmaceuticals.¹⁴

1.2.2. Polycarbonates

Conventional polycarbonate is produced by reaction of bisphenol A with phosgene or with diphenyl carbonate (Figure 1.8). In this type of process, in addition to the dangerousness of the phosgene, there is also the use of bisphenol A which is highly toxic to humans, being a powerful endocrine disruptor, and currently, there are no threshold values below which an exposure to it can be considered harmless. In this regard, in the last decades, an intense research activity has been

developed in order to replace these reagents and find alternative synthetic processes.¹⁵

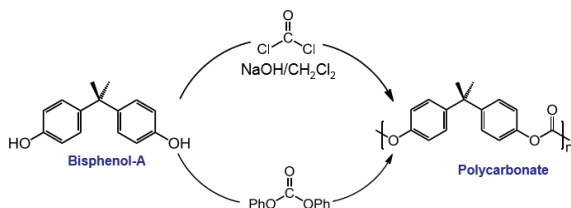


Figure 1.8. Synthesis of conventional polycarbonates.

In this context, the coupling reaction between carbon dioxide and epoxides is arousing particular interest for the synthesis of aliphatic polycarbonates, as they represent an eco-sustainable alternative to the conventional polycarbonates (Figure 1.9).¹⁵

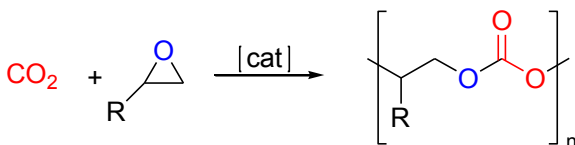


Figure1.9. Copolymerization of CO₂ with epoxides.

Bisphenol-based polycarbonate has excellent properties as engineering plastic for a broad range of applications including data storage, electronics, optical components and as construction materials. Polycarbonates obtained by CO₂/epoxide reaction have the advantage to be biodegradable but have poor mechanical and physical

properties. These characteristics limit their application at the industrial level, however many efforts are being made at improve their properties and reduce production costs in order to guarantee their use. Recent studies have shown that the nature of epoxide can significantly affect the mechanical properties of the corresponding polycarbonates. Generally, linear aliphatic polycarbonates, such as polypropylene carbonate (PPC), have a low glass transition temperature, T_g (35-40 °C), and consequently a low rigidity; they can not be used as technopolymers, as they do not show a high stability in a wide temperature range and under drastic chemical-physical conditions. However, they show the peculiar characteristic of decomposing in a controlled manner, forming CO₂ and water, representing an excellent material for environmentally friendly packaging. On the other hand, cyclic aliphatic polycarbonates, such as polycyclohexene carbonate (PCHC), by virtue of the higher T_g (115 °C), lend themselves to a wider range of applications. PCHC is, in fact, the polymer that shows the best mechanical properties, presenting characteristics similar to polystyrene, but its use is limited because it is particularly fragile ¹⁵

More recently, several research groups focused on the use of limonene oxide (LO) in polycarbonate synthesis.^{16,17} LO is an epoxide produced from fully renewable sources, it is extracted from the peel of citrus fruits and has a distinct orange odor. The use of LO as monomer is desirable, because its rigidity imparts good thermal properties to the polymer material to overcome the main limitation of propylene oxide derived

polycarbonates, that is the low glass transition temperature. Moreover, the double bond functionality of limonene oxide offers opportunities for post-polymerization modifications.¹⁸ These chemical modifications allow the tuning of the properties of the aliphatic polycarbonate in nearly any direction.¹⁸

1.3. Catalytic systems for the CO₂/epoxide reaction

Over the last decades, numerous efforts have been devoted to the design of efficient catalytic systems to promote the coupling reaction between carbon dioxide and epoxides, under mild reaction conditions. Typically, the catalytic systems have a general formula L_nMX , in which L_n is a set of ancillary ligands that influence the electronic and steric properties of the metal center and consequently the catalytic activity, M is the metallic center and X is a labile ligand. Various studies have highlighted the influence of the chemical environment of the metal on the catalytic activity; for this purpose, the attention has been focused on the modification of the ligand skeleton to increase the efficiency of the catalyst itself.^{6,8} Furthermore, there is an increasing interest to search sustainable catalytic systems that combine low toxicity and low costs. From this point of view, complexes based on zinc, iron and aluminium metals, which fully respect these requests, may be considered as preferred catalytic systems.

1.3.1. General mechanism

The CO₂/epoxide reaction, promoted by metallic complexes, proceeds through a coordination-insertion mechanism. Initially, the epoxide coordination occurs at the metal center which activates the epoxide and makes it susceptible to the nucleophilic attack, where the nucleophile may derive from a cocatalyst present in the reaction medium or by the catalyst itself.^{8,15,19} This leads to the opening of the ring and the formation of a first reaction intermediate characterized by the presence of a metal-alkoxide bond. The subsequent insertion of CO₂ in the M-O bond leads to the formation of a metal-carbonate species. In turn, this intermediate can follow two different paths, an intramolecular process, consisting in a self-folding of the chain with the consequent formation of cyclic carbonate, or regular and alternating insertion reactions of epoxide and CO₂ that produce aliphatic polycarbonates (Figure 1.10). In some cases, repeated insertions of epoxide units are observed with the formation of a polymeric chain with polyether sequences. The consecutive insertion of CO₂, on the other hand, is a thermodynamically unfavorable reaction, for this reason, dicarbonate bonds have never been observed.^{8,15}

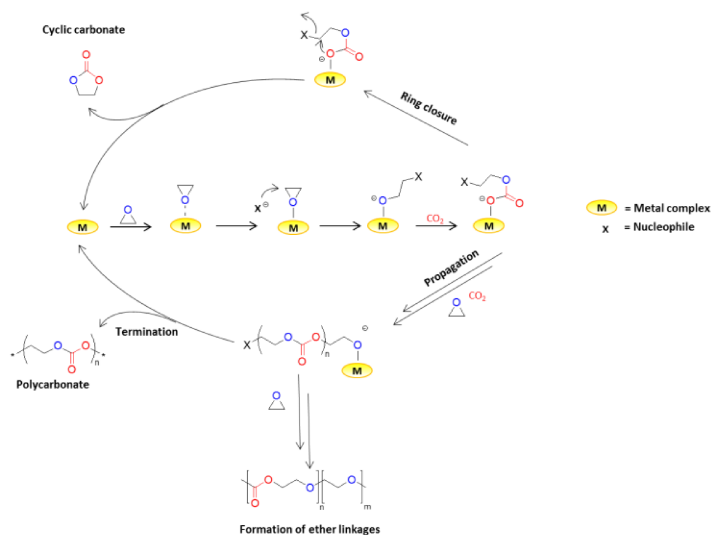


Figure 1.10. General mechanism for CO_2 /epoxides reaction.

Although cyclic carbonates are the thermodynamically most favored products, the ratio between the cyclic carbonate and the polymer produced depends on various factors such as the type of used catalyst, the presence of the cocatalyst, the CO_2 pressure, nature and concentration of the epoxide and finally the temperature. It is interesting to note that in the case of internal epoxides, the cyclic carbonates can be of the *trans* or *cis* type, such as, for example, cyclohexene-oxide (CHO). CHO is a *meso* epoxide, since one carbon has a configuration R and the other S; the breakdown of the C-O bond typically occurs with the inversion of configuration at the attack site ($\text{S}_{\text{N}}2$ mechanism). According to the mechanism proposed in the literature, the *trans*-cyclic carbonate (Figure 1.11 (A)) is formed following the attack of the alkoxide terminal at the

nearest carboxylic group of the growing chain, while the *cis*-carbonate (Figure 1.11 (B)) is obtained through the attack of the carbonate end to the carbon bearing the nucleophile which then undergoes a double inversion of configuration (formal retention of the configuration).²⁰

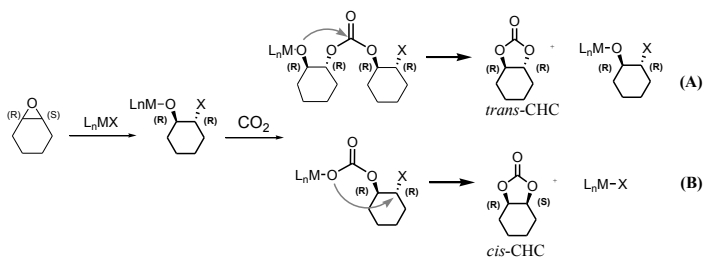


Figure 1.11. Synthesis of *cis*- and *trans*-cyclohexenecarbonate.

The common homogeneous catalysts, active in this class of reactions, can be classified into two broad families:

- (a) **Bicomponent catalyst systems:** *binary systems* comprising metal complexes with an exogenous co-catalyst or, *bifunctional systems* that present the co-catalyst attached to the ancillary ligand scaffold of the complex. The catalysts are usually complexes of Co(III), Cr(III), Mn(III) or Al(III) coordinated by ligands such as salens or porphyrins. The co-catalyst are typically ionic compounds, the most common are bis(triphenylphosphoranylidene)ammonium chloride (PPNCI) and quaternary ammonium salts (TBAX, X=I, Cl, Br, etc.) or Lewis bases, commonly 4-dimethylaminopyridine (DMAP).^{6,9,17}

- (b) **Dinuclear or bimetallic catalysts** comprising metal(II/III) complexes. Most commonly these are complexes where two metals are coordinated by tethered 'mononucleating' ligands, such as Zn(II) β -diiminates (BDIs) or tethered Co(II)/Cr(III) salens. There are also examples of deliberately dinucleating ligands, such as macrocyclic ligands coordinated to Zn(II), Mg(II), Co(II/III) or Fe(III).^{6,9,17}

Following, an *excursus* on some of the most important catalytic systems active in CO₂/epoxides reactions is done. In particular, a special attention has been devoted to catalysts deriving from inexpensive, earth-crust abundant and no toxic metals, such as aluminium, zinc, iron.^{3,8,17}

1.3.2. Catalytic systems for the synthesis of cyclic carbonates

1.3.2a Aluminum catalysts

Inoue *et al.* reported the synthesis of an tetraphenylporphyrin (TPP) aluminum complex **1a** (Figure 1.12) that, in the presence of N-methylimidazole (NMIM), as a co-catalyst, is able to promote the CO₂ reaction with propylene oxide (PO), producing propylene carbonate (PC).²¹ The reaction was carried out using 5% mol of catalyst **1a** (Figure 1.12) and 8% mol of NMIM at atmospheric temperature and pressure. In 45 hours a conversion of 39% of PO in PC was observed. A similar aluminum porphyrin catalyst **1b** (Figure 1.12) was

used to study the reaction mechanism with spectroscopic methods.²²

Later, Kasuga *et al.* reported the synthesis of phthalocyanine aluminum complexes **2a,b** (Figure 1.12) for the production of propylene carbonate.²³ Unfortunately, these systems, in the presence of NMIM **3** (Figure 1.12) as cocatalyst, exhibit a low catalytic activity, producing only 2% propylene carbonate operating under mild conditions. Subsequently, Ji *et al.* showed that, working at 140 °C, phthalocyanine aluminum complex **2b** (Figure 1.12) with NMIM was able to produce propylene carbonate with a yield of 96% after 72 minutes.²⁴

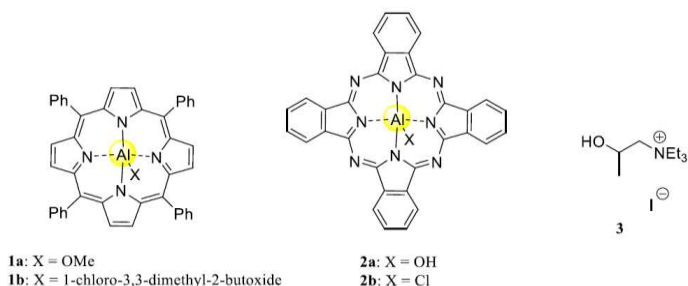


Figure 1.12. Examples of aluminum porphyrin and phthalocyanine catalysts.

Kleij and collaborators have extensively studied aluminum triphenolate complexes such as Lewis acid catalysts. They reported hexachlorinated aluminum(III)-aminetriphenolate complex **4a** (Figure 1.13) for the synthesis of organic carbonates by coupling reaction of CO₂ with epoxides.^{25,26,27} The first experiments were conducted using 1,2-epoxyhexane as a substrate and tetrabutylammonium iodide (TBAI) as co-catalyst. A good conversion of cyclic carbonate, using a

catalyst loading of 0.05 mol% and co-catalyst loading of 0.25 % mol, was observed. The reaction was carried out at 90 °C and 10 bar of CO₂ pressure in 2 hours, showing a TOF of 960 h⁻¹. Furthermore, by decreasing the amount of catalyst/co-catalyst ratio to 0.0005/0.05 mol%, higher initial TOF of 24000 h⁻¹ was achieved. In order to improve the catalytic activities, a series of analogous complexes **4b-d** and the asymmetric complex **5** were synthesized. These were tested as promoters of the CO₂ /epoxide reactions and, working, under the same conditions, complex **4a** proved to be the most active.

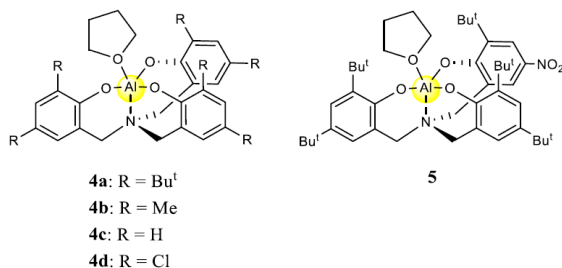


Figure 1.13. Aluminum triphenolate complexes developed by Kleij and co-workers.

He and co-workers reported the synthesis of an aluminium chloride complex **6** bearing a salen ligand (Figure 1.14).²⁸ This complex was active in the CO₂/ethylenoxide reaction, producing the corresponding cyclic carbonate. The reaction was carried out using 1 equivalent of tetrabutylammonium bromide (TBAB) as a co-catalyst, at 110 °C and under supercritical carbon dioxide conditions of 150 bar pressure (TOF up to 3070 h⁻¹). However, the conversion of ethylene

oxide to ethylene carbonate decreased significantly in the absence of the co-catalyst. Furthermore, working at 40 bar of CO₂ pressure a diminution of the conversion was observed. Lu *et al.* demonstrated that the **6**/TBAI binary catalyst system (Figure 1.14.) showed better catalytic activity in the synthesis of propylene carbonate, working in extremely mild conditions compared to other catalytic systems reported. At 25°C and 6 bar of CO₂, and in the presence of 1 equivalent of TBAI, the reaction gave a yield of 61% after 8 h (TOF = 61.5 h⁻¹).²⁹ Darensbourg *et al.* reported a series of bifunctional aluminum(salen) complexes bearing appended pyridinium salt substituents **7a**, **b** (Figure 1.14) for the synthesis of propylene carbonate by coupling reaction of CO₂ with PO. Complexes **7a**, **b**, in the absence of cocatalyst and operating at 120 °C and 30 bar of CO₂, proved to be highly efficient for the production of propylene carbonate (TOF up to 297 h⁻¹). They also had good recyclability not showing significant loss of catalytic activity.^{30,31}

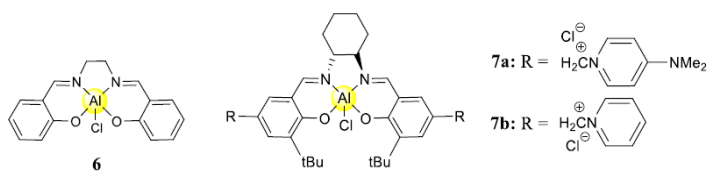


Figure 1.14. Monometallic aluminum salen complexes.

North and co-workers reported the dinuclear μ -oxo-bridged Al(salen) complex **8** (Figure 1.15) which resulted active for the formation of cyclic carbonate even under mild reaction

conditions (25°C and 1 atm).³² These reactions require the presence of a quaternary ammonium salt such as TBAB. Detailed mechanistic studies on this binary catalytic system have revealed that this cocatalyst plays a key role in the catalytic cycle, i.e. it provides the bromide necessary for the opening of the epoxide generating *in situ* tributylamine, which in turn reacts with carbon dioxide to form a carbamate salt. The aluminum bimetallic complex will coordinate both species allowing their intramolecular combination and thus completing the catalytic cycle (Figure 1.15).³³

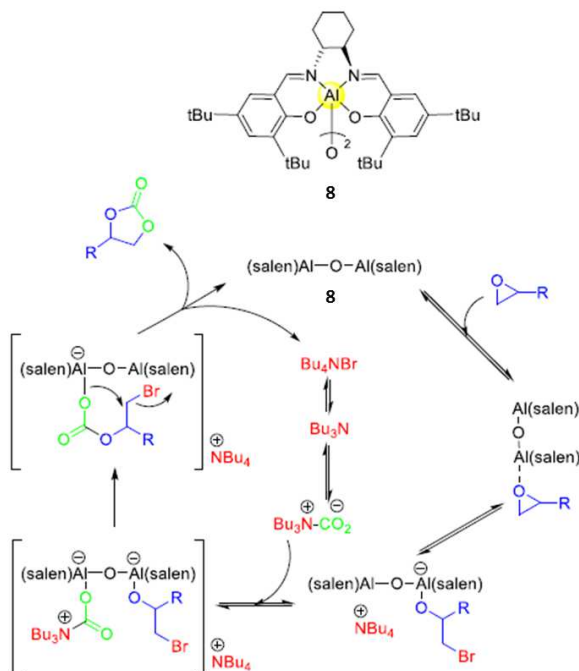


Figure 1.15. Catalytic cycle for the addition of CO₂ to epoxides catalyzed by complex **8**³⁷

To avoid the need for adding a co-catalyst, the same group developed a one-component analog of their bimetallic aluminum(salen) complex, in which quaternary ammonium bromide groups were covalently attached to the salen ligand **9** (Figure 1.16). Finally, in a more recent work, North designed an analog catalyst **10** which was able to carry out cycloaddition reactions using CO₂ in continuous flow coming from the outlet of industrial discharges.³⁴

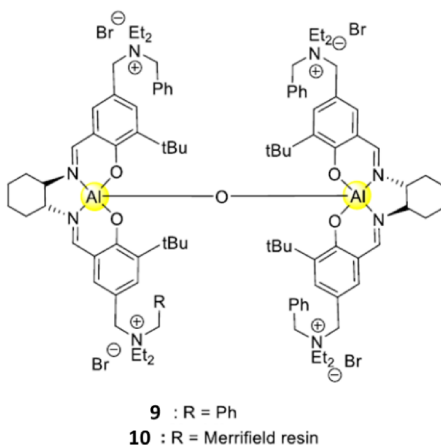


Figure 1.16. One-component bimetallic aluminum(salen) catalyst system developed by North and co-workers:

Lamberti *et al.* recently reported bimetallic aluminum complexes **11a-d** (Figure 1.17) bearing salen ligands (hybrid structures between salen and salan ligands) which were active in the CO₂/epoxide cycloaddition reaction with both cyclohexene oxide and propylene oxide. By proper choice of the reaction conditions, *cis*-cyclohexene carbonate

and propylene carbonate were obtained as exclusive products.³⁵

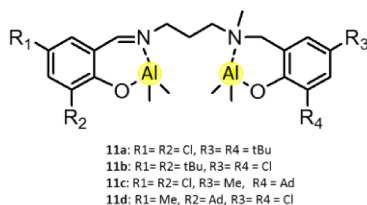


Figure 1.17. Bimetallic aluminum salen complexes reported by Lamberti *et al.*

The behaviour of one of these bimetallic salen-Al complexes in the CO₂/cyclohexene oxide reaction was compared with that of a similar bimetallic salen Al complex and that of a monometallic half-salen Al complex. The obtained results allowed to conclude that the formation of *cis*-CHC takes place on a single Al center, whereas the formation of both the polycarbonate and *trans*-CHC (which originates from the back-biting of the polymer) involves two metal centers.

1.3.2b Zinc catalysts

Kleij's group reported a mononuclear Zn(salphen) complex **12** (Figure 1.18) active towards CO₂ coupling with terminal epoxides under moderate CO₂ pressures (P_{CO2}= 0.2-1 MPa) and mild operating temperatures (25-45 °C). The high activity of the Zn(salphen) complex was ascribed to its constrained geometry imposed by the ligand scaffold, which imparts increased Lewis acid character to the catalytically active Zn ion.^{36,37} The same research group reported an analogue

bifunctional system containing a Lewis acid nucleophilic center in a single molecule **13** (Figure 1.18).³⁸ This complex, was also active for the synthesis of cyclic carbonates with terminal epoxides under mild conditions.

Furthermore, they conducted kinetic studies to compare both systems. In particular, the two different catalytic systems have shown different behavior. In fact, a dependence of the first order from the catalyst concentration for the **12**/TBAI binary system was found, while a second speed dependence on the bifunctional catalyst **13** has been found (Figure 1.18). These observations thus support a monometallic mechanism for the binary catalyst system and a bimetallic mechanism in the case of the bifunctional system (Figure 1.18)³⁹

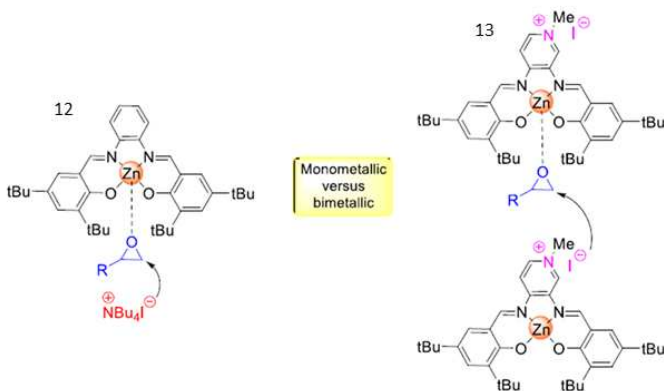


Figure 1.18. On the left a monometallic mechanism for binary catalyst **11**/TBAI and on the right a bimetallic mechanism for bifunctional catalyst **12**.³⁷

Bifunctional Zn-salen complexes with multiple hydrogen bonding donors and protic ammonium bromides **14** (Figure 1.19) was reported by He et al.⁴⁰ This complex was active in

the fixation of CO₂ in cyclic carbonate products with both terminal and internal epoxides under 0.1 MPa CO₂ pressure. High TON and TOF values of 49288 and 39473 h⁻¹ respectively, were obtained. This was one of the most effective phenoxy imminates complexes reported for the epoxide/CO₂ coupling, but showed lower activity compared with the highly symmetrical and bifunctional porphyrin complexes **15** (Figure 1.19) developed by Ema and coworkers.⁴¹ The latter showed much greater activity in the CO₂ and epoxide reactions, producing cyclic carbonate under 1.7 MPa CO₂ pressure and at 120°C and very low catalyst loadings (0.0003 mol %). Catalytic Zn systems with NNO-donor ligands have been less extensively studied. The tridentate ligands may offer different possibilities to stabilize the intermediate species. Recently Aghmiz and co-workers reported mononuclear Zn complexes **16** with NNO-donor ligands (Figure 1.20) which in the presence of a co-catalyst were active for the cycloaddition of CO₂ with both terminal and internal epoxides, under 1-100 atm CO₂ pressure and at 100°C, at very low catalyst loading (0.14-0.2 mol%).⁴² Dinjus's group reported zinc complexes **17** (Figure 1.19) based on a N,Nbis (2-pyridine-carboxamide)-1,2-benzene framework displaying either electron donating- or electron withdrawing substituents located at the diamido-spacer.⁴³ These complexes in the presence of an onium salt as cocatalyst were active in the coupling of different epoxides with carbon dioxide to afford cyclic carbonates in good yields,

even under mild reaction conditions and low catalyst loadings (0.2 mol%).

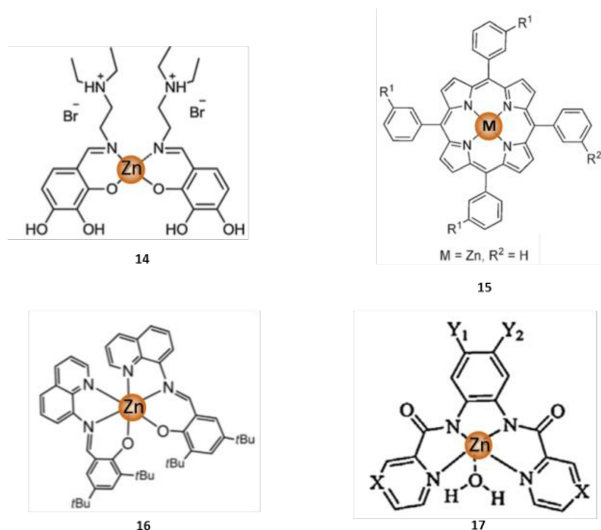


Figure 1.19. Examples of zinc complexes for synthesis of cyclic carbonates.

1.3.2c Iron catalysts

Kleij and co-workers developed monometallic and dimetallic iron (III) complexes chelated with amino-triphenolate ligands. These complexes can be both monomeric **18** and dimeric **19** (Figure 1.20), depending on the substituent present on the ortho position of the phenoxy rings.^{44,45} The bimetallic complexes have proved to be significantly less active than the monometallic complexes. In particular, the monometallic complexes, at the CO₂ pressure of 80 bar, at the temperature of 80 °C and in the presence of 10 equivalents of bis(triphenylphosphoranylidene)ammonium chloride (PPNCl), are able to give cyclohexene carbonate as exclusive product,

while in the presence of 1 equivalent of the cocatalyst give the polymer.

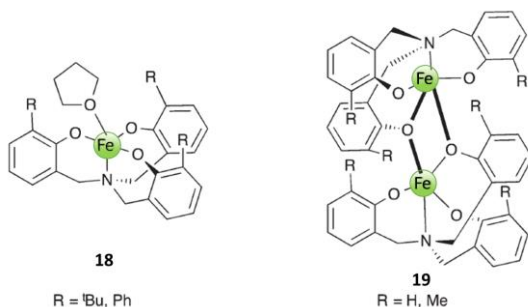


Figure 1.20. Iron triphenolate complexes developed by Kleij and co-workers.

An iron(II) tetramine complex **20** (Figure 1.21) has been investigated as catalyst for the synthesis of propylene carbonate by Rieger and co-workers.⁴⁶ This complex was able to achieve complete conversion of propylene oxide within 2 hours at 100 °C and 15 bar of CO₂, using 1.5 mol % of catalyst **20** (Figure 1.21) without the use of an additional co-catalyst. Döring and co-workers reported some easy-to-handle ionic iron(III) complexes. Among all, the most active **21** (Figure 1.21.) incorporate iodide as a counterion and two coordinated pyridines, which act as a nucleophilic co-catalyst.⁴⁷ This catalyst gave almost complete conversion of propylene oxide to propylene carbonate after 20 h, at 50 bar and 80 °C, at a low catalyst loading (only 0.2 mol%)

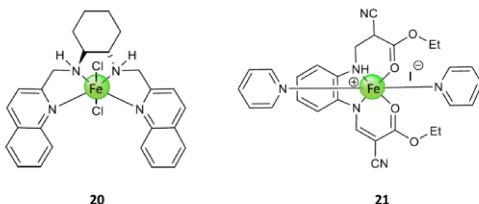


Figure 1.21. Examples of iron complexes for the cycloaddition of CO₂ and epoxides.

The same group reported catalyst **22**, bearing a bis pyridine bis amide ligand, (Figure 1.22). This catalyst was shown to be effective for a range of monosubstituted terminal epoxides.⁴⁸ In particular, in the CO₂/PO reaction produced yields of propylene carbonate up to 91 % after 20 h at 80 °C and 35 bar of CO₂ at low catalyst loading of 0.5 mol%. Moreover, iron(III) porphyrin complexes have also been used as catalysts for cyclic carbonate synthesis by Bai *et al.*⁴⁹ Complex **23** (Figure 1.22), does not require a cocatalyst as it contains iodide anions in its structure. Not only it can convert propylene oxide to propylene carbonate with high yields at low catalyst loading of 0.1 mol %, but it also can be recovered for five sequential reaction cycles with no significant reduction of activity.

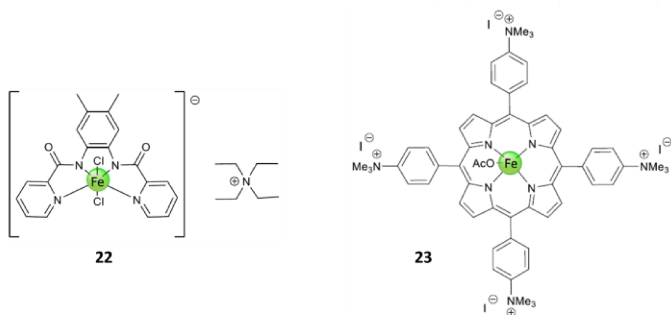


Figure 1.22. Examples of iron complexes for the cycloaddition of CO₂ and epoxides.

Particularly interesting was the bimetallic complex of Fe (III) **24** containing a macrocyclic ligand (Figure 1.23), reported by Williams and collaborators.⁵⁰ This complex showed a good catalytic activity for the copolymerization of cyclohexeneoxide with carbon dioxide to produce both cyclic carbonates and polycarbonates. In particular, at a CO₂ pressure of 10 atm and in the absence of the cocatalyst the polycarbonate was selectively obtained, while at a CO₂ pressure of 1 atm and in the presence of co-catalyst, selectivity towards cyclohexenecarbonate was obtained. Recently, Capacchione et al developed a new catalytic system based on a dimeric complex of Fe (III) **25** (Figure 1.23) bearing a dithioether-triphenolate ligand, containing a combination of "hard" and "soft" donor atoms such as oxygen and sulfur to modulate the acidity of metal centers. This catalytic system showed a high activity for the synthesis of propylene carbonate from the coupling of CO₂ with propylene oxide (PO), working in the

absence of solvent. One of the highest TOF reported in the literature, was obtained.⁵¹

Finally, iron salan complexes **26** (Figure 1.23) reported by Kerton and co-workers, were shown to be particularly active in the synthesis of propylene carbonate starting from propylene oxide (PO), in the presence of 4 equivalents of a quaternary ammonium salt, used as a cocatalyst. These reactions were conducted at 20 bar of CO₂ pressure and at 100 °C.⁵²

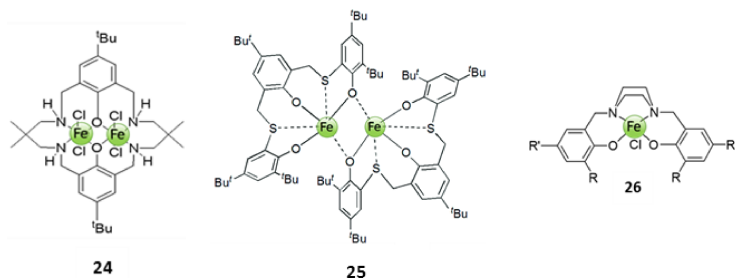


Figure 1.23. Examples of iron complexes for the cycloaddition of CO₂ and epoxides.

1.3.3. Catalytic systems for the synthesis of polycarbonates

1.3.3a Aluminum catalysts

In 1978, Inoue and co-workers synthesized the first single-site catalyst for copolymerization of CO₂/epoxide, it was a pentacoordinate complex of Al with tetraphenylporphyrin (tpp) as ancillary ligand and chloride or methoxide as a labile ligand **27** (Figure 1.24).⁵³ The complexes **27a** and **27b** were found to be active for the polymerization of CO₂ and propylene oxide

to poly(propylene carbonate) (PPC) with narrow polydispersity (PDIs) between 1.07-1.15. The reactions were carried out at 20 °C and 8 bar of CO₂, giving PPC ($M_n = 3900 \text{ g mol}^{-1}$; $M_w/M_n = 1.15$) with only 40 % carbonate linkages over 19 days of reaction. Although the low carbonate linkages and long reaction time, this reaction was the first example of polycarbonate having a narrow PDI.^{22,54}

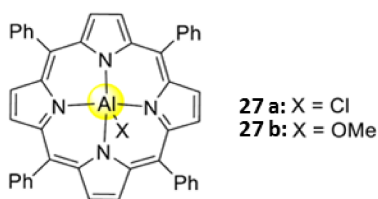


Figure 1.24. Aluminum porphyrin for the copolymerization of CO₂ and epoxides. (R = alkyl, oligomer of PPO).

In 2005, Darensbourg and collaborators developed a series of Al complexes with salen ligands **28** (Figure 1.25), with various substituents on the ligand skeleton, as promoters of the CO₂/CHO copolymerization reaction.⁵⁵ This study revealed that the most active complexes was the complexes that presented nitro groups and t-butyl groups in positions 3 and 5 of the aromatic rings, respectively. In fact, the nitro groups were necessary to increase the electrophilicity of the metal center while the t-butyl substituents served to increase the solubility of the catalytic system in the reaction mixture. These catalytic systems were also used as catalysts in CO₂/PO reactions leading to the production of cyclic carbonates.

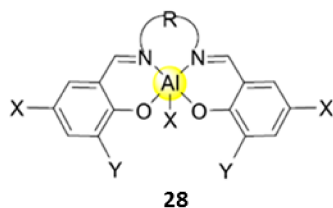


Figure 1.25. Aluminum(salen) complexes for copolymerization of CHO and CO₂.

Aluminum alkoxides were able to convert epoxides and CO₂ into polycarbonates.^{56,57,58} Beckman and collaborators synthesized several aluminum complexes, including **29**, **30** and **32** (Figure 1.26) which reacted with CHO and CO₂ to give PCHC with a maximum TOF of 2.7 h⁻¹. The reactions were conducted at 80 bar CO₂ and 60 °C. Furthermore, the aluminum complex **29** promoted the CO₂/PO reaction producing PPC (M_n = 5000 g mol⁻¹; M_w / M_n = 2.89) with only 22% of carbonate linkages and a TOF of 2.0 h⁻¹. These low-carbonate content polymers have shown potential applications as solubilizers in supercritical CO₂ (scCO₂).

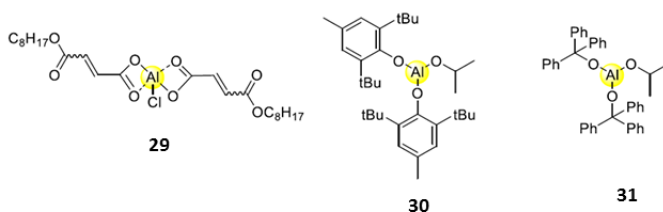


Figure 1.26. Several aluminum alkoxides for the copolymerization of CO₂ and epoxides.

1.3.3b Zinc catalysts

One of the first well-characterized class of dinuclear catalysts for CO₂/epoxides ROCOP was a zinc β -diiminato (BDI) **32**, reported by Coates and co-workers (Figure 1.27).⁵⁹ This complex showed high activity and excellent control in the CO₂ and CHO reactions, producing PCHC under 7 atm CO₂ pressure and at 50°C. A lower activity was obtained in the reaction of CO₂ with PO. The mechanism proposed for this class of complexes involved a bimetallic pathway, with one metal pre-coordinating the epoxide, enabling the second metal to feed the growing copolymer chain which ring-open the epoxide (Figure 1.27).

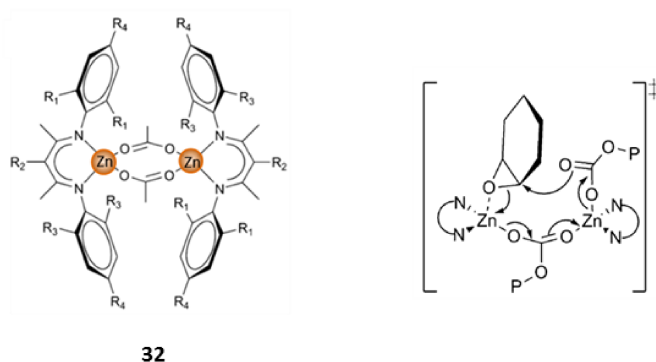


Figure 1.27. Zinc β -diiminato complex reported by Coates and co-workers and the supposed state of transition for CO₂/CHO reaction promoted by this complex.

Since this pivotal finding, many highly active dinuclear catalysts have been developed including those based on anilido-alimine, Trost type “pro-phenolate”, macrocyclic and porphyrin, typically coordinated to zinc. In 2005, Lee and co-workers reported a series of zinc anilido-alimine complexes

33 (Figure 1.28), which showed extremely high TONs in the production of PCHC having high molecular weights.⁶⁰ The activity increased in the presence of electron-withdrawing substituents (such as fluorine) on the ligand skeletal. This effect was attributed to two reasons: firstly, the electron-withdrawing fluorine substituents could reduce the electron density at the metal centers, aiding CO₂/epoxide binding, and secondly, the electron-withdrawing substituents could decrease the basicity of the anilido nitrogen donor, making the complex less sensitive to protic impurities. In the same year, Xiao *et al.* reported a dizinc complex coordinated with the Trost phenolate ligand **34** (Figure 1.28), which was moderately active for CO₂/CHO copolymerization, although the precise nature of the catalyst was not described as it was prepared *in situ*.⁶¹

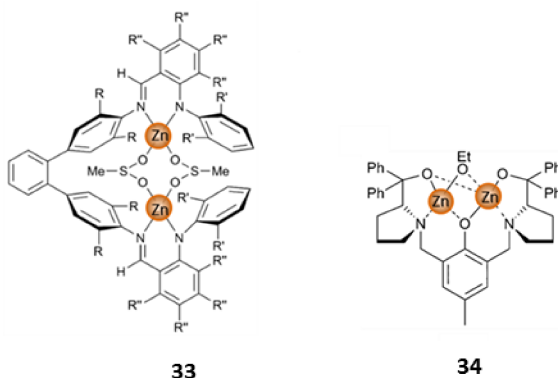


Figure 1.28. Zinc complexes for copolymerization of CHO and CO₂.

Williams *et al.* reported a series of bimetallic complexes coordinated by a novel reduced Robson's type macrocyclic ligand **35** (Figure 1.29), which were highly active with CHO

under 1 atm CO₂ pressure and at 100 °C giving a TOF of 13 h⁻¹.⁶² The macrocyclic ligand environment and the bimetallic structure were both proposed to be essential to the activity of the catalysts. Indeed the high activity of these complexes at low pressures was attributed to the coordinative flexibility of the ligand and the proximity of the two metal centers, both of which could facilitate a bidentate carboxylate chain binding mode, lowering the energy barrier of the CO₂ insertion. Rieger and co-workers reported a dizinc complex coordinated by two β-diiminate moieties that were linked through the phenyl rings **36** (Figure 1.29).⁶³ This complex was one of the most active catalyst systems for the synthesis of PCHC under 30 bar of CO₂ pressure, at 100 °C and at a catalyst loading of 0.0125 mol%. In 2015 Williams et al. reported dizinc complexes coordinated by salan ligand (or salen ligand) with an additional neutral O donor **37** (Figure 1.29), which showed activity in the CO₂ and CHO reactions, producing PCHC under 1 bar CO₂ pressure and at 80 °C.⁶⁴ The stability of the dinuclear complexes was dependent on the ligand structure, with the most stable complexes based on salen ligands.

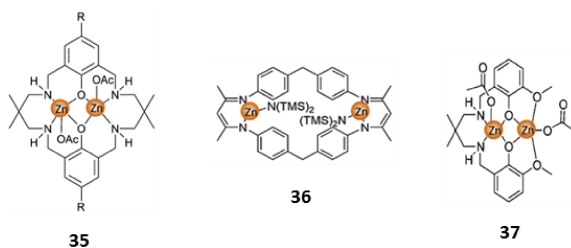


Figure 1.29. Zinc complexes for copolymerization of CHO and CO₂.

1.3.3c Iron catalyst

To date, only few examples of iron-based catalysts, active in the copolymerization of CO₂ epoxides have been reported in the literature. Among these, the bimetallic complex of Fe (III) with a macrocyclic ligand **24** (Figure 1.23, in 1.3.2c), developed by Williams and collaborators,⁶⁵ showed a good activity for the copolymerization of CHO and CO₂ at 10 bar giving a TOF of 107 h⁻¹ at 80 °C. The polymer presented a M_n up to 17200 Da and narrow polydispersity of 1.03-1.29. Nozaki *et al.* reported dinuclear oxo-bridged iron complexes **38** (Figure 1.30) with a corrole ligand as the first examples of iron complexes applicable not only in CHO/CO₂ but also in propylene oxide PO/CO₂ and glycidyl phenyl ether GPE/CO₂ copolymerization.⁶⁶ The copolymerization of epoxide and CO₂ was carried out at 60°C, 20 bar of CO₂ pressure and in the presence of PPNCl as cocatalyst. The catalytic activity was depended on the [PPN]Cl/Fe molar ratio, with the highest activity observed for an equimolar mixture, leading to TOF up to 1300 h⁻¹. In particular, by the GPE/CO₂ reaction an isotactic enriched crystalline CO₂ polymer was obtained, with a melting point of 180 °C. The other active catalyst, in this reaction class, iron(III) amine triphenolate complexes **19** (Figure 1.20 in 1.3.2c), was reported by Kleij and co-workers. They found that, depending on the cocatalyst nature and the cocatalyst/catalyst ratio, the selectivity of the reaction could be driven towards polycarbonates or cyclic carbonates.⁴⁴ Recently Capacchione and co-workers described the synthesis of a new family of OSSO-type iron (III) complexes **39** (Figure

1.30). These complexes, in the presence of TBAC as cocatalyst, were able to promote the co-polymerization of CO₂ with CHO giving the corresponding polycarbonate with the highest activity and selectivity so far reported for iron-based catalysts.⁶⁷

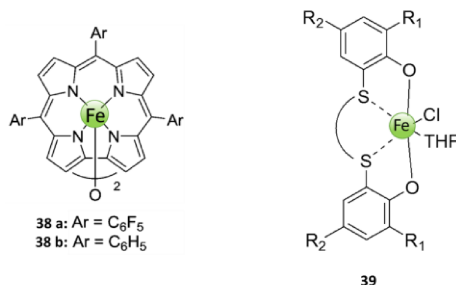


Figure 1.30. Iron complexes for copolymerization of epoxides and CO₂.

1.4. Aims of the thesis

Several examples of catalytic systems bearing salen ligands employed as promoters of CO₂/epoxides reactions have been described in the literature.^{28-34,36,39,53} Salen ligands are characterized by the presence of two imino-type nitrogen donors and two phenolate rings, thus, they are tetradentate dianionic ligands. These ligands present several advantages, in fact, they are easily synthesized and have an N₂O₂ coordination pocket in which a wide range of metal ions can be accommodated; moreover, their aromatic rings can be easily functionalized, depending on the substituents introduced, allowing the tuning of the electronic and steric properties of the metal center (Figure 1.31).

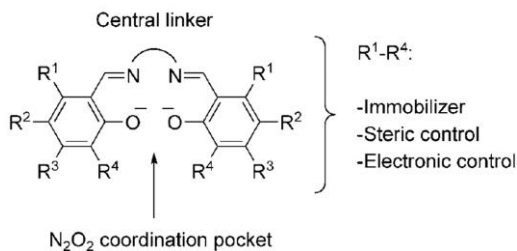


Figure 1.31. General structure of salen ligand. Substitution on the phenyl rings and linking fragment allows control over the ligand properties.

Salan and salalen ligands derive from the best known salen ligands (Figure 1.32). In particular, salan ligands are the reduced form of salen ligands and are characterized by the presence of two amino-type nitrogen donors; while salalen ligands have an intermediate structure between salan and salen, and contain both the amine and the imine moieties. The synthesis of salalen ligand has been developed by Kol's group,⁶⁸ and, to date, these ligands are still poorly explored with respect to salen and salan ligands. For this reason, in this PhD project, we have focused our attention on this innovative class of ligands and in some cases, on the comparison with its counterparts, salen and salan ligands. Salan and salalen ligands show similar advantages of salen ligands. The different hybridization of the nitrogen atoms of these classes of tetradentate ligands may differentiate the behaviour of the corresponding complexes in a substantial way.⁶⁸

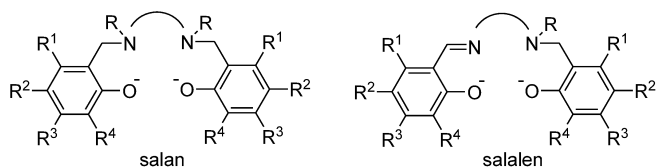


Figure 1.32. General structure of salan and salalen ligands.

For example, chromium complexes bearing salan **40** (Figure 1.33) and salalen **42** ligands (Figure 1.33), showed a notable increase in catalytic activity in the CO₂/epoxide reaction, compared to the analogous complexes with salen ligands **41** (Figure 1.33).^{69,70} This increment in activities was attributed to the greater flexibility of the salan and salalen ligands, compared to the salen, which facilitates the coordination of the carbonate and thus decreases the activation energy related to the insertion of CO₂.

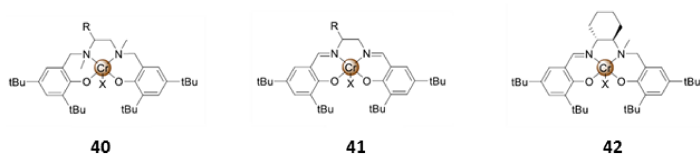


Figure 1.33. Chromium salan, salen and salalen complexes.

From our previous studies on bimetallic salalen aluminium complexes as catalysts for the CO₂/CHO reaction, we observed that the formation of *cis*-CHC takes place on a single Al center, whereas the formation of both the polycarbonate and *trans*-CHC (which originates from the back-biting of the polymer) involves two metal centers³³ (Figure 1.17 in **1.3.2a**). On the basis of these considerations,

and in order to maximize the formation of cyclic carbonate, the first part of this thesis project, was focused on the preparation of monometallic salalen aluminum complexes, (Figure 1.34) and their use as catalysts in the reaction of CO₂ with epoxides. Some modifications of the ligand skeleton were realized to modify the steric and electronic properties of the metallic center with the aim to evaluate the effects on catalytic activity. Moreover, the effect of the reaction conditions (nature of epoxide, temperature, pressure of CO₂) on the productivity and selectivity of the catalytic systems was evaluated. Finally NMR mechanistic studies allowed the characterization of an intermediate species of the catalytic cycle.⁷¹

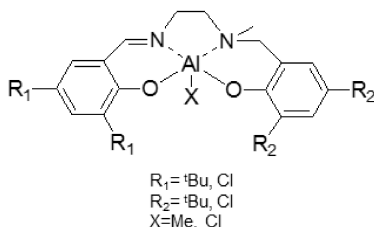


Figure 1.34. Monometallic salalen aluminum complexes used in this project.

In the same work, the behavior of aluminium complexes bearing salen, salan and salalen ligands in the CO₂/cyclohexene oxide reactions was studied. For these aluminium complexes, only small differences were observed, since in the explored conditions, *cis*-CHC was obtained in all cases, with similar conversions for all complexes.

Intrigued by the different behavior, in the CO₂/epoxide reactions, found for our monometallic aluminum complexes compared to the similar chromium complexes reported in the literature, we decided to extend our study to monometallic complexes of iron bearing salen, salan and salalen ligands (Figure 1.35).

With this aim in mind, we synthesized iron complexes with the same substituents on the phenolate rings and the same bridge between the two donor nitrogen atoms, while they differ in the nature of the donor nitrogen atoms. A study of their behavior as promoters of the CO₂/epoxide reaction was carried out, optimizing the reaction conditions and evaluating how the nature of the nitrogen atoms, (amine and / or imine atoms) and the length of the bridge between the nitrogen donors affect the activity of the complexes in CO₂/epoxide reaction. Finally, the same complexes were tested as catalysts in the ring-opening polymerization of L-lactide and ϵ -caprolactone.⁷²

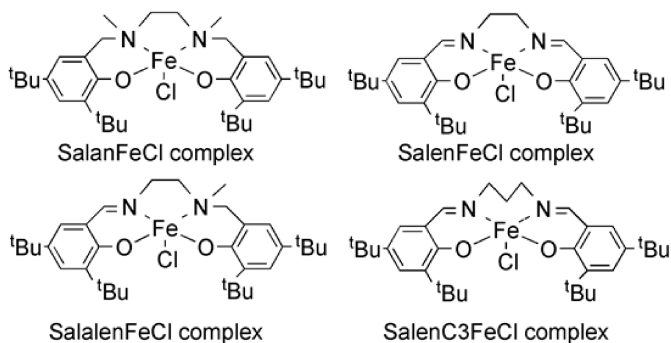


Figure 1.35. Monometallic “salen like” iron complexes used in this project.

In the last part of this project, we focused our attention on zinc complexes. As discussed before (see paragraph **1.3.3b**) bimetallic zinc complexes showed a greater activity and selectivity towards the production of polycarbonate with respect to their monometallic counterparts (see paragraph **1.3.2b**). With the aim to synthesize a salalen-based bimetallic zinc complex, we initially followed the same strategy used for the synthesis of aluminum bimetallic complexes (see paragraph **1.3.2a**). The reaction between salalen ligands, with a propylenic bridge between the two nitrogen atoms, and two equivalents of different zinc precursor (diethylzinc, zinc acetate, $\text{Zn}[\text{N}(\text{SiMe}_3)_2]_2$,) was conducted. Unfortunately, in all cases, the formation of the monometallic species was observed (Scheme 4.2 and 4.3 in chapter 4). Reasonably, the monometallic species is favored with respect to the bimetallic species because the tetracoordination of the zinc atom realized in the monometallic complex could be energetically more favorable with respect to the tricoordination, into bimetallic complex.

On the basis of these considerations, we thought to increase the coordination number of each metal centres, modifying the salen skeleton by adding two extra donor atoms. Thus, we designed new hexadentate dianionic ligands characterized by the presence of two OS-type units linked by a diimminic bridge (Figure 1.36). The new ligand scaffold closely resembles the salen skeleton and preserves some of its advantages, i.e., for example, it is possible to vary the nature of the nitrogen donor atoms (amine and imine), the

substituents on the aromatic rings, to modulate the length of the bridge and to find the optimal distance for the cooperation between the two metallic centers. During this PhD project, a methodology for the synthesis of this class of new hexadentate dianionic ligands has been developed. The first ligand of this class has been synthesized and characterized, it present hydrogen atoms as R substituents, t-butyl groups as the R₁ substituents and ethylene bridge between the two imino nitrogen donors.

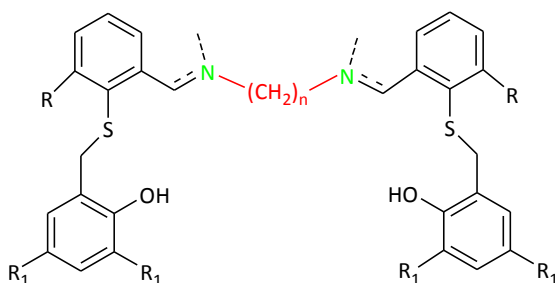


Figure 1.36. Structure of the hexadentate dianionic ligands.

Afterwards, we were pleased to get the desired bimetallic zinc complex (Figure 1.37). through direct reaction between the ligand and two equivalents of $\text{Zn}[\text{N}(\text{SiMe}_3)_2]_2$. Subsequently, this new bimetallic complex has been employed as catalyst for CO_2/CHO reactions. The effect of the reaction conditions (nature of epoxide, temperature pressure of CO_2) on the productivity and selectivity of the reaction has been evaluated.

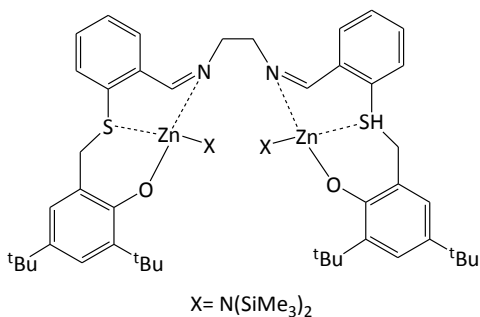


Figure 1.37. Structure of the bimetallic zinc complex synthesized in this project.

During my third year of PhD, I spent a research period (six months) at the laboratories of ICIQ, Institut Català d'Investigació Química, working under the supervision of Prof. Arjan W. Kleij. During this period I had the opportunity to work in the field of coupling reactions of CO_2 with epoxide promoted by several organocatalytic systems

References

- 1 International Energy Agency. CO₂ Emission from Fuels Combustion Highlights, 2012 Edition; Imprimerie Centrale: Luxembourg, October **2012**.
- 2 A. W. Kleij, M. North, A. Urakowa, ChemSusChem **2017**, 10, 1036-1038.
- 3 M. R. Kember, A. Buchard, C. K. Williams, Chem. Commun, **2011**, 47, 141-163.
- 4 International Energy Agency. Energy Technology Perspectives **2012**, ETP 2012; OECD/IEA: Paris, 2012.
- 5 M. Aresta, A. Di Benedetto, A. Angelini, Chem. Rev. **2014**, 114, 1709-1742.
- 6 Q. W. Song, Z. H. Zhou, L. N. He, Chem. Chem., **2017**, 19, 3707-3728
- 7 M. Aresta, A. Dibenedetto, Dalton Trans. **2007**, 2975-2992.
- 8 G. W. Coates, D. R. Moore, Angew. Chem. Int. Ed. **2004**, 43, 6618-6639.
- 9 J. W. Comerford, I. D. V. Ingram, M. North, X. Wu, Green Chemistry, **2015**, 17, 1966-1987.
- 10 C. Beattie, M. North, P. Villuendas, Molecules **2011**, 16, 3420-3432.
- 11 V. Etacheri, R. Marom, R. Elazari, G. Salitra, D. Aurbach, Energy Environ. Sci. **2011**, 4, 3243-3262.
- 12 M. Fleischer, H. Blattmann, R. Mülhaupt, Green Chem. **2013**, 15, 934-942.
- 13 Z. Liu, V. Jensen, W. Fenical, Phytochemistry **2003**, 64, 571-574.
- 14 J. Y. Gauthier, Y. Leblanc, W. C. Black, C. C. Chan, W. A. Cromlish, R. Gordon, B. P. Kennedy, C. K. Lau, S. Léger, Z. Wang, D. Ethier, J. Guay, J. Mancini, D. Riendeau, P. Tagari, P. Vickers, E. Wong, L. Xu, P. Prasit, Bioorg. Med. Chem. Lett. **1996**, 6, 87-92.

-
- 15 M. Taherimehr, P. P. Pescarmona, J. Appl. Polym. Sci. Rev. **2014**, 131, 41141-41158.
- 16 S. Paul, Y. Zhu, C. Romain, R. Brooks, P. K. Saini, C. K. Williams Chem. Commun., **2015**, 51, 6459—6479
- 17 S. J. Poland and D. J. Darensbourg, Green Chem., **2017**, 19, 4990-5011
- 18 A. W. Kleij, ChemSusChem, **2018**, 11, 2842-2844.
- 19 A. Decortes, A. M. Castilla, A. W. Kleij, Angew. Chem., Int. Ed. **2010**, 49, 9822-9837.
- 20 C. Martin, G. Fiorani, A. W. Kleij, ACS Catal. **2015**, 5, 1353-1370.
- 21 N. Takeda, S. Inoue, Bull. Chem. Soc. Jpn. **1978**, 51, 3564-3567.
- 22 T. Aida, S. Inoue, J. Am. Chem. Soc. **1983**, 105, 1304-1309.
- 23 K. Kasuga, T. Kato, N. Kabata, M. Handa, Bull. Chem. Soc. Jpn. **1996**, 69, 2885-2888.
- 24 D. Ji, D., X. Lu, R. He, Appl. Catal. A: General **2000**, 203, 329-333.
- 25 C. J. Whiteoak, N. Kielland, V. Laserna, V.; E. C. Escudero-Adán, E. Martin, A. W. Kleij, J. Am. Chem. Soc. **2013**, 135, 1228-1231.
- 26 C. J. Whiteoak, N. Kielland, V. Laserna, V. Castro-Gómez, E. Martin, E. C. Escudero-Adán, C. Bo, A. W. Kleij Chem. Eur. J. **2014**, 20, 2264-2275.
- 27 J. Rintjema, A. W. Kleij, ChemSusChem, **2017**, 10, 1274-1282.
- 28 X. B. Lu, X, J. Feng, R. He, Appl. Catal. A: General **2002**, 234, 25-33.
- 29 X. B. Lu, Y. J. Zhang, K. Jin, L. M. Luo, H. Wang, J. Catal. **2004**, 227, 537-541.
- 30 D. J. Darensbourg, Yarbrough, J. Am. Chem. Soc. **2002**, 124, 6335-6342.
- 31 D. J. Darensbourg, A. I. Moncada, Macromolecules **2010**, 43, 5996-6003.

-
- 32 J. Meléndez, M. North, R. Pasquale, *Eur. J. Inorg. Chem.* **2007**, 3323-3326.
- 33 W. Clegg, R. Harrington, M. North, R. Pasquale, *Chem. Eur. J.* **2010**, 16, 6828-6843.
- 34 J. Meléndez, M. North, P. Villuendas, *Chem. Commun.* **2009**, 2577-2579.
- 35 M. Cozzolino, K. Press, M. Mazzeo, M. Lamberti, *ChemCatChem* **2016**, 8, 455-460
- 36 A. Decortes, M. Martinez-Belmonte, J. Benet-Buchholz, A. W. Kleij, *Chem. Commun.* **2010**, 46, 4580-4582.
- 37 A. Decortes, A. W. Kleij, *ChemCatChem* **2011**, 3, 831-834.
- 38 C. Martín, C. J. Whiteoak, E. Martin, M. Martinez-Belmonte, E. C. Escudero-Adán, A. W. Kleij, *Catal. Sci. Technol.* **2014**, 4, 1615-1621.
- 39 C. Martín, A. W. Kleij, *J. Beilstein Org. Chem.* **2014**, 10, 1817-1825.
- 40 X. D. Lang, Y. C. Yu, L. N. He, *Journal of Molecular Catalysis A: Chemical*, **2016**, 420, 208-215.
- 41 C. Maeda, T. Taniguchi, K. Ogawa, T. Ema, *Angew. Chem., Int. Ed.* **2015**, 54, 134-138.
- 42 L. C. Aluja, A. C. Carrasco, J. Castilla, M. Reguro, A. M. M. Bulto, A. Aghmiz, *Journal of CO₂ Utilization*, **2016**, 14, 10-22.
- 43 M. Adolph, T. A. Zevaco, C. Altesleben, S. Staudt, E. Dinjus, *Journal of Molecular Catalysis A: Chemical*, **2015**, 400, 104-110
- 44 M. Taherimehr, S. M. Al-Amsyar, C. J. Whiteoak, A. W. Kleij, P. P. Pescarmona, *Green Chem.* **2013**, 15, 3083-3090.
- 45 C. J. Whiteoak, E. Martin, E. C. Escudero-Adán, A. W. Kleij, *Adv. Synth. Catal.* **2013**, 355, 2233-2239.
- 46 J. E. Dengler, M. W. Lehenmeier, S. Klaus, C. E. Anderson, Herdtweck, E.; Rieger, B., *Eur. J. Inorg. Chem.* **2011**, 336-343.
- 47 M. A. Fuchs, T. A. Zevaco, E. Ember, O. Walter, I. Held, V. Dinjus, M. Döring, *Dalton Trans.* **2013**, 42, 5322-5329.

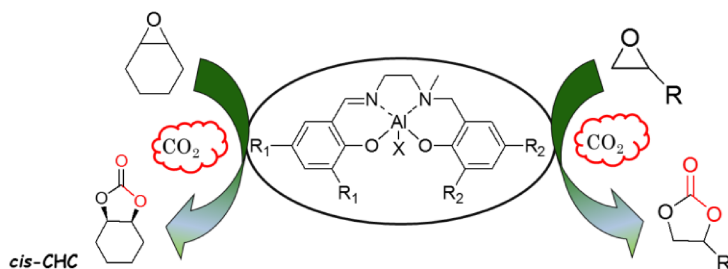
-
- 48 M. Adolph, T. A. Zevaco, C. Altesleben, O. Walter, E. Dinjus, *Dalton Trans.* **2014**, 43, 3285-3296.
- 49 D. Bai, X. Wang, Y. Song, B. Li, L. Zhang, P. Yan, H. Jing, J. *Chin, Catal.*, **2010**, 31, 176-180.
- 50 A. Buchard, M. R. Kember, K. G. Sandeman, C. K. Williams, *Chem. Commun.* **2011**, 47, 212-214.
- 51 A. Buonerba, A. De Nisi, A. Grassi, S. Milione, C. Capacchione, S. Vagin, B. Rieger, *Catal. Sci. Technol.*, **2015**, 5, 118–123.
- 52 D. Alhashmialameer, J. Collins, K. Hattenhauera, F. M. Kerton, *Catal. Sci. Technol.*, **2016**, 6, 5364 –5373.
- 53 S. Inoue, J. Polym. Sci. Part A, Polym. Chem. **2000**, 38, 2861-2871.
- 54 T. Aida, S. Inoue, *Macromolecules* **1982**, 15, 682-684.
- 55 D. J. Darensbourg, D. R. Billodeaux, *Inorg. Chem.* **2005**, 44, 1433-1442.
- 56 T. Sarbu, T. Styranec, E. J. Beckman, *Nature* **2000**, 405, 165-168.
- 57 T. Sarbu, E. J. Beckman, *Macromolecules* **1999**, 32, 6904-6912.
- 58 T. Sarbu, T. J. Styranec, E. J. Beckman, *Ind. Eng. Chem. Res.* **2000**, 39, 4678-4683.
- 59 M. Cheng, D. R. Moore, J. J. Reczek, B. M. Chamberlain, E. B. Lobkovsky and G. W. Coates, *J. Am. Chem. Soc.*, **2001**, 123, 8738-8749.
- 60 B. Y. Lee, H. Y. Kwon, S. Y. Lee, S. J. Na, S.-I. Han, H. Yun, H. Lee, Y.-W. Park, *J. Am. Chem. Soc.*, **2005**, 127, 3031-3037.
- 61 Y. L. Xiao, Z. Wang, K. L. Ding, *Chem. Eur. J.*, **2005**, 11, 3668-3678.
- 62 M. R. Kember, P. D. Knight, P. T. R. Reung, C. K. Williams, *Angew. Chem., Int. Ed.*, **2009**, 48, 931-933.
- 63 S. Kissling, M. W. Lehenmeier, P. T. Altenbuchner, A. Kronast, a M. Reiter, P. Deglmann, U. B. Seemann and B. Rieger, *Chem. Commun.*, **2015**, 51, 4579—4582.

-
- 64 A. Thevenon, J. A. Garden, A. J. P. White, C. K. Williams, *Inorg. Chem.* **2015**, *54*, 11906–11915.
- 65 A. Buchard, M. R. Kember, K. Sandeman, C. K. Williams, *Chem. Commun.* **2011**, *47*, 212-214.
- 66 K. Nakano, K. Kobayashi, T. Ohkawara, H. Imoto, K. Nozaki, *J. Am. Chem. Soc.*, **2013**, *135*, 8456-8459.
- 67 F. Della Monica, B. Maity, T. Pehl, A. Buonerba, A. De Nisi, M. Monari, A. Grassi, B. Rieger, L. Cavallo, C. Capacchione, *ACS Catal.* **2018**, *8*, 6882-6893.
- 68 A. Yeori, S. Gendler, S. Groysman, I. Goldberg, M. Kol, *Inorganic Chemistry Communications*, **2004**, *7*, 280–282.
- 69 D. Y. Rao, B. Li, R. Zhang, H. Wang, X. B. Lu, *Inorg. Chem.*, **2009**, *48*, 2830-2836.
- 70 K. Nakano, M. Nakamura, K. Nozaki, *Macromolecules*, **2009**, *42*, 6972-6980.
- 71 M. Cozzolino, T. Rosen, I. Goldberg, M. Mazzeo, M. Lamberti, *ChemSusChem*, **2017**, *10*, 1217-1223
- 72 M. Cozzolino, V. Leo, C. Tedesco, M. Mazzeo, M. Lamberti, *Dalton Trans.*, **2018**, *47*, 13229-13238.

CHAPTER 2

CO₂ Fixation in Cyclic Carbonates by Salalen Aluminum Complexes and Mechanistic studies

In chapter 2, we report synthesis and characterization of aluminum complexes bearing salalen ligands. These complexes have been employed as catalysts for CO₂/epoxide cycloaddition reactions. In particular, the effect of the reaction conditions (nature and equivalents of the cocatalyst, CO₂ pressure and temperature) and of the ligands (substituents on the ancillary ligand, nature of the labile ligand and nature of the nitrogen donor atoms) on the outcome of these reactions was studied. Interestingly, NMR mechanistic studies allowed the characterization of an intermediate species of the catalytic cycle.



2.1. Introduction

Carbon dioxide can be considered as a non-toxic, abundant, renewable and low cost C1-building block. In particular, the transformation from epoxides and CO₂ into either cyclic carbonates or polycarbonates have received much attention recently.¹ Polycarbonates are considered a promising class of biodegradable polymers²; while cyclic carbonates find application as environmentally friendly polar aprotic solvents, electrolytes in lithium ion batteries and as intermediates in the synthesis of fine and bulk chemicals.³

Several metal based catalytic systems for the synthesis of cyclic carbonates from epoxides and CO₂, have been developed, including complexes of aluminum, chromium, cobalt, zinc and magnesium. Among the various metals, aluminum is very interesting because it is an abundant and inexpensive and main group metal which generally leads to a good control of the reaction process.^{4,5} The dinuclear μ -oxo-bridged Al(salen) complex reported by North *et al* was one of the most active aluminum complexes for the synthesis of cyclic carbonates, even under mild reaction conditions.⁶ Among the most active complexes, noteworthy are aluminum triphenolate complexes reported by Kleij and collaborators. They are able to promote the coupling reaction of CO₂ with both terminal and internal epoxides, working in the presence of TBAI, at 10 bar and 70-90 ° C.⁷ Aluminum porphyrine complex had a special importance from a historical point of view, as it was the first single-site catalyst for the CO₂ / epoxide reaction.⁸ Recently, Qin and Wang reported aluminum porphyrine complexes as highly active catalysts for the synthesis of cyclic carbonates with

TOF values up to $1.85 \cdot 10^5 \text{ h}^{-1}$, although working under drastic conditions (120°C and 30 bar).⁹ Finally, aluminum complexes with different ancillary ligands, such as: phthalocyanine, salen, acen, scorpionate and aminoethanol, active in this class of reactions have been also described in the literature.^{10,11,12,13,14}

We recently reported bimetallic salalen-aluminum complexes, which under appropriate reaction conditions, were able to selectively produce *cis*-cyclohexene carbonate (*cis*-CHC) and propylene carbonate by reacting CO_2 with cyclohexene and propylene oxide, respectively.¹⁵ In this chapter, we describe the behavior of, strictly related, monometallic salalen aluminum complexes in the CO_2 / epoxide reaction. Different modifications were made to the skeleton of the ligand to study the effect of substituents and the nature of nitrogen atoms both on the selectivity and the activity of the catalysts. Furthermore, NMR mechanistic studies have been carried out to get information on the catalytic cycle active with this class of catalysts.

2.2. Results and Discussion

2.2.1. Characterization of Salalen ligands

The ligands H_2L_{1-3} (Figure 2.1), used for the synthesis of aluminum complexes, were provided by the research group of professor Moshe Kol of the University of Tel Aviv. The purity of the H_2L_{1-3} ligands was confirmed by ^1H NMR analysis.

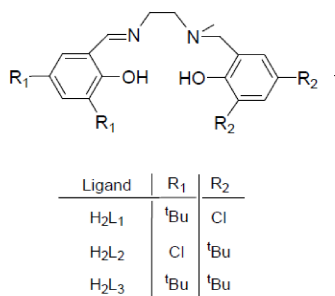
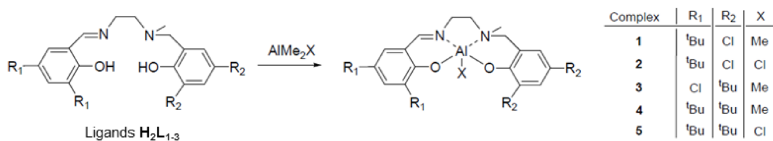


Figure 2.1. Structure of the salalen ligands used in this project.

2.2.2. Synthesis and characterization of Salalen Aluminum complexes

The synthesis of aluminum complexes **1-5** (Scheme 2.1) was performed following a previously reported procedure, which involves the reaction of the ligand with 1 equivalent of aluminum precursor (trimethyl aluminum for complexes **1**, **3** and **4** and dimethyl aluminum chloride in the case of complexes **2** and **5**) in benzene at room temperature.



Scheme 2.1. Synthesis of Aluminum Salalen Complexes **1-5**

Complexes **1-5** were obtained in high yields (78 ÷ 96 %). All compounds were characterized by ¹H, ¹³C and COSY NMR spectroscopy. Complexes **3** and **4**, which have been previously reported in the literature, showed NMR spectra superimposable with those reported.^{16,17}

The ^1H NMR spectra of complexes **1-5** were consistent with the formation of the desired monometallic complexes in which aluminum is pentacoordinate as it is bound to the four donor atoms of the salalen ligand and one methyl or chloride as labile ligand. In the spectra of complexes **1**, **3** and **4** the appearance of a signal for the protons of the methyl bound to the aluminum atom, is observed in the high field region (around -0.4 ppm). While the spectra of complexes **2** and **5** show no signals in the high field region, as the aluminum is bound to the chloride. As expected, the protons of the bridge ($\text{NCH}_2\text{CH}_2\text{N}$), as well as the methylene protons adjacent to the amino nitrogen atom (NCH_2Ar) are diastereotopic and resolve into A_xB_x patterns, suggesting the coordination of both neutral nitrogen atoms to the aluminum centre. The 2D COSY analysis allowed the complete assignment of all the protons of the ligand skeleton.

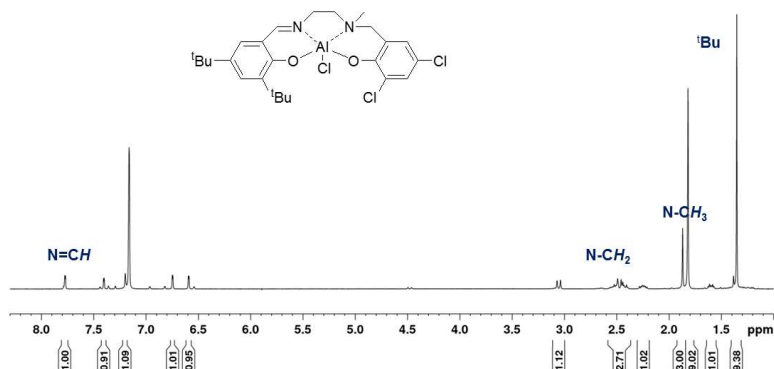


Figure 2.2. ^1H NMR spectrum (400 MHz, C_6D_6 , 298K) of complex **2**.

2.2.3. Single-crystal structure analysis

Single crystals of complex **2** suitable for X-ray diffraction analysis were obtained by a solution of the complex in hexane at room temperature. Complex **2** crystallized in space group *P*-1, and the asymmetric unit contains two enantiomeric molecules of the Al-complex (Figure 2.3) and half a molecule of the solvent (which resides on crystallographic inversion). The structure features a pentacoordinate mononuclear aluminum complex in which all donors of the (ONNO) ligand are bound to the aluminum center.

Commonly pentacoordinate complexes can adopt two geometries: square-pyramidal (sqp) or trigonal bipyramid (tbp), parameter τ ($\tau = |\beta - \alpha|/60$, where $\beta = \text{N1—Al—O2}$ angle and $\alpha = \text{N2—Al—O1}$ angle) is used to describe to which geometry between sqp and tbp the complex is closer. When τ is equal to 0 the complex has a perfect sqp geometry, whereas when τ is equal to 1 the complex assumes a perfect tbp geometry. The τ values for the two crystallographically independent molecules were 0.61 and 0.65.¹⁸ The geometry around Al is closer to trigonal bipyramidal (with N3 and O1 in the apical positions) than to square-pyramidal (with Cl at the apical position). The bond lengths of the (ONNO) donors to aluminum are unexceptional. Evidently, the Al-N(sp³) bonds are considerable longer than the Al-N(sp²) ones, as previously observed for similar salalen aluminum complexes.¹⁷ As expected, the phenoxide *trans* to the imine nitrogen has an Al-O bond distance shorter than that of the phenoxide *trans* to the amine nitrogen.

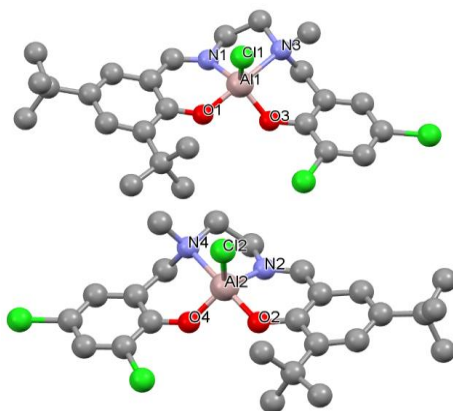


Figure 2.3. Ball-and stick illustration of the two crystallographically independent molecules of complex **2**. The chirality on N3 is S and on N4 is R. Selected bond lengths (Å): Al1-O1 1.792(2), Al1-O3 1.760(2), Al1-N1 1.949(2), Al1-N3 2.168(2), Al1-Cl1 2.165(1), Al2-O2 1.798(2), Al2-O4 1.755(2), Al2-N2 1.941(2), Al2-N4 2.197(2), Al2-Cl2 2.177(1).

2.2.4. Cycloaddition of carbon dioxide with epoxides

Complexes **1-5** were employed as catalysts in the reaction of CO₂ with epoxides. We first tested the catalytic activity and the product selectivity of complexes **1-5** in the reaction of CO₂ with cyclohexene oxide (CHO). Subsequently we extended our study, testing complex **1** with several terminal epoxides. Usually, the selectivity between the *cis*-cyclic carbonate and the polycarbonate derived from cyclohexene oxide is determined by means of IR spectroscopy, due to the overlapping of the signals of these two products in the NMR spectrum. Indeed the signals of the hydrogen atoms on the carbonate ring in *cis*-CHC (H_a in Figure 2.4) and on the polymer backbone in PCHC (H_d in Figure 2.5) are partially overlapped in the ¹H NMR spectra. However, recently reported in the literature that using a 600 MHz NMR instrument, a good resolution of the signals

at $\delta=2.0$ (He) and 1.9 ppm (Hb) is possible, enabling the determination of the ratio of the two products.¹⁵ The conversion was measured by ^1H NMR spectrum by integrating the signal at 4.6 ppm (methine protons of both PCHC and *cis*-CHC) and the signal at 4.0 ppm (methine protons of the *trans*-CHC) with respect to the analogue protons of the CHO (3.1 ppm).

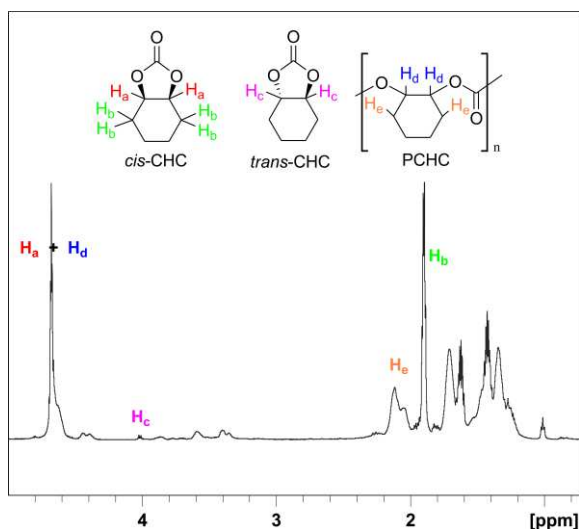
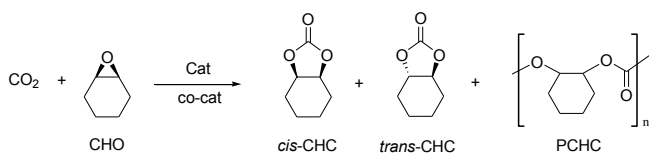


Figure 2.4. ^1H NMR spectrum of a mixture of CHC and PCHC, (CDCl_3 , 600 MHz, 298 K).¹⁵

Previous studies have shown that the ammonium derived cocatalyst does not present a good solubility in the epoxide and, working in the absence of solvent, a class of similar complexes tends to homopolymerize the CHO.^{15,19} For this reason the experiments were conducted in the presence of a small amount of methylene chloride (0.3 mL) in order to dissolve the salts used as

cocatalysts. The effect of the experimental conditions (i.e., nature and equivalent of the cocatalyst, nature and loading of the catalyst, temperature and CO₂ pressure) on the outcoming of the reactions has been investigated. Complex **1** was initially employed as catalyst for the cycloaddition of CO₂ to CHO in combination with different ammonium salts as cocatalysts namely tetrabutylammonium bromide (TBAB), tetrabutylammonium chloride (TBAC), tetrabutylammonium acetate (TBAAc), bis(triphenylphosphoranylidene)ammonium chloride (PPNCl). These reactions were carried out in autoclave, at a CO₂ pressure of 30 bar and at a temperature of 80 °C for a time of 20 hours. The reactions were quenched by adding CH₂Cl₂ at air. A ¹H NMR spectrum of the reaction mixture allowed the determination of the cyclohexene oxide conversion. The results obtained are summarized in Table 2.1. The turnover numbers (TON) were calculated according to the following equation: mol of epoxide consumed / mol of cat. These experiments show that, in all cases, cyclohexenecarbonate (CHC) was the most abundant product (Scheme 2.2). Nevertheless there were small differences in the activities of this aluminum complex by varying the cocatalyst. The most active system was obtained by the combination of complex **1** with TBAB or PPNCl, with TONs of 328 and 340, respectively.



Scheme 2.2. CO₂/CHO reaction promoted by complexes **1-5** in combination with a quaternary ammonium salt.

Table 2.1. CO₂/CHO reaction promoted by complex **1** and ammonium salts.^[a]

Entry ^[a]	Cocat.	Conv.(%)	<i>Cis</i> CHC: <i>trans</i> CHC:PCHC ^[b]	TON
1	TBAB	28	90 : 2 : 8	328
2	TBAC	16	81 : 3 : 10	187
3	TBAAc	20	84 : 2 : 9	235
4	PPNCl	29	88 : 2 : 10	340

^[a] **General conditions:** cat **1** = 42.1 μmol (0.08 mol %), CH₂Cl₂ = 0.3 mL, CHO = 5 mL (1174 equiv), P_{CO₂} = 30 bar, T = 80 °C, ^[b] complement to 100 = polyethers.

To study the effect of the reaction conditions and the substrate scope, TBAB was chosen as cocatalyst, because it is cheaper and more selective towards the formation of *cis*-CHC compared to PPNCl. Results of these reactions are summarized in Table 2.2.

As shown in Table 2.2 (entries 1-4), conducting reactions at 30 bar and 80 °C, both activity and selectivity towards the formation of *cis*-CHC seem to increase with the increase of the equivalents of TBAB. It is interesting to note that when 4 equivalents of ammonium salt are used, *cis*-CHC was the exclusive product. Indeed, as already known in the literature, an excess of nucleophile can induce the detachment of the carbonate intermediate from the catalyst, encouraging the ring closure reaction and, subsequently the formation of the cyclic carbonate.²

Table 2.2. CO₂/CHO reaction promoted by complex **1** and tetrabutylammonium bromide (TBAB).^[a]

Entry ^[a]	TBAB (eq)	P _{CO₂} (bar)	Temp (°C)	<i>Cis</i> - CHC ^[b]	TON	TOF (h ⁻¹)
1	1	30	80	91	106	5
2	2	30	80	96	340	17
3	4	30	80	>99	505	25
4	8	30	80	>99	810	40
5	8	30	100	>99	904	45
6	8	10	100	>99	927	46
7	8	2	100	>99	575	29
8 ^[c]	8	30	100	>99	1291	64

^[a] **General conditions:** **1** = 42.1 μmol, CHO = 5 mL (1174 equiv), CH₂Cl₂ = 0.3 mL, time = 20 h. ^[b] complement to 100 = PCHC. ^[c] **1** = 21.05 μmol.

Comparing entries 4 and 5 of Table 2.2 it can be observed that an increase of the temperature leads to an improvement in the catalytic activities of the complex **1**. While by lowering the CO₂ pressure, from 30 to 2 bar, the activity decreased (cf entries 5, 6 and 7, Table 2.2) while no effect on the selectivity was observed. Then, we investigated the reaction in the presence of reduced amounts of complex **1** (entries 8, Table 2.2) and we were delighted

to find that considerable conversion could still be achieved working at a catalyst loading of 0.04 mol% under 30 bar and 100 °C. Worth of noting, these salalen monometallic aluminum complexes exhibit excellent selectivity towards *cis*-CHC formation. When compared with salalen bimetallic aluminum complexes, previously reported,¹⁵ these salalen monometallic aluminum complexes show similar catalytic activities but higher selectivity towards the *cis*-CHC product. This effect could be ascribed to the fact that the production of polycarbonates by the salalen bimetallic aluminum complexes involves two metallic centers, while the formation of cyclic carbonates involves only one metallic center.

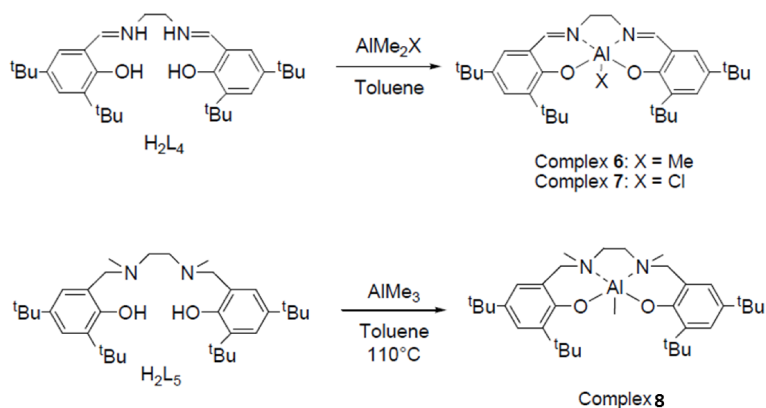
To understand if the substituents on the ligand skeleton, the labile ligand and the nature of the donor nitrogen atoms play a role on the progress of the reaction, we used complexes **1-5** as catalysts in the CO₂/CHO coupling reaction. The reactions were carried out in the presence of 8 equivalents of TBAB, at 100 °C and 2 bar of CO₂ pressure. Results of these reactions are summarized in Table 2.3. In all cases, *cis*-CHC were obtained as exclusive product. In general, the effect of the ligands on the conversion was not considerable, however some tendencies can be outlined. First, methyl derivatives gave better conversions with respect to chloride derivatives (entries 1 vs 2 and 4 vs 5 of Table 2.3). Complex **1**, which features halo substituents on the amine-side phenol and bulky alkyl groups on the imine-side phenol, and complex **3**, with the opposite phenolate substitution pattern, showed similar conversion (entries 1 and 3 in Table 2.3). Whereas complex **4**, bearing *t*-butyl substituents on both sides, resulted less active (entry 4 in Table 2.3).

Table 2.3. CO₂ / CHO reaction promoted by complexes **1-8** and TBAB.^[a]

Entry	Cat		Conv (%)	TON	TOF (h ⁻¹)
1	^t BuClAlMe	1	49	575	29
2	^t BuClAlCl	2	38	399	20
3	Cl ^t BuAlMe	3	47	551	28
4	^t Bu ^t BuAlMe	4	34	446	22
5	^t Bu ^t BuAlCl	5	34	446	22
6	salenAlMe	6	48	563	28
7	salenAlCl	7	41	481	24
8	salanAlMe	8	34	446	22

^[a] **General conditions:** cat **1-8** = 42.1 μmol, TBAB = 8 equiv, CH₂Cl₂ = 0.3 mL, CHO = 50 mmol (5 mL). Temperature = 100°C, P_{CO₂} = 0.2 MPa, time = 20 h.

This can be explained taking into account that electron withdrawing substituents may increase the Lewis acidity of the aluminum centre, irrespectively of their position. To evaluate the effect of the nature of nitrogen atoms in the ligand skeleton we synthesized the aluminum complexes **6**²⁰ and **8**.²¹ These aluminum complexes **6** and **8** bear respectively salen and salan ligands with t-butyl substituents on the phenolate rings of ligands and one methyl as a labile ligand (see Scheme 2.3).

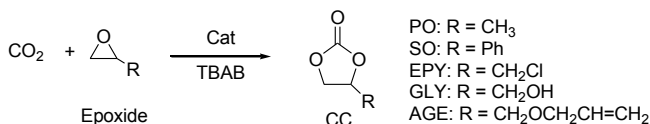


Scheme 2.3. Synthesis of Aluminum Salalen Complexes **6-8**

Comparing complexes **4**, **6** and **8**, which have the same substituents on the phenolate rings and the same labile ligand it can be noted that the aluminum complexes with salan and salalen ligands show comparable activities and the aluminum salen-based complex is the most active of the three. Likely, the planar conformation of the complex bearing the salan ligand is beneficial in this reaction.^{22,23} Complex **7**,²⁴ bearing the same salan ligand of complex **6** but a chlorine as labile ligand, confirmed that methyl derivatives are more active than chloride ones (cfr entries 6 and 7 in Table 2.3).

Finally, we explored the behavior of complex **1** in the scope of cycloaddition of CO₂ with a variety of functionalized terminal epoxides (Scheme 2.4). Results are summarized in Table 2.4 The reactions were carried out at 100 °C and 10 bar of CO₂ pressure. All of the studied substrates were conveniently converted into the corresponding cyclic carbonates. The selectivity for the cyclic

carbonate product was >99% in all cases, as determined by ^1H NMR. Importantly, this result indicates that this catalytic system show a high versatility and a good tolerance towards different functional groups as halogen, aryl, alkenyl, ether and hydroxyl.



Scheme 2.4. Cycloaddition of terminal epoxides and CO₂ promoted by complex **1**.

Table 2.4. Cycloaddition of terminal epoxides and CO₂ promoted by complex **1** and TBAB. ^[a]

Entry ^[a]	Epoxide R =	Time (h)	Conv (%)	TON	TOF (h ⁻¹)
1	CH ₃	1	54	1830	1830
2	Ph	5	43	900	180
3	CH ₂ Cl	5	86	2612	522
4	CH ₂ OH	5	92	3295	659
5	CH ₂ OCH ₂ CH=CH ₂	5	42	840	170

^[a] **General conditions:** **1** = 21.05 μmol, TBAB = 8 equiv, CH₂Cl₂ = 0.3 mL, epoxide = 5 mL. Temperature = 100°C, P_{CO₂} = 10 bar.

2.2.5. NMR mechanistic studies of the CO₂/CHO reaction promoted by complex 1.

The mechanism usually proposed for the formation of cyclic carbonates involves the coordination of the epoxide to the metal centre through the oxygen atom, the following opening of the epoxide by a nucleophilic attack, the insertion of CO₂ into the metal-oxygen bond and finally the ring closing by an intramolecular nucleophilic attack with the formation of the cyclic carbonate.

However, in most of the papers such mechanism is proposed on the basis of theoretical studies and/or experimental results (such as kinetics analysis, stereochemistry of the products, etc) to the best of our knowledge only in few cases intermediate species of the catalytic cycle have been observed.²¹ With the aim to get a more in depth study of the mechanism active with our catalysts, NMR studies have been carried out on reaction mixtures purposely prepared.

Stoichiometric reactions were carried out in NMR tube between the aluminum complex **1** and the cyclohexeneoxide and/or CO₂ in order to obtain mechanistic information about the CO₂/CHO reaction catalyzed by this class of complexes. The aluminum monometallic complex **1** was first reacted with a small amount of CHO to understand if it was able to promote the opening of the epoxide. The studies were conducted by using ¹H NMR analysis.

The ¹H NMR spectra of complex **1** (10 mg, 1.98 * 10⁻⁵ mol) and the CHO (1.5 eq, 3 μL) at room temperature in CD₂Cl₂ were recorded. In the collected spectra was observed the formation of polycyclohexeneoxide (PCHO) and the disappearance of the CHO signals, while the signals of the starting complex were unchanged.

This suggested that this complex homopolymerizes the CHO under these conditions; and that the process concerns only a small part of the metal centers, therefore propagation rate should be much faster of the initiation rate.

Next, the opening reaction of CHO promoted by complex **1** in the presence of TBAC as a cocatalyst was investigated. In this case the homopolymerization process of the CHO is not observed as evidenced by the presence of the unaltered signals of the initial species. Thus the addition of an external nucleophile, deriving from the cocatalyst, inhibits the opening of the CHO ring and therefore its homopolymerization.² After the subsequent addition of CO₂ (by gurgling the gas at one atmosphere in the CD₂Cl₂ solution) the appearance of new signals was observed in the ¹H NMR spectrum (see Figure 2.5).

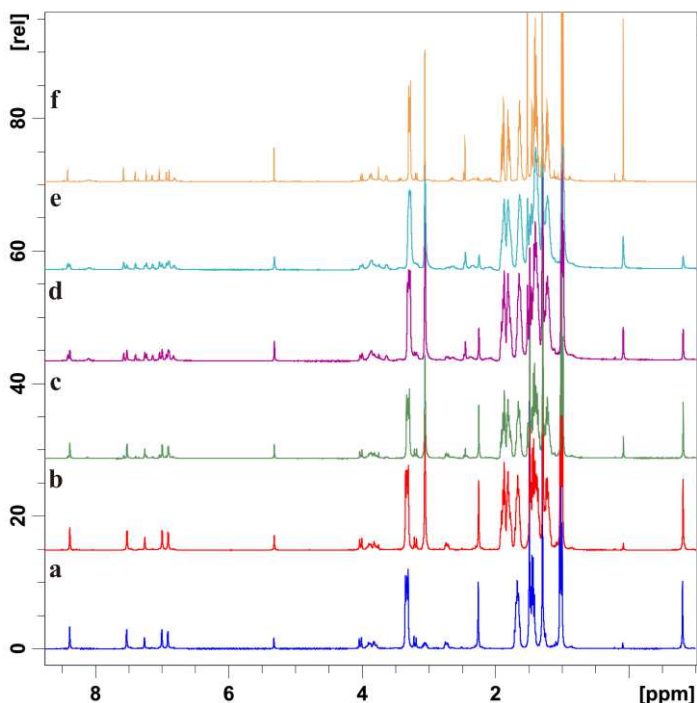


Figure 2.5. ^1H NMR spectra (600 MHz, CD_2Cl_2 , 298K) of the reaction mixture constituted by: a) complex **1** + TBACl; b) after the addition of CHO; c) after the addition of CO_2 ; d) after 2 days; e) after 4 days; f) after 8 days.

In the aromatic region of the spectrum (see Figure 2.6) close to the five peaks of the starting complex, ten new peaks of equal intensity were observed. These new signals suggested either the formation of a bimetallic intermediate (involving two ligands in different surroundings) or the formation of equimolar amount of two different species (A and B).

It is important to underline that if the CO_2 was not occasionally gurgled in the reaction mixture, the reaction did not evolve towards the formation of the products. In 8 days, and after further additions of CO_2 , the reaction came to completion, as the signals of the

starting complex disappeared completely. The reaction was carried out twice using different amounts of complex **1** and in both cases led to the formation of the same products, demonstrating the reproducibility of the experiment.

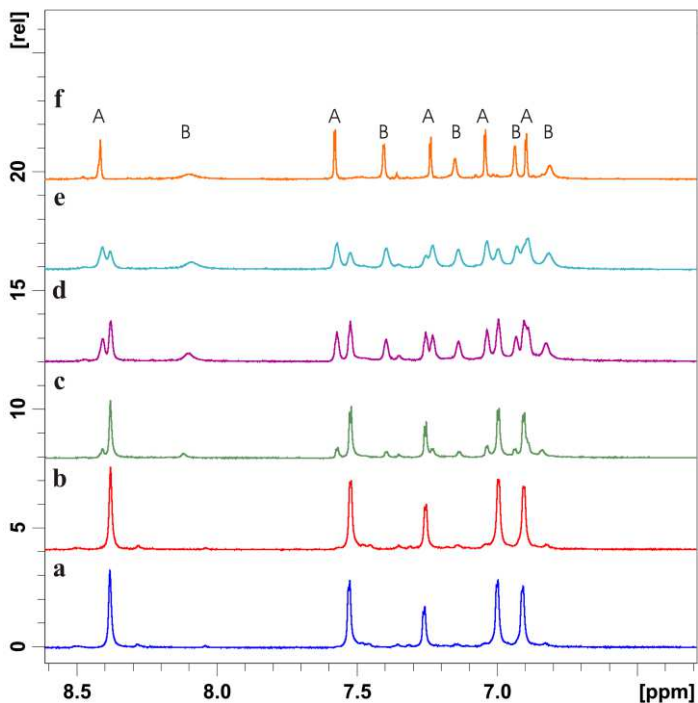


Figure 2.6. ^1H NMR aromatic region of the reaction mixture detailed in the caption of figure 2.4.

To obtain more indications about the product of this reaction, a DOSY NMR experiment was conducted. This experiment provides the diffusion coefficients of molecules in relation to the hydrodynamic radius and molecular weight, so it can give information on the number of species present in the reaction

mixture. In our case the aromatic region of the DOSY spectrum (Figure 2.7) showed the presence of two series of peaks corresponding to different diffusion coefficients, and therefore belonging to different species.

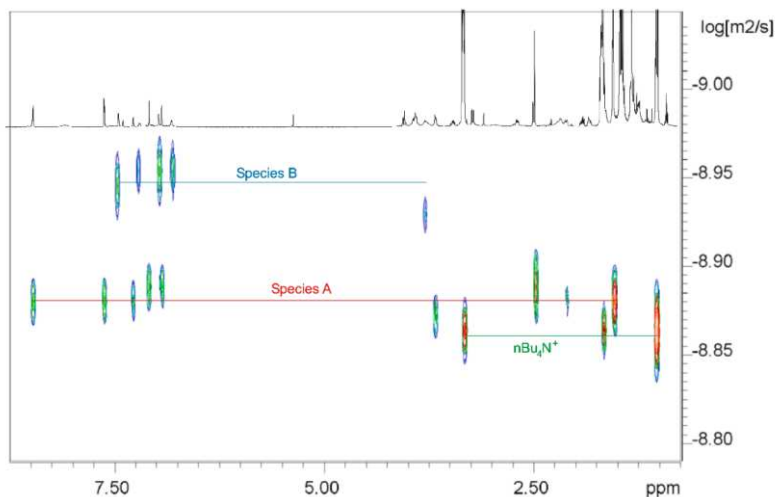


Figure 2.7. ^1H DOSY spectrum (600 MHz, CD_2Cl_2 , 298K) of the reaction mixture containing species A and species B.

Subsequent experiments showed that the ratio between A and B resulted dependent on the reaction conditions, i.e. the reaction temperature and the amount of CHO. In particular, working at 40 °C (or even at 60 °C) and in the presence of 10 equivalents of CHO, only the formation of species A was obtained. Species A were completely characterized by ^1H , ^{13}C , HSQC and NOESY NMR spectroscopy (see Figures 2.8, 2.9, 2.20 and 2.21). In the ^{13}C NMR spectrum five signals attributable to the open epoxide were observed: two of which at 74.58 and 70.57 ppm attributable to CH

carbons and three signals at 37.79, 36.11 and 26.27 ppm attributable to CH₂ carbons (see Figure 2.8). The missing signal for one of the methylene carbon may be reasonably overlapped with other signals in the aliphatic region of the spectrum.

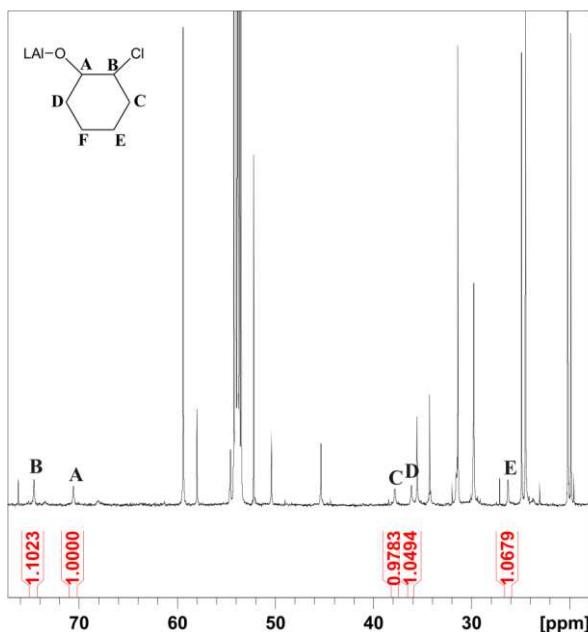


Figure 2.8. Aliphatic region of the ¹³C NMR spectrum (150.9 MHz, CD₂Cl₂, 298K) of the species A. Signals of the opened cyclohexene oxide are denoted by capital letters.

The HSQC spectrum allowed us to individuate some of the corresponding signals in the ¹H NMR spectrum (Figure 2.20 in the Experimental Section).

The described results combined with literature data allowed us to formulate the hypothesis depicted in figure 2.9 for the structure of species A consisting of the salalen ligand wrapped around an

aluminum centre which also bound an open CHO molecule. Moreover, all the signals of the ^1H NMR spectrum of the ligand skeleton in the structure of species A have been attributed, thanks to the 2D COSY (Figure 2.21 in the Experimental Section) and NOESY NMR spectra (Figure 2.21 in the Experimental Section).

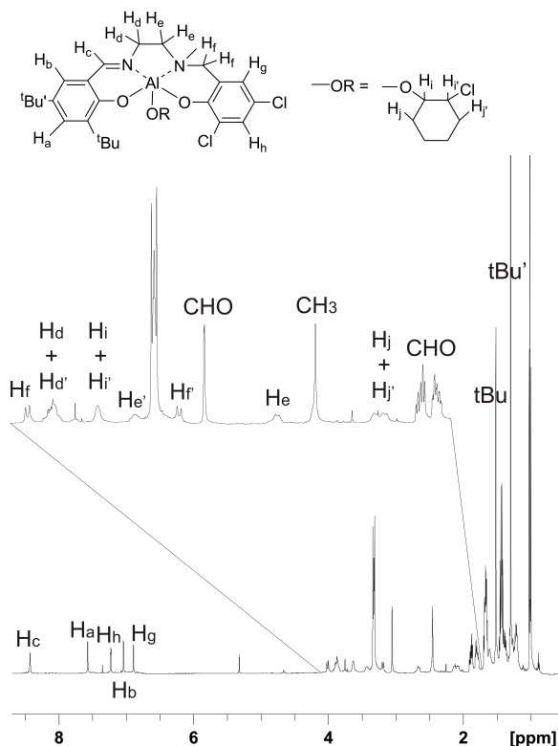


Figure 2.9. ^1H NMR spectrum and hypothesized structure of species A.

It was interesting to note that continuing the bubbling of CO_2 in a solution containing species A, an increasing amount of CHC was observed by ^1H NMR (see figure 2.10).

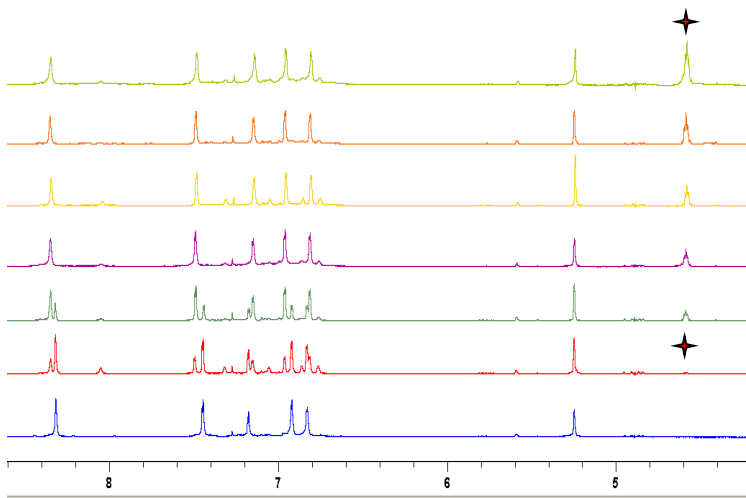


Figure 2.10. ^1H NMR spectra (600 MHz, CD_2Cl_2 , 298K) of the reaction mixture containing complex **1**, TBAC and 10 equivalents of CHO. After the complete formation of species A the bubbling of CO_2 in the solution produced an increasing amount of *cis*-cyclohexencarbonate, as can be appreciated by looking to the signal at 4.64 ppm (indicated with \star)

All these results indicate that species A is an intermediate in the catalytic cycle. Finally, a control experiment was conducted to confirm this hypothesis. Before species A was prepared in the NMR J Young tube by mixing complex **1**, 1 equiv of TBAC and 10 equivalents of CHO in the CD_2Cl_2 solution. Then it was used in the autoclave reactor working at 80 ° C and 30 bar and by adding other 7 equivalents of TBAC. The same CO_2/CHO coupling reaction was performed using complex **1** under the same reaction conditions (see entry 2 Table 2.5). Excitingly, *cis*-CHC was the exclusive product in both experiments and very similar conversions were obtained.

Table 2.5. CO₂/CHO reaction promoted by Species A and complex **1**.^[a]

Entry ^[a]	Cat	P _{CO2}	Temperature (°C)	Con (%)
1	Species A	30	80	62
2	Complex 1	30	80	54

^[a] **General conditions:** cat = 45.3 μmol, CH₂Cl₂ = 1.0 mL, TBAC = 8 equiv, CHO = 5 mL, time = 20 h.

Regarding species B, not much information has been collected, since, as can be seen from the aliphatic ¹H NMR spectrum region, the signals related to this species are broad (see for example, broad signals at 3.75 and 2.17 ppm in the ¹H NMR spectrum, related to signals at 59.9, 51.5 and 45.0 ppm in the ¹³C NMR spectrum, by means of HSQC spectrum, reported in Figures 2.17, 2.18 and 2.20 in the Experimental Section. For this reason, it was not possible to assign all the signals belonging to species B and therefore it was not possible to hypothesize a structure for this species.

On the other hand, it is important to note that the formation of species B was not observed when the experiments were conducted at temperatures above RT and in the presence of an excess of CHO, both conditions used to conduct the reactions in the autoclave reactor. This allowed us to hypothesize that species B is not an intermediate of the catalytic cycle.

Thanks to the collected results, it was possible to propose the mechanism described in Figure 2.11 where the species A is one of the intermediate in the catalytic cycle and is formed by the S_N2 attack of the chloride to the cyclohexene oxide coordinated to the aluminum. After the introduction of CO_2 into the Al-O bond of species A, the reaction continues with the S_N2 attack of the oxygen of the carbonate group to the carbon bearing the chloride, thus providing the *cis*-cyclohexene carbonate and the free chloride.

Reasonably, in the presence of one equivalent of cocatalyst (such as in the NMR tube experiments) the reaction follows pathway 1, whereas in the autoclave reactor, where an excess of cocatalyst is present, the ring closing reaction may take place after the displacement of the carbonate ion promoted by the excess of chloride (pathway 2). In both cases the double S_N2 attack preserves the original configuration of the cyclohexene oxide allowing the formation of *cis*-cyclohexene carbonate.^{5,25}

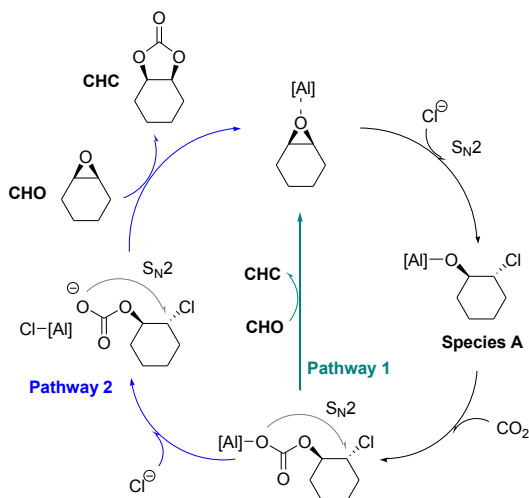


Figure 2.11. Proposed mechanism for the formation of *cis*-cyclohexene carbonate promoted by complex 1/TBAC.

2.3. Conclusions

In summary, salalen aluminum complexes were found to be active in the CO₂/epoxide cycloaddition reaction. The effect of the reaction conditions on the productivity and selectivity of the catalytic systems was evaluated. Under the optimized reaction conditions, *cis*-cyclohexene carbonate (CHC) was obtained as the exclusive product with good TON values (from 106 to 1290) even operating at 2 bar of CO₂, in the presence of an ammonium salt as cocatalyst. Furthermore, terminal epoxides with several functional groups were easily transformed by complex 1 under mild conditions and at a low catalyst loading. The effect of the substituents of the ligand skeleton on the activity of the catalyst was evaluated: the presence of electron withdrawing substituents increased the activity.

Comparative studies of salen, salan and salalen aluminum complexes bearing the same substitution pattern on the different ligands indicated that the salen aluminum complex was the most active in the CHO/CO₂ reaction. Finally, NMR analysis of reaction mixtures prepared in J-Young tube allowed us to shed light on the reaction mechanism. Interestingly, an intermediate species of the catalytic cycle was individuated and characterized by NMR spectroscopy. A control experiment showed that this species was catalytically active allowing us to propose a catalytic cycle for the formation of *cis*-cyclohexene carbonate promoted by this class of salalen aluminum complexes.

2.4. Experimental Section

2.4.1 General considerations

All manipulations of air- and/or water-sensitive compounds were performed under a dry N₂ atmosphere by using a Braun Labmaster glovebox or standard Schlenk techniques. The glassware and autoclave used in the polymerization were dried in an oven at 120°C overnight. Benzene and hexane were distilled over sodium benzophenone. Dichloromethane, cyclohexene oxide, and propylene oxide were distilled over calcium hydride. CD₂Cl₂ and C₆D₆ were dried with molecular sieves. All other chemicals were commercially available and used as received unless otherwise stated. Elemental analyses were performed by using a Flash EA 1112 elemental analyzer (THERMO).

2.4.2. Synthesis of Salalen Ligands

The ligands were prepared according to published procedures^{16, 17} which involves the reaction of condensation of N-methyl-1,2-diaminoethane with a substituted salicylaldehyde followed by nucleophilic substitution on a substituted bromomethylphenol. The identity of the compounds was determined by ¹H NMR.

2.4.3. Synthesis and Characterization of Salalen Aluminum Complexes (1-5)

Complex 1

The synthesis was carried out in a glove-box under a nitrogen atmosphere. In a 20 mL vial with a magnetic stirrer bar, 31.9 mg ($4.30 \cdot 10^{-4}$ mol) of AlMe_3 (97% wt) were dissolved in 2 mL of dry benzene. In a 5 mL vial, 200 mg ($4.30 \cdot 10^{-4}$ mol) of H_2L_1 were dissolved in 2 mL of dry benzene. The ligand solution was added dropwise in the solution containing AlMe_3 , and other 0.5 mL of dry benzene were used to wash the vial containing the ligand. The resulting mixture was stirred at room temperature for 2 hours. The solvent was then removed under vacuum and the solid residue was washed with pentane. Complex **1** was obtained as a yellow powder. Yield: 96%. Elemental analysis, calculated for $\text{C}_{26}\text{H}_{35}\text{AlCl}_2\text{N}_2\text{O}_2$ (%): C, 61.78; H, 6.98; N, 5.54. Found: C, 61.69; H, 6.95; N, 5.56.

^1H NMR (400 MHz, C_6D_6 , 298 K): δ -0.42 (s, 3H, Al-CH₃), 1.37 (s, 9H, CCH₃), 1.58 (s, 3H, NCH₃), 1.81 (s, 9H, CCH₃), 2.01 (m, 1H, CH₂), 2.35 (d, J = 12.80 Hz, 1H, CH₂), 2.53 (m, 1H, CH₂), 3.13 (d, J = 12.80 Hz, 1H, CH₂), 6.67 (d, J = 2.40 Hz, 1H, Ar-H), 6.77 (d, J = 2.40 Hz, 1H, Ar-H), 7.27 (s, 1H, C=N), 7.43 (d, J = 2.65 Hz, 1H, Ar-H), 7.75 (d, J = 2.40 Hz, 1H, Ar-H)

^{13}C NMR (250 MHz, C_6D_6 , 298 K): δ -9.15 (AlCH₃), 29.90 (CCH₃)₃, 31.62 (CCH₃)₃, 34.19 (CCH₃)₃, 35.74 (CCH₃)₃, 43.91 (N-CH₃), 50.96 (CH₂), 54.29 (CH₂), 57.80 (CH₂), 117.58 (Cq), 120.59 (Cq), 125.32 (Cq), 125.73 (Cq), 127.43 (2 CH), 129.81 (CH), 132.15 (CH), 137.47 (Cq), 141.61 (Cq), 155.33 (Cq), 165.59 (Cq), 173.52 (CH=N).

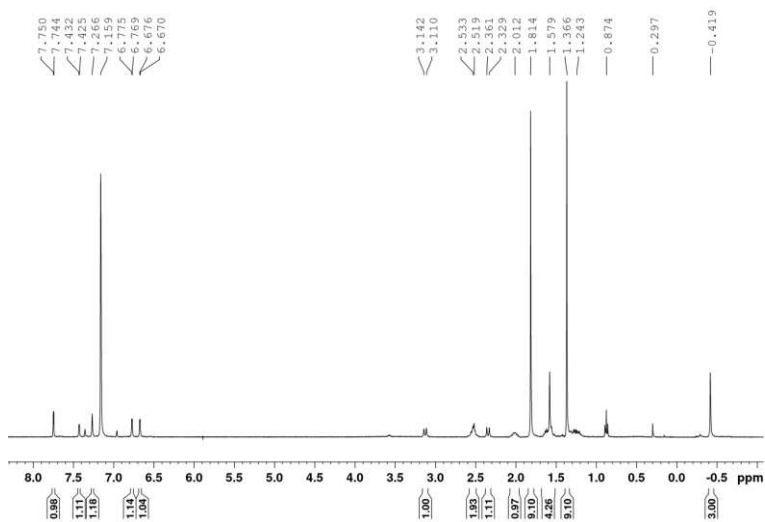


Figure 2.12. ¹H NMR spectrum (400 MHz, C₆D₆, 298K) of complex 1.

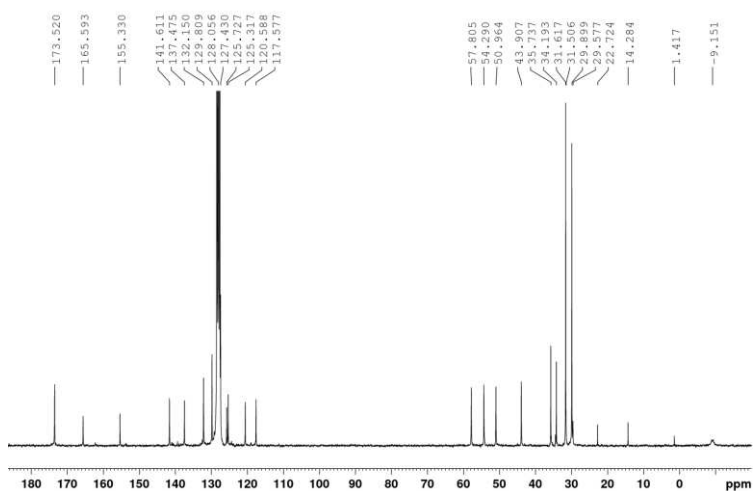


Figure 2.13. ¹³C NMR spectrum (62.9 MHz, C₆D₆, 298K) of complex 1.

Complex 2

The same procedure used for complex **1** was followed by using 215 μL ($2.15 \cdot 10^{-4}$ mol) of Me_2AlCl (1M solution in Hexane) and 100 mg ($2.15 \cdot 10^{-4}$ mol) of H_2L_1 . Complex **2** was obtained as a yellow powder in 89% yield. Elemental analysis, calculated for $\text{C}_{25}\text{H}_{32}\text{AlCl}_3\text{N}_2\text{O}_2$ (%): C, 57.10; H, 6.13; N, 5.33; Found: C, 57.17; H, 6.11; N, 5.39.

^1H NMR (400 MHz, C_6D_6 , 298 K): δ 1.35 (s, 9H, CCH_3), 1.60(m, 1H, CH_2), 1.82 (s, 9H, CCH_3), 1.87 (s, 3H, N-CH_3), 2.25 (m, 1H, CH_2), 2.46 (m, 3H, CH_2), 3.05 (d, $J = 13.20$ Hz, 1H, CH_2), 6.60 (d, $J = 2.80$ Hz, 1H, Ar-H), 6.74 (d, $J = 2.40$ Hz, 1H, Ar-H), 7.20 (s, 1H, C=N), 7.40 (, $J = 2.40$ Hz, 1H, Ar-H), 7.77 (d, $J = 2.40$ Hz, 1H, Ar-H).

^{13}C NMR (300 MHz, C_6D_6 , 298 K): δ 29.86 (CCH_3)₃, 31.54 (CCH_3)₃, 34.22 (CCH_3)₃, 35.79 (CCH_3)₃, 45.00 (N-CH_3), 49.41 (CH_2), 53.83 (CH_2), 57.66 (CH_2), 117.53 (Cq), 121.47 (Cq), 123.76 (Cq), 125.71 (Cq), 127.04 (CH), 127.23 (CH), 130.14 (CH), 132.96 (CH), 138.47 (Cq), 142.23 (Cq), 154.39 (Cq), 165.32 (Cq), 174.43 (CH=N).

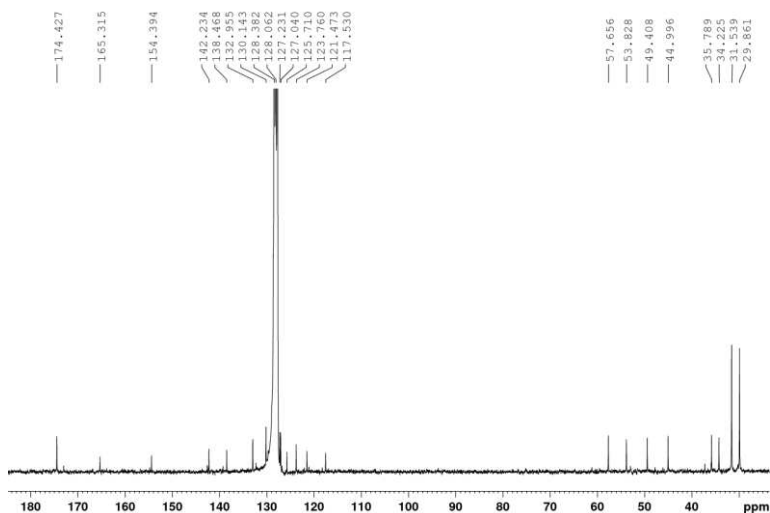


Figure 2.14. ^{13}C NMR spectrum (75.4 MHz, C_6D_6 , 298K) of complex **2**.

Complex 3

The same procedure used for complex **1** was followed by using 32.6 mg ($4.381 \cdot 10^{-4}$ mol) of AlMe_3 (97% wt) and 203.9 mg ($4.381 \cdot 10^{-4}$ mol) of H_2L_2 . Complex **2** was obtained as a yellow powder in 85% yield. The ^1H NMR spectrum was in agreement with the spectrum reported in the literature.^{15,17}

Complex 4

The synthesis was carried out in a glove-box under a nitrogen atmosphere. In a 20 mL vial with a magnetic stirrer bar, 22.6 mg ($3.04 \cdot 10^{-4}$ mol) of AlMe_3 (97% wt) were dissolved in 2 mL of dry toluene. In a 5 mL vial, 155.9 mg ($3.04 \cdot 10^{-4}$ mol) of H_2L_3 were dissolved in 2 mL of dry toluene. The ligand solution was dropped in the solution containing AlMe_3 and other 0.5 mL of dry toluene

were used to wash the vial containing the ligand. The resulting mixture was stirred at 110°C overnight. After cooling to room temperature, the solvent was removed under vacuum and the solid residue was washed with hexane. Complex **4** was obtained as a yellow powder. Yield: 78%. The ^1H NMR spectrum was in agreement with the spectrum reported in the literature.¹⁷

Complex 5

The same procedure used for complex **1** was followed by using 400 μL ($4.00 \cdot 10^{-4}$ mol) of Me_2AlCl (1 M solution in Hexane) and 203.5 mg ($4.00 \cdot 10^{-4}$ mol) of H_2L_3 . Complex **5** was obtained as a yellow powder in 86% yield. Elemental analysis, calculated for $\text{C}_{33}\text{H}_{50}\text{AlClIN}_2\text{O}_2$ (%): C, 69.63; H, 8.85; N, 4.92. Found: C, 69.71; H, 8.82; N, 4.96.

^1H NMR (400 MHz, C_6D_6 , 298 K): δ 1.36 (s, 9H, CCH_3), 1.47 (s, 9H, CCH_3), 1.76 (m, 1H, CH_2), 1.86 (d, $J = 10.46$ Hz, 18H, CCH_3), 2.07 (s, 3H, N-CH_3), 2.37 (m, 2H, CH_2), 2.68 (m, 1H, CH_2), 2.83 (m, 1H, CH_2), 3.68 (d, $J = 12.80$ Hz, 1H, CH_2), 6.78 (d, $J = 2.40$ Hz, 1H, Ar-H), 6.91 (d, $J = 2.40$ Hz, 1H, Ar-H), 7.26 (s, 1H, C=N), 7.66 (d, $J = 2.40$ Hz, 1H, Ar-H), 7.80 (d, $J = 2.40$ Hz, 1H, Ar-H).

^{13}C NMR (300 MHz, C_6D_6 , 298 K): δ 30.26 (CCH_3), 30.35 (CCH_3), 31.56 (CCH_3), 32.18 (CCH_3), 34.18 (CCH_3), 34.38 (CCH_3), 35.81 (CCH_3), 35.88 (CCH_3), 45.39 (N-CH_3), 50.82 (CH_2), 54.85 (CH_2), 59.10 (CH_2), 117.82 (Cq), 121.64 (Cq), 123.70 (CH), 124.33 (CH), 128.59 (CH), 132.66 (CH), 138.08 (Cq), 138.89 (Cq), 139.33 (Cq), 142.06 (Cq), 155.92 (Cq), 165.59 (Cq), 174.09 (CH=N).

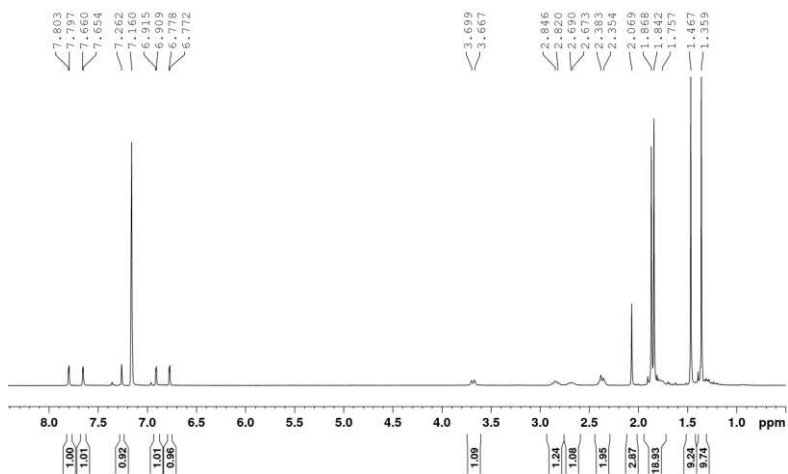


Figure 2.15. ¹H NMR spectrum (400 MHz, C₆D₆, 298K) of complex **5**.

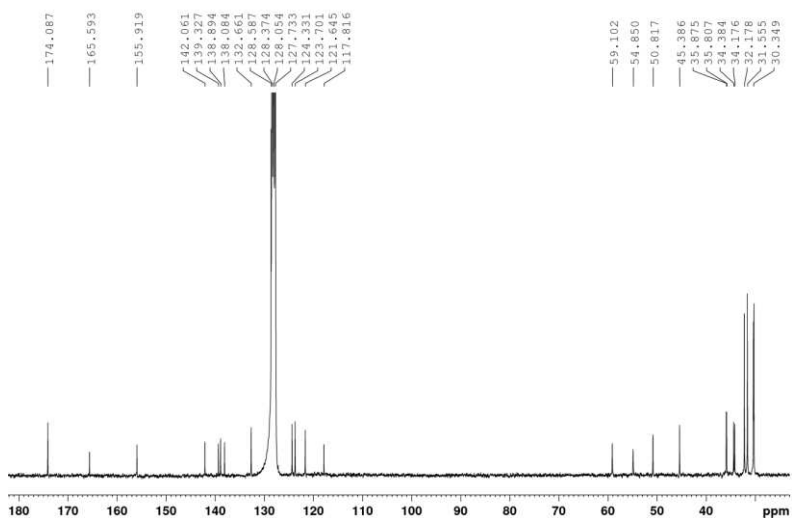


Figure 2.16. ¹³C NMR spectrum (75.4 MHz, C₆D₆, 298K) of complex **5**.

2.4.4. Synthesis of Salen and Salan Aluminum Complexes (6-8)

Complex 6

The synthesis was carried out in a glove-box under a nitrogen atmosphere. In a 5 mL vial, 22.6 mg ($3.04 \cdot 10^{-4}$ mol) of AlMe_3 (97% wt) were dissolved in 2 mL of dry toluene. In a second vial, 150 mg ($3.04 \cdot 10^{-4}$ mol) of H_2L_4 were dissolved in 2 mL of dry toluene. The ligand solution was slowly dropped in the solution containing AlMe_3 and other 0.5 mL of dry toluene were used to wash the vial containing the ligand. The resulting mixture was transferred into a 10 mL tube with a magnetic stirrer bar and stirred at 110°C overnight. After cooling to room temperature, the solvent was removed under vacuum and the solid residue was washed with pentane. Complex **6** was obtained as a yellow powder. Yield: 76%. The ^1H NMR spectrum was in agreement with the spectrum reported in the literature.²⁰

Complex 7

Complex **7** was prepared in a glove-box under a nitrogen atmosphere. In a 10 mL tube with a magnetic stirrer bar, 457 μL ($4.57 \cdot 10^{-4}$ mol) of Me_2AlCl (1M solution in Hexane) were dissolved in 2 mL of dry toluene. In a second tube, 200 mg ($4.06 \cdot 10^{-4}$ mol) of H_2L_4 were dissolved in 2 mL of dry toluene. Then both solutions were cooled at -78°C . The solution of aluminum precursor was slowly dropped in the solution containing the ligand. The resulting mixture was gradually warmed to 25°C over 2 h and stirred for an additional 10 h. After the solvent was removed under vacuum and the solid residue was washed with pentane. Complex **7** was

obtained as a yellow powder. Yield: 80%. The ^1H NMR spectrum was in agreement with the spectrum reported in the literature.²⁴


Complex 8

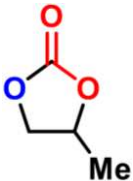
The synthesis was carried out in a glove-box under a nitrogen atmosphere. In a 5 mL vial, 42.5 mg ($5.72 \cdot 10^{-4}$ mol) of AlMe_3 (97% wt) were dissolved in 2 mL of dry toluene. In a second vial, 300 mg ($5.72 \cdot 10^{-4}$ mol) of H_2L_5 were dissolved in 2 mL of dry toluene. The ligand solution was slowly dropped in the solution containing AlMe_3 and other 0.5 mL of dry toluene were used to wash the vial containing the ligand. The resulting mixture was transferred into a 10 mL tube with a magnetic stirrer bar and stirred at 110°C overnight. After cooling to room temperature, the solvent was removed under vacuum and the solid residue was washed with pentane. Complex **8** was obtained as a white powder. Yield: 68%. The ^1H NMR spectrum was in agreement with the spectrum reported in the literature.²¹

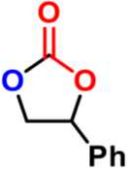
2.4.5. CO_2/CHO reaction procedure


A representative procedure for the CO_2/CHO reaction is described as follows. The reaction was carried out using $\text{CHO}/\text{complex } 1=1200$ and $\text{TBAB}/\text{complex}=8$. In a glove-box, complex **1** (21.3 mg, $4.21 \cdot 10^{-5}$ mol) was dissolved in 0.1 mL of CH_2Cl_2 in a 2 mL vial, in a second vial TBAB (108.6 mg, $3.371 \cdot 10^{-4}$ mol) was dissolved in 0.2 mL of CH_2Cl_2 . Both solutions were transferred into a 20 mL vial. Then, CHO (5 mL) was added to the vial. The mixture was charged into the autoclave. The autoclave was pressurized to the appropriate pressure of CO_2 , whilst the reaction mixture was stirring

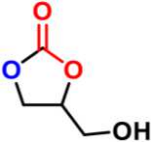
for 20 minutes at room temperature, in order to facilitate CO₂ dissolution. The reaction mixture was stirred at the desired temperature. After the prescribed time, the reaction was quenched by dipping the autoclave in an ice bath, opened at air and adding 0.5 mL of CH₂Cl₂. The product was analyzed by ¹H NMR spectroscopy.

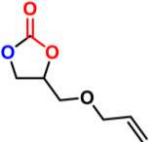
	<p>Cis-Cyclohexene carbonate: ¹H NMR (600 MHz, CDCl₃): δ 1.43 (m, 2H, CH₂), 1.63 (m, 2H, CH₂), 1.90 (m, 4H, 2 x CH₂), 4.68 (m, 2H, 2 x CH).</p>
---	---

	<p>Propylene carbonate: ¹H NMR (300 MHz, CDCl₃): δ 1.49 (d, J= 6.30 Hz, 3H, CH₃), 4.02 (t, J= 8.40 Hz, 1H, CH₂), 4.55 (t, J= 8.40 Hz, 1H, CH₂), 4.84 (m, 1H, CH).</p>
--	---

	<p>Styrene carbonate: Purification by flash column chromatography with n-hexane/EtOAc (8:2).</p> <p>^1H NMR (300 MHz, CDCl_3): δ 4.35 (t, J= 8.00 Hz, 1H, CH_2), 4.80 (t, J= 8.20 Hz, 1H, CH_2), 5.68 (t, J= 8.00 Hz, 1H, CH_2), 7.41 (m, 5H, Ph).</p>
---	--

	<p>3-Chloropropylene carbonate: Purification by flash column chromatography with nhexane/ EtOAc (6:4).</p> <p>^1H NMR (400 MHz, CDCl_3): δ 3.76 (m, 2H, CH_2Cl), 4.41 (m, 1H, CH_2), 4.59 (t, J= 8.46 Hz, 1H, CH_2), 4.96 (m, 1H, OCH).</p>
---	--

	<p>Glycerol carbonate: Purification by flash column chromatography with n-hexane/EtOAc (6:4).</p> <p>^1H NMR (300 MHz, CDCl_3): δ 3.73 (dd, J= 12.59, 3.54 Hz, 1H, CHOH), 4.01 (dd, J= 12.73, 4.00 Hz, 1H, CHOH), 4.47 (t, 2H, CH_2), 4.81 (m, 1H, CH).</p>
---	--

	<p>4-((allyloxy)methyl)-1,3-dioxolan-2-one:</p> <p>Purification by flash column chromatography with nhexane/ EtOAc (6:4).</p> <p>^1H NMR (250MHz, CDCl_3): δ 3.66 (m, 2H, CH_2), 4.06 (d, J= 5.62 Hz, 2H, CH_2), 4.46 (m, 2H, CH_2), 4.82 (m, 1H, CH), 5.27 (m, 2H, $\text{CH}=\text{CH}_2$), 5.88 (m, 1H, $\text{CH}=\text{CH}_2$).</p>
---	--

2.4.6. NMR mechanistic studies of the CO₂/CHO reaction promoted by complex 1.

The reaction mixtures were prepared in a glove-box under a nitrogen atmosphere and transferred in J-Young tubes for NMR analysis. A typical experiment was carried out as follows. In a 2 mL vial, 20 mg ($3.96 \cdot 10^{-5}$ mol) of complex 1 were dissolved in 0.4 mL di CD₂Cl₂. In another vial 11 mg ($3.96 \cdot 10^{-5}$ mol) of TBAC were dissolved in 0.6 mL CD₂Cl₂. Both solutions were transferred into a J-Young NMR tube into which was introduced the desired equivalents of CHO. A 100 mL Schlenk flask, equipped with rubber septa, was exposed to several vacuum/CO₂ cycles, afterwards the flask was filled with CO₂. 20 mL of CO₂ were bubbled into the reaction mixture by syringe equipped with a metal needle. In the NMR tube was introduced a magnetic stirrer bar and the reaction mixture was stirred at the desired temperature. The reaction was followed by ¹H NMR spectroscopy, bubbling the CO₂ in the solution after each NMR analysis till the reaction went to completion.

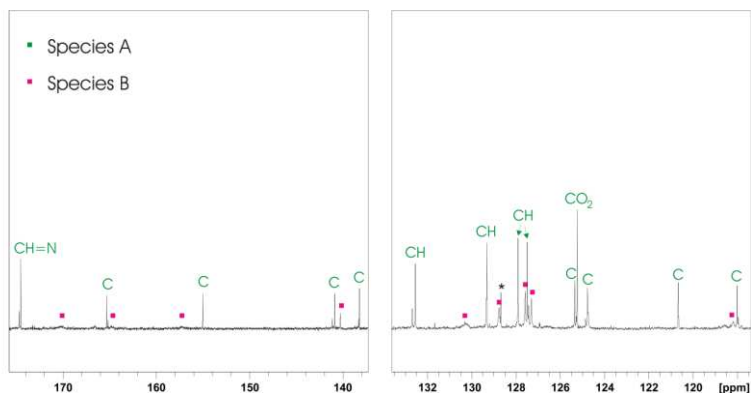


Figure 2.17. Aromatic region of the ¹³C NMR spectrum (150.9 MHz, CD₂Cl₂, 298K) of the reaction mixture containing species A and species B. The black star denotes the peak of the dissolved CO₂.

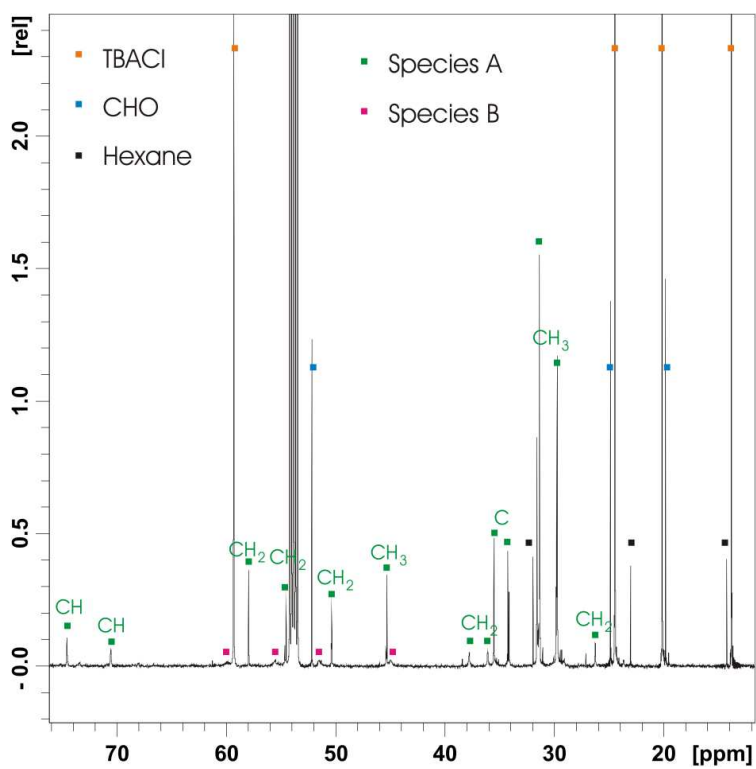
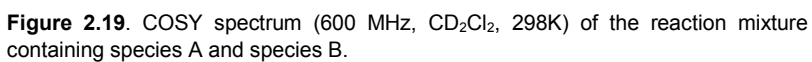


Figure 2.18. Aliphatic region of the ^{13}C NMR spectrum (150.9 MHz, CD_2Cl_2 , 298K) of the reaction mixture containing species A and species B.



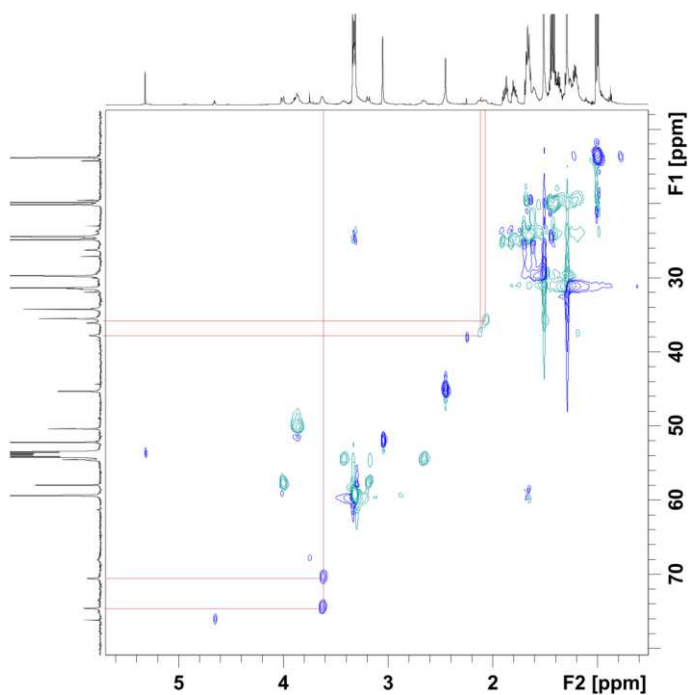


Figure 2.20. Aliphatic region of the HSQC NMR spectrum (600 MHz, CD₂Cl₂, 298K) of the species A. Cross peaks of the opened cyclohexene oxide are linked by red lines.

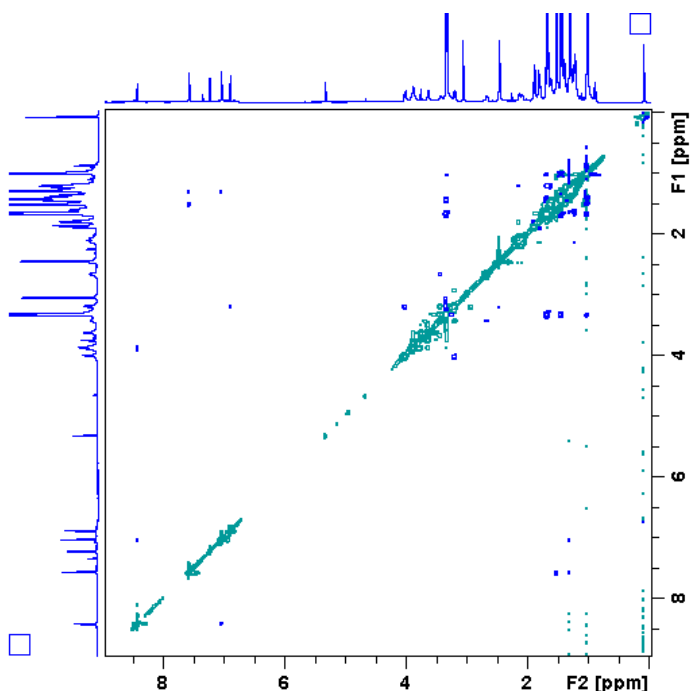


Figure 2.21. ¹H NOESY NMR spectrum (600 MHz, CD₂Cl₂, 298K) of the species A.

References

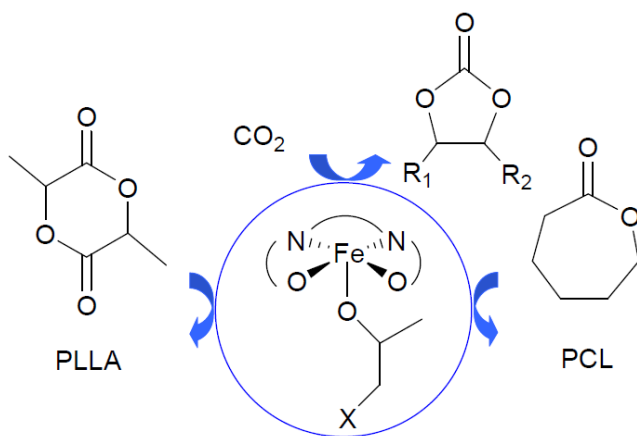
- 1 M. Aresta, A. Dibenedetto, A. Angelini, *Chem. Rev.* **2014**, 114, 1709–1742
- 2 M. Taherimehr, P. P. Pescarmona, *J. Appl. Polym. Sci.* **2014**, 121, 41141–41158.
- 3 M. North, R. Pasquale, C. Young, *Green Chem.* **2010**, 12, 1514–1539.
- 4 J. W. Comerford, I. D. V. Ingram, M. North, X. Wu, *Green Chem.* **2015**, 17, 1966–1987.
- 5 C. Martín, G. Fiorani, A. W. Kleij, *ACS Catal.* **2015**, 5, 1353–1370.
- 6 C. Beattie, M. North, P. Villuendas, C. Young, *J. Org. Chem.* **2013**, 78, 419–426.
- 7 J. Rintjema, R. Epping, G. Fiorani, E. Martín, E. C. Escudero-Adán, A. W. Kleij, *Angew. Chem., Int. Ed.* **2016**, 55, 3972–3976.
- 8 T. Aida, S. Inoue, *J. Am. Chem. Soc.* **1983**, 105, 1304–1309.
- 9 Qin, H. Guo, X. Sheng, X. Wang, F. Wang, *Green Chem.* **2015**, 17, 2853–2858.
- 10 K. Kasuga, T. Kato, N. Kabata, M. Handa, *Bull. Chem. Soc. Jpn.* **1996**, 69, 2885–2888.
- 11 X.–B. Lu, Y.–J. Zhang, K. Jin, L.–M. Luo, H. Wang, *J. Catal.* **2004**, 227, 537–541.
- 12 M. North, C. Young, *Catal. Sci. Technol.* **2011**, 1, 93–99.
- 13 J. A. Castro–Osma, C. Alonso–Moreno, A. Lara–Sánchez, J. Martínez, M. North, A. Otero, *Catal. Sci. Technol.* **2014**, 4, 1647–1684.
- 14 S. H. Kim, D. Ahn, M. J. Go, M. H. Park, M. Kim, J. Lee, Y. Kim, *Organometallics* **2014**, 33, 2770–2775.
- 15 M. Cozzolino, K. Press, M. Mazzeo, M. Lamberti, *ChemCatChem* **2016**, 8, 455–460.
- 16 A. Pilone, N. De Maio, K. Press, V. Venditto, D. Pappalardo, M. Mazzeo, C. Pellecchia, M. Kol, M. Lamberti, *Dalton Trans.* **2015**, 44, 2157–2165.

-
- 17 E. L. Whitelaw, G. Loraine, M. F. Mahon, M. D. Jones, *Dalton Trans.* **2011**, 40, 11469-11473.
- 18 A. W. Addison, T. N. Rao, J. Reedijk, J. van Rijn, G. C. Verschoor, *Dalton Trans.* **1984**, 1349– 1356.
- 19 D. J. Darensbourg, D. R. Billodeaux, *Inorg. Chem.* **2005**, 44, 1433 – 1442.
- 20 P. Hormnirun, E. L. Marshall, V. C. Gibson, R. I. Pugh, A. J. P. White, *PNAS* **2006**, 103, 15343–15348.
- 21 P. Hormnirun, E. L. Marshall, V. C. Gibson, A. J. P. White, D. J. Williams, *J. Am. Chem. Soc.* **2004**, 126, 2688-2689.
- 22 N. Ikpo, J. C. Flogeras, F. M. Kerton, *Dalton Trans.* **2013**, 42, 8998– 9006.
- 23 A. Decortes, A. M. Castilla, A. W. Kleij, *Angew. Chem.* **2010**, 10016-10032.
- 24 D. Rutherford, D. A. Atwood, *Organometallics* **1996**, 15, 4417-4422.
- 25 G. A. Luinstra, G. R. Haas, F. Molnar, V. Bernhart, R. Eberhardt, B. Rieger, *Chem. Eur. J.* **2005**, 11, 6298-6314.

CHAPTER 3

“Salen like” Iron (III) Complexes as Catalysts for CO₂/Epoxides Reactions and ROP of Cyclic Esters

In chapter 3 we describe the synthesis of iron (III) complexes bearing salen, salan and salalen ligands with the same substituents on the aromatic rings. All the complexes were employed in the coupling reaction of CO₂ with reference epoxide substrates (PO, SO, CHO) and in the ring-opening polymerization of L-lactide and ϵ -caprolactone. In particular, we evaluated how the nature of nitrogen atoms, (amine and / or imino) influences their activity in these reactions. By comparing their behavior we identified an order of reactivity of the different classes of complexes.



3.1. Introduction

3.1.1. Iron-based catalysts for CO₂/epoxide reactions and ROP of cyclic esters

Iron complexes are a promising class of catalysts thanks to the nearly unlimited supply of iron and its biocompatibility. Moreover in the literature, there are some recent examples of iron complexes that have shown exceptional catalytic activity in the reaction of CO₂ with epoxides or in the ROP of cyclic esters.¹ The dinuclear iron complex based on Robson-type ligand reported by Williams *et al.* was one of the most active iron complexes for the synthesis of cyclic carbonates (in the presence of 1 equivalent of PPNCI as cocatalyst) or polycarbonates (in the absence of the cocatalyst), even under mild reaction conditions (1 atm pressure of CO₂).² Monometallic and dimetallic iron (III) complexes chelated with amino-triphenolate ligands reported by Kleij and collaborators were able to promote the reaction of CO₂ with CHO. In particular, working in the presence of 10 equivalents of PPNCI these systems produced *cis*-CHC as the exclusive product, while in the presence of 1 equivalent of the cocatalyst, they converted CHO into PCHC.^{3,4,5} Recently, Capacchione *et al.* reported bimetallic iron(III) thioether-triphenolate complexes, as highly active catalysts for synthesis of cyclic carbonates with TON value up to 3480, in only 6 h.^{6,7} Moreover, iron complexes with different ancillary ligands active in CO₂/epoxide reactions (such as: bis-phenoxyimine^{8,9} phenoxyamine,¹⁰ iminopyridine,¹¹ bis-CNN pincer,¹² tetraamine,¹³ bis-aminepyridine¹⁴ and bis-imido¹⁵) have been described in the literature.

Iron catalysts active in the ROP of lactones and/or lactides consist predominantly in inorganic or organic iron salts, such as, oxides,¹⁶ halides,^{17,18} carboxylates,¹⁹ alkoxides,^{20,21,22} and lactate.²³ However, some examples of L_nMX_m complexes, bearing ancillary ligands, have also been reported in this catalysis (for example, L_n = benzamidinate,²⁴ iminopyridine,²⁵ β -ketimine,²⁶ NNN-pincer,²⁷ β -diminate,²⁸ calixarene²⁹ and N-heterocyclic carbene³⁰ ligands).

Complexes bearing salen ligands or its derivatives are ubiquitous in several kinds of catalysis since they are cheap, facile to synthesize, and may be easily modulated whether from a steric or an electronic point of view. Salen-based iron complexes with aromatic bridges between the two imino nitrogen donors were active in the synthesis of styrene carbonate, from the CO_2 / SO reaction.³¹

Other examples of salen based iron complexes have also been found to be active in the ROP of cyclic esters.³²

Iron complexes based on salan with a homopiperazine bridge and different substituents on the aromatic rings were synthesized by the Kerton's research group. These complexes, in combination with TBAB, showed promising activity towards the catalytic formation of cyclic carbonates. Studies conducted on these catalytic systems have shown that electronic effects play a fundamental role in catalytic activity. In particular, it was observed that electron withdrawing groups in the *ortho* and *para*-positions of the phenolate rings increased the reactivity of the catalysts.³³

Our interest in the study of salen and its derivatives aluminum complexes in the CO_2 / epoxide^{34,35} reaction led us to explore the behavior of iron complexes in this reaction. Moreover, considering that in the literature there are several examples of iron complexes

active both in the CO₂ epoxide reaction and in the ROP of cyclic esters, we decided to extend our study also to the ROP of L-lactide and ϵ -caprolactone. In this chapter we report the synthesis and the characterization of iron complexes with salen, salan and salalen ligands. The ligands present the same substituents on the phenolate rings, the same bridge, and differ only in the nature of the donor nitrogen atoms (amine and/or imino). All complexes were first tested in the reaction of CO₂ with benchmark epoxides (PO, SO, CHO) and subsequently in the ring-opening polymerization of L-lactide and ϵ -caprolactone, with the aim to compare their behaviour in catalysis.

3.1.2. Ring-Opening Polymerization of Cyclic esters.

Aliphatic polyesters are very interesting synthetic polymers because they are biodegradable and biocompatible materials.

Among the linear aliphatic polyesters, the polylactide (PLA) and the polycaprolactone (PCL) play a fundamental role, because they present excellent physical and mechanical properties which make them the best candidates for the replacement of thermoplastic polymers from petrochemical sources such as polystyrene and polyethylene. At the same time they are biodegradable and biocompatible, in fact, the degradation of their chain can be done by hydrolytic or enzymatic way, making these substances well tolerated by every living being. These characteristics are sought in the biomedical field, for the preparation of implants and for tissue engineering and in the pharmaceutical field as vectors for controlled release of drugs.^{36,37} For many years the use of these two polymers has been limited to niche or medical applications, but now it is

possible to obtain them with a greater definition of the microstructure and with better physico-chemical properties, allowing their use in the packaging and fiber industries. Moreover, these biopolymers have the advantage of deriving from bio-renewable resources. In the case of PLA, the lactic acid used to obtain the monomer is produced by the fermentation of glucose which may derive from corn or sugar beets;³⁸ while in the case of the PCL, a synthetic strategy for the preparation of the caprolactone starting from the starch has been identified.³⁸

The synthetic methods to make PLA and PCL are substantially two:

- 1) Polycondensation: it is the condensation of molecules of hydroxy-acid (lactic acid for PLA and caproic acid for PCL). The reaction proceeds by the elimination of water molecules so it requires reduced pressure and very high temperatures. The disadvantage of polycondensation is that it is a reaction of equilibrium and it is very difficult to remove residual quantities of water, thus limiting the molecular weight that can be reached in the final product. Consequently, with polycondensation only low molecular weight or intermediate molecular weight polymers can be produced, which result fragile and similar to glass, unusable because of the scarce mechanical properties.³⁹
- 2) Ring-Opening Polymerization (ROP): this type of reaction was realized for the first time by Carathes in 1932, but high molecular weight polymers were obtained when DuPont, in 1954, improved the purification techniques of the respective monomers. The process was then refined by Carfile Dow. The driving force of the reaction is the opening of the

tensioned ring of the cyclic ester. The mechanism involved in the ROP can be: cationic, anionic or coordination-insertion type, depending on the catalytic system that is used. However, the first two processes, due to their high reactivity, often meet inconveniences such as racemization and *trans*-esterification reactions. Polymers with more controlled microstructures can be obtained through ROP that occurs with coordination-insertion mechanism (Figure 3.2). In this case metal complexes of the L_nMX_m type (where L is an ancillary ligand, X is an initiator group, generally an alkoxide or amide, and M is the metal) are used as catalysts. The process involves the coordination of the monomer to the metallic center of the catalyst which acts as Lewis acid, followed by the breakdown of the carbonyl oxygen-carbon bond with consequent opening of the cycle and insertion of the monomer into the metal initiator bond (X). During propagation, the growing chain is linked to the metal through an alkoxy bond, on which propagation continues.³⁹

As it can be observed, both the catalyst type and the mechanism are very similar to those described for the CO₂/epoxide reaction.

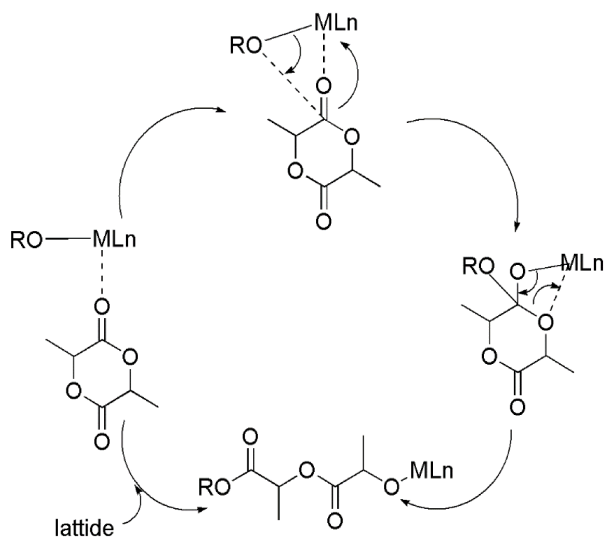


Figure 3.1. Coordination-insertion mechanism in the ROP of lactide.

3.2. Results and Discussion

3.2.1. Synthesis and characterization of ligands H₂L₁₋₄

The ligands H₂L₁₋₄ have the structures shown in figure 3.2; they have been synthesized using a synthetic procedure reported in the literature.^{40,41} The formation of the ligands H₂L₁₋₄ was verified by ¹H NMR analysis. The results of the analysis compared with the data reported in the literature confirmed the formation of the desired product and the absence of impurities.

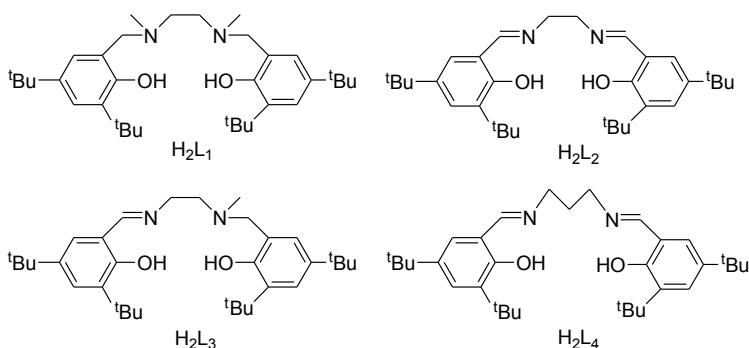


Figure 3.2. Structure of the ligands H₁L₁₋₄.

3.2.2. Synthesis of Complexes 1-4

The synthesis of the complexes **1-4** (Figure 3.3) was performed following a previously reported procedure, which involves the direct reaction between the ligand and the metal precursor, anhydrous FeCl₃, in methanol. The reaction involves the development of HCl which is neutralized using NEt₃. The mixture is taken to dryness and subsequently the extraction in an appropriate solvent, such as acetone, followed by the filtration and removal of the solvent allowed to obtain the desired paramagnetic complexes.

Complexes **1**,^{42,43} **2**^{32,44,45} and **4**³² have been previously reported in the literature while complex **3** is a new species.

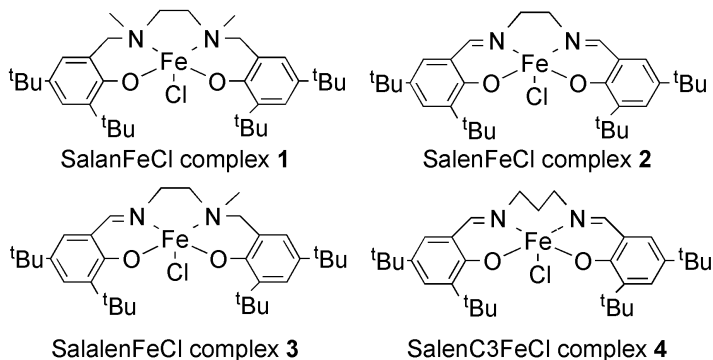


Figure 3.3. Structure of the complexes **1-4**

3.2.3. Characterization of Complexes **1-4**

The monometallic complexes were analyzed using MALDI-ToF mass spectrometry, UV spectroscopy, IR spectroscopy and Evans method.

MALDI-ToF mass spectrometry

Firstly, all the complexes were characterized by MALDI-ToF mass spectrometry. In the MALDI-ToF spectra, the highest peak for the salan, salalen and salenC3-iron complexes **1**, **3** and **4** (Figures 3.4 and 3.20-3.23 in Experimental Section) corresponded to the species formed after the loss of a chloride while for the salen-iron complex **2** the most intense peak was attributable to the molecular ion (Figures. 3.18 and 3.19 in Experimental Section).

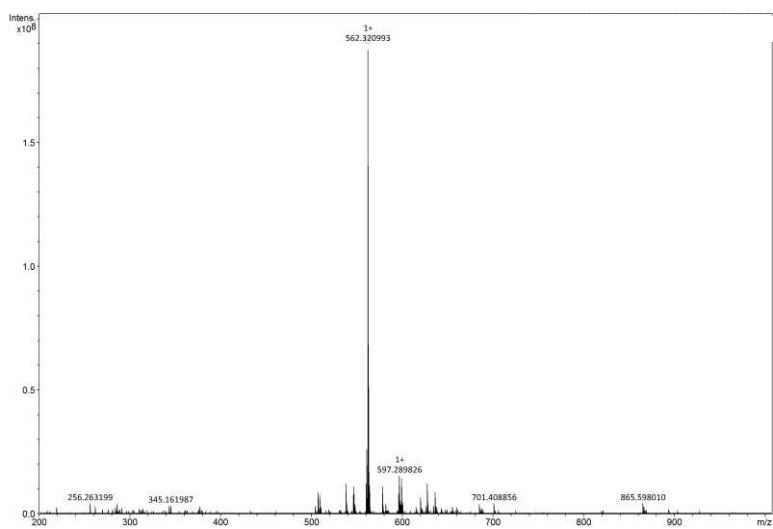


Figure 3.4. MALDI-TOF mass spectrum of **3**, peak at 597.3 m/z belongs to the species of complex **3**, 562.3 m/z belongs to the dechlorinated species of complex **3**

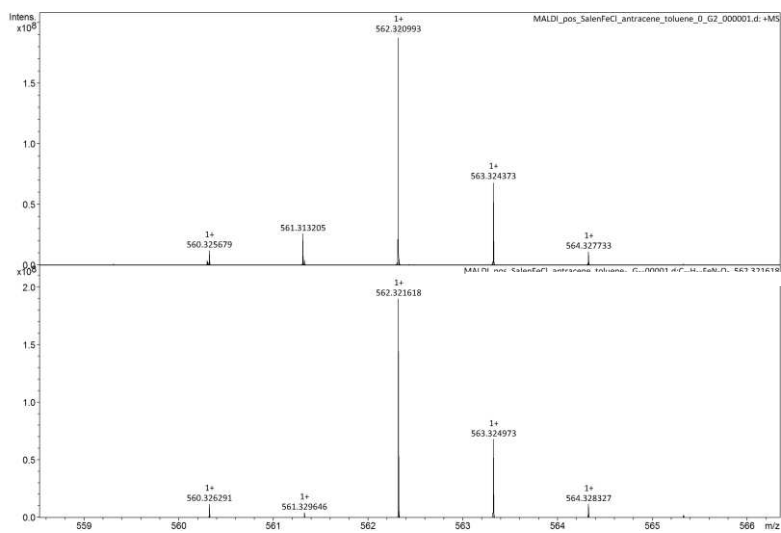


Figure 3.5. Experimental and Theoretical isotopic distribution pattern for complex **3**

UV-visible spectroscopy

Both the precursors of the ligands and the complexes **1-4** were analyzed by UV-visible spectroscopy. All samples were dissolved in acetonitrile (80 μmol) and the absorbance was recorded from 200 to 1000 nm (see Fig.3.6-3.8).

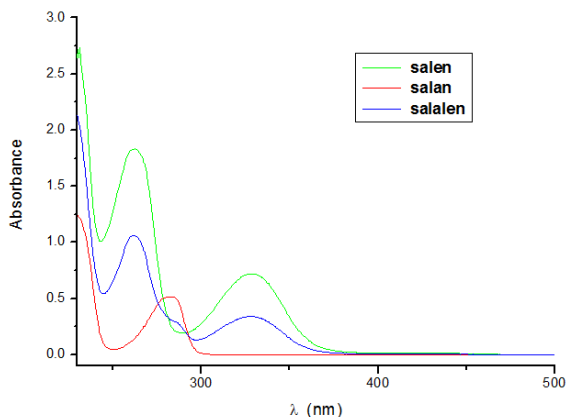


Figure 3.6. Electronic absorption spectra of salen, salan and salalen ligands in acetonitrile.

Spectra of salan, salen and salalen ligands are reported in figure 3.6, it can be seen that the spectrum of salan ligand shows an absorption band at 281 nm, while spectrum of salenFeCl ligand has two bands at 265 and 327 nm. These bands were attributed to the $\pi \rightarrow \pi^*$ transitions of the phenolic chromophores. It is interesting to note that the spectrum of the salalen ligand shows both the salen and salan bands, albeit with a half intensity (see Figura 3.6). This observation is in agreement with the fact that salalen has a hybrid structure between salan and salen, in fact it has both amine and imine units.

Spectra of complexes **1** and **2** were consistent with those already reported in literature (Figure 3.7).^{43,45} As expected, these spectra, shows absorption bands similar to those of the related ligands. In addition, two absorption bands (337 and 552 nm) for complex **1** and an absorption band (504 nm) for complex **2** a lower energy and at lower intensity are present. These bands were attributed to the ligand-metal charge transfer transitions (LMCT)..

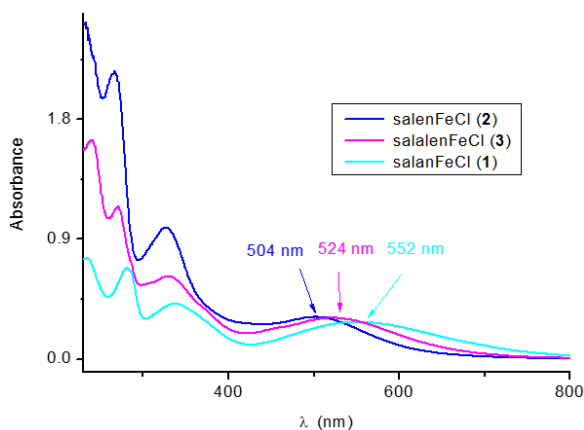


Figure 3.7. Electronic absorption spectra of salenFeCl **2**, salanFeCl **1** and salalenFeCl **3** complexes in acetonitrile.

The salalenFeCl complex **3** has two absorption bands at 270 and 329 nm due to phenol chromophore transitions and a band at 524 nm band attributable to a phenol LMCT transition. Finally, in the spectrum of the salenC3FeCl complex **4** there are three bands at 242, 273 and 332 nm, due to the transitions of the ligands and a band at 520 nm attributable to a LMCT transition (Figure 3.8).

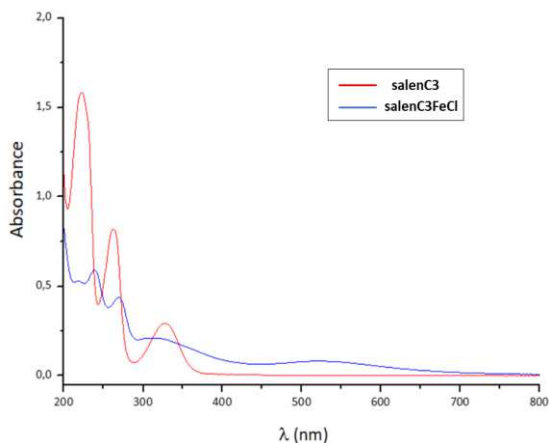


Figure 3.8. Electronic absorption spectra of salenC3 ligand and salenC3FeCl complex **4** in acetonitrile

Lewis acidity of the iron center can be related to the absorption energy of the LMCT bands. In particular, greater energy should indicate a lower acidity of the metal.³⁰

From the comparison of the observed transitions for complexes **1-4**, the data suggest the following order of acidity: salanFeCl **1** > salalenFeCl **3** > salenC3FeCl **4** > salenFeCl **2**.

IR spectroscopy

Both ligand precursors and complexes **1-4** were analyzed by IR spectroscopy. Comparing the IR spectra of the ligands, with those of the corresponding complexes, the successful coordination of the ligand to the metal was demonstrated (Figures 3.9 and 3.24 in Experimental Section).

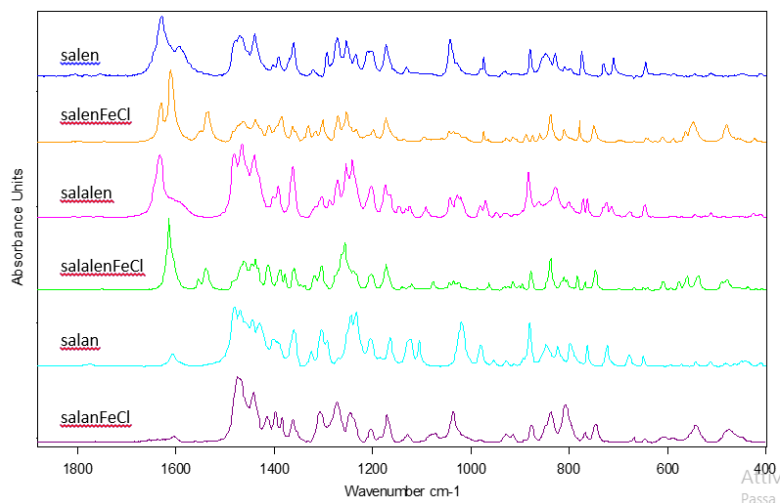


Figure 3.9. FT-IR spectra of salen, salalen, salan ligands and of the corresponding complexes **1-3**

In particular, in the spectra the salen, salalen and salenC3 ligands we observe of peaks attributable to C = N stretching respectively at 1629, 1632 and 1634 cm^{-1} . For the corresponding complexes, **2**, **3** and **4**, these peaks moved respectively to 1610, 1614 and 1609 cm^{-1} , suggesting the coordination of the ligand to the iron metal. Moreover, in the spectra of all complexes **1-4**, the appearance of two peaks, absent in the spectra of the ligands, around 540 and 480 cm^{-1} , is particularly significant as these peaks are indicative of the M-O and M-N bonds. Finally, as predictable, the IR spectra of salalen ligand and complex **3** can be conceived as the sum of the corresponding spectra of salan and salen.

Evans NMR method

The measurement of the magnetic susceptibility of iron complexes **1-4** was performed using the Evans NMR method. The values of magnetic moments found for complexes **1-4**

(range 5.3-6.0 μ_B), were consistent with the formation of high-spin Fe(III) complexes (5.92 μ_B for $S=5/2$).

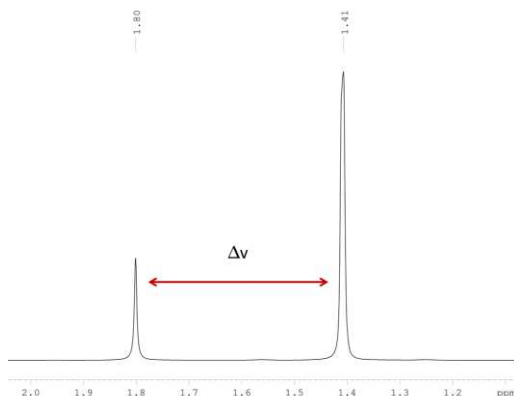


Figure 3.10. Example of measurement of the magnetic susceptibility of iron complex using the Evans NMR method.

Crystal structure determination

Single crystals of the salalenFeCl complex **3**, suitable for X-ray diffraction analysis, were obtained by slow evaporation of a solution of the complex in acetone at room temperature.

The X-ray molecular structure is shown in Figure 3.11. Selected bond lengths and angles for complex **3** and the analogous complexes **1**⁴³ and **2**³² are reported in Table 3.1.

The five-coordinate coordination geometry around Fe atom in complex **3** can be described as a distorted trigonal bipyramidal (tbp) geometry. The O1 and N2 atoms occupy the apical positions, while the N1, O2 and Cl atoms lie in the equatorial plane (Figure. 3.11). Commonly pentacoordinate complexes can adopt two geometries: square-pyramidal (sqp) or trigonal bipyramid (tbp), parameter τ ($\tau = |\beta - \alpha|/60$, where $\beta = \text{N1—}$

Fe—O2 angle and $\alpha = \text{N2—Fe—O1}$ angle) is used to describe to which geometry between sqp and tbp the complex is closer. When τ is equal to 0 the complex has a perfect sqp geometry, whereas when τ is equal to 1 the complex assumes a perfect tbp geometry. For complex **3** τ is 0.78 indicating a distorted trigonal bipyramid, interestingly for complex **1** τ is 0.31 indicating a distorted sqp geometry, while for complex **2** τ is 0.47.

In particular, for the complex **3**, the carbon atom of the methyl lies on the same part of the Cl atom deviating from the N1FeN2 mean plane by 0.95 Å. The bridge C atoms (C16 and C17) are on the opposite side with respect to the N1FeN2 mean plane and deviates from it by 0.31 Å and 0.33 Å, respectively.

As for complex **1**, the methyl groups are on the opposite side with respect to the N1FeN2 mean plane deviating by 1.22 and 1.36 Å. As for the bridge C atoms, one deviates from the mentioned plane by 0.60 Å and the other only by 0.09 Å. Similarly to **1** also in complex **2** one bridge C atoms deviates by 0.68 Å and the other only by 0.09 Å.

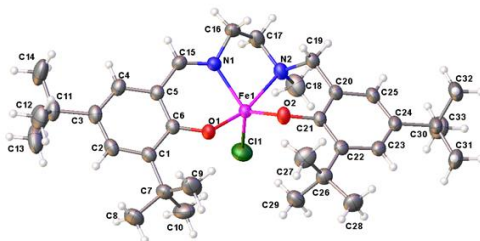


Figure 3.11. ORTEP diagram of complex **3**. Ellipsoids are drawn at 50% probability level.

As for the Fe-N1 and Fe-N2 distances in the three complexes, the following trends **1>2>3** and **3≈1>2** (confirmed by standard deviations) can be determined, respectively. Whereas, less significant differences resulted for the Fe-O1, the Fe-O2 and the Fe-Cl distances. Since longer distances indicate weaker bonds and thus more acidic iron center, the following order of acidity **salanFeCl 1 > salalenFeCl 3 > salenFeCl 2** can be inferred for the examined complexes, in agreement with what gathered from the LMCT bands of the electronic absorption spectra.

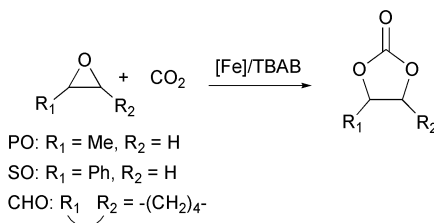
Table 3.1. Selected bond lengths (Å) and angles (°) for complexes **1-3**

Complex	1	2	3
Fe—N ₁	2.1623(18)	2.082(3)	2.0647(14)
Fe—N ₂	2.2824(18)	2.086(3)	2.2980(14)
Fe—O ₁	1.8636(16)	1.868(2)	1.9091(12)
Fe—O ₂	1.8615(14)	1.882(2)	1.8517(13)
Fe—Cl	2.2481(6)	2.2351(12)	2.2325(19)
O ₁ —Fe—N ₂	158.39(7)	132.78(12)	164.03(5)
O ₁ —Fe—N ₁	85.15(7)	86.17(10)	85.47(5)
O ₂ —Fe—N ₁	140.08(7)	161.23(11)	117.26(6)
O ₂ —Fe—N ₂	88.06(6)	86.76(11)	88.55(5)
Cl—Fe—N ₁	107.03(5)	92.64(9)	124.64(4)
Cl—Fe—O ₂	112.00(5)	101.77(9)	117.27(5)
Cl—Fe—N ₂	96.43(5)	108.00(9)	93.68(4)
Cl—Fe—O ₁	102.59(6)	116.78(9)	97.70(5)
N ₁ —Fe—N ₂	79.49(6)	77.30(11)	78.83(5)
O ₁ —Fe—O ₂	94.17(7)	97.77(11)	96.09(6)
τ	0.31	0.47	0.78

3.2.4. Catalytic cycloaddition of carbon dioxide with epoxides

The Fe (III) complexes **1-4** were tested as promoters of the CO₂ coupling reaction with three different epoxides, such as: propylene oxide (PO), a terminal aliphatic epoxide, cyclohexene oxide (CHO), an internal aliphatic epoxide, and the styrene oxide (SO), a typical aromatic epoxide (Scheme 3.1). The effect of the nature of the donor nitrogen atoms in the ligand skeleton, amino and / or imino, on the behavior of the catalysts has been evaluated.

The turnover numbers and frequencies (TON and TOF) were calculated respectively, according to the following equations: TON = mol epoxide consumed / mol of cat. and TOF = TON / time (h).



Scheme 3.1. Coupling reaction of epoxides with CO₂

We first tested the catalytic activity and the product selectivity of complexes **1-4** in the reaction of CO₂ with propylene oxide (PO). The reaction conditions and the results obtained are summarized in Table 3.2. The reactions were carried out in autoclave, at a CO₂ pressure of 20 bar and at 100 °C for a time of 16 hours, in the presence of TBAB (tetrabutylammonium-bromide), as a cocatalyst, using a catalyst ratio: PO equal to 1: 4000. The reactions were quenched by adding of CH₂Cl₂ at air, a ¹H NMR spectrum of the reaction mixture allowed to determine the conversion of the

propylene oxide. The analysis of the NMR spectra showed that all complexes produced propylencarbonate (PC) as the only product.

Table 3.2. CO₂/PO reaction promoted by complexes 1-4 and tetrabutylammonium bromide (TBAB)^[a]

Entry	Cat	TBAB (eq)	Conversion (%)	TON ^b	TOF ^c (h ⁻¹)
1	1	4	85	3400	213
2	1	1	58	2320	145
3	1	2	77	3080	192
4	2	2	64	2560	160
5	3	2	44	1760	110
6	4	2	78	3120	193
7	-	2	24	-	-
8	4	-	12		

^[a] **General conditions:** Complexes: **1-4** = 17.5 μ mol (0.025mol%), PO = 5 mL (4000 equiv), Pco₂ = 20 bar, Temperature = 100°C, time = 16 h. ^b Overall turnover number (mol_{PC}/mol_{cat}). ^c Overall turnover frequency (TON/reaction time).

Initially, the CO₂ / PO coupling reaction (see entry 1 in Table 3.2) was carried out under the same conditions reported in literature, by Kerton *et al*,³³ for a similar salanFeCl complex (Figure 3.12). Complex **1**, which differs for the ethylene bridge between the two nitrogen atoms with respect to the salanFeCl reported in the literature with a homopiperazine based bridge, in the presence of 4 equivalents of TBAB as a cocatalyst, has shown an epoxide conversion in the corresponding cyclic carbonate of 85% and

therefore showed an activity ($\text{TOF} = 213 \text{ h}^{-1}$) about twice the activity of the salanFeCl complex reported in the literature (135 h^{-1}).³³

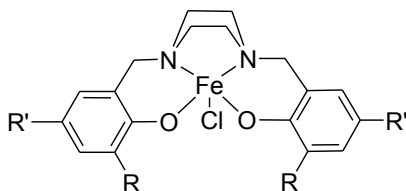


Figure 3.12. SalanFe complex synthesized by Kerton's research group.

On the basis of these initial results, it was thought to reduce the cocatalyst equivalents using complex **1**/ cocatalyst ratios of 1 : 2 and 1 : 1. The conversion of the PO into propylene carbonate (PC) decreases, decreasing the cocatalyst equivalents (cf entry 1-3 in Table 3.2), however decreasing the TBAB equivalents from 4 to 2, the variation was small. Therefore, it was decided to evaluate the activity of the other complexes under the same conditions of entry 3 (Table 3.2)., since the use of 2 equivalents is a good compromise to get high conversion while saving up the cocatalyst. For this purpose, complexes **2** and **3**, which respectively bear salen and salalen ligands, were used as catalysts in the CO_2/PO reactions working under the same conditions (see entry 4-5 in Table 3.2), obtaining the PC as the only product.

The following order of reactivity was found: $\text{salanFeCl } \mathbf{1} > \text{salenFeCl } \mathbf{2} > \text{salalenFeCl } \mathbf{3}$.

The behavior of complex **3** (salalenFeCl) was unexpected: since the salalen ligand has a hybrid structure between salan and salen ligands, an intermediate activity between those of complexes **1** and **2** would have been expected, while experimental data show that complex **3** (salalenFeCl) is the least active of the three.

The same order of reactivity was observed by comparing the behavior of complexes **1-3** as catalysts in the CO₂/PO reaction carried out using bis(triphenylphosphoranylidene)ammonium chloride (PPNCl) as a cocatalyst (see Table 3.3). But, in this case, when we conducted the reference reaction in the presence of PPNCl alone, a higher conversion than the binary system (iron complexes-PPNCl) was obtained.

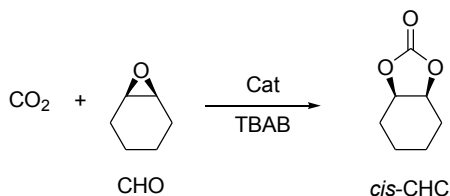
Table 3.3. CO₂/PO reaction promoted by complexes **1-3** and PPNCl ^[a]

Entry	Cat	Cocat	Conv. (%)	TON	TOF (h ⁻¹)
1	1	PPNCl	85	3723	233
2	2	PPNCl	79	3463	216
3	3	PPNCl	55	2409	151
4	-	PPNCl	64		

^[a] **General conditions:** Complexes: **1-3** = 16.3 μ mol (0.023mol%), PO = 5 mL (4400 equiv), PPNCl = 0.075 mmol (8 equiv), Pco₂ = 28 bar, Temperature = 100°C, time = 16 h.

The comparison of the behavior of complex **1** (salanFeCl) with that of complex reported in the literature (Figure 3.13) suggests that greater flexibility of the bridge may lead to greater activity. The same conclusion can be reached by comparing the activity of complex **1** (salanFeCl) with that found for complex **2** (salenFeCl) (entry 3 and 4 in table 3.2), taking into account the lower flexibility of the salen ligand with respect to the salan ligand. On the basis of these considerations, complex **4** was synthesized, with a salen type

ligand having a bridge with three carbon atoms between the two nitrogen atoms, and therefore more flexible than complex **2**. Thus, complex **4** was used in the CO₂/PO reaction under the same conditions of complex **2** (cf entries 4 and 6 in Table 3.2). Complex **4** showed higher activity than the analogous complex **2** (salenFeCl), bearing an ethylene bridge between the two nitrogen atoms, and comparable activity to complex **1** (salanFeCl) (cf entries 3 and 6 in Table 3.2) confirming the hypothesis of the importance of the flexibility of the ligand. Finally, two reference reactions in the presence of TBAB alone or complex **4** alone (entries 7 and 8 in Table 3.2) were conducted. In both cases low conversions of PO into PC were achieved. These results confirm the necessity to use the catalyst/cocatalyst binary system to promote the CO₂/PO coupling reaction and to obtain the corresponding cyclic carbonate. Subsequently we extended our study testing complexes **1-4** with styrene oxide (SO) and cyclohexene oxide (CHO). In general, SO and CHO have a lower reactivity than PO, for this reason we decided to conduct the reactions in the presence of 4 equivalents of TBAB. Furthermore, a longer reaction time was required for CHO, as it is a very unreactive internal epoxide. The obtained results are summarized in Table 3.4. In all cases, cyclic carbonates were obtained as exclusive products. In particular, in the case of CHO, the *cis*-CHC (see scheme 3.2) was obtained as an exclusive product; but with low conversions, resulting in a decline of the differences among the different complexes. Finally, even in these reactions with less reactive epoxides, the order of activity was the same observed in the case of the CO₂/PO reaction.



Scheme 3.2. CO_2/CHO reaction promoted by complexes **1-4** in combination with a quaternary ammonium salt (TBAB).

Table 3.4. Reaction of CO_2 with styrene oxide (SO) and cyclohexeneoxide (CHO) promoted by complexes **1-4** and tetrabutylammonium bromide (TBAB)^[a]

Entry	Cat	Epoxide	Conversion (%)	TON ^b	TOF ^c (h ⁻¹)
1	1	SO	53	2120	132
2	2	SO	46	1840	115
3	3	SO	44	1760	110
4	4	SO	53	2120	132
5	-	SO	15	-	-
6	1	CHO	19	760	35
7	2	CHO	18	720	32
8	3	CHO	13	520	24
9	4	CHO	19	760	35
10	-	CHO	10	-	-

^[a] **General conditions:** Complexes: **1-4** = 17.5 μmol (0.025mol%), Epoxide = 4000 equiv (7 mL of CHO, 8 mL of SO), P_{CO_2} = 20 bar, Temperature = 100°C, time = 16 h for SO, 22 h for CHO. ^b Overall turnover number ($\text{mol}_{\text{PO}}/\text{mol}_{\text{cat}}$). ^c Overall turnover frequency (TON/reaction time).

For salen M (III) Cl complexes (with M = Cr, Al and Co), the mechanism involved in the CO₂ / epoxide reaction has been extensively studied and revised.^{46,47,48} The initiation step contemplates the epoxy coordination in the *trans* position to the nucleophile. At this point, the reaction can proceed either by a bimetallic initiation pathway, where the nucleophile bound to the metal of another complex, attacks the coordinated epoxide, or by a binary initiation pathway, where the opening of the coordinated epoxide, initiates by a nucleophile present in the reaction mixture. The subsequent insertion of CO₂ in the metal-oxygen bond produces a metal carbonate which, by intramolecular S_N2 attack to the carbon that carries the nucleophile, leads to the formation of cyclic carbonate (Figure. 3.14).

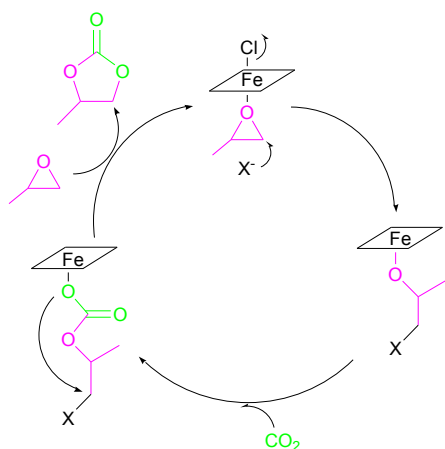


Fig. 3.14. Catalytic cycle for the formation of cyclic propylene carbonate

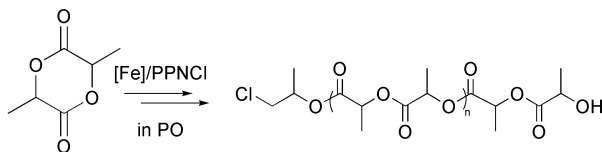
A possible explanation of the different activity observed for the catalysts could be related to the different geometries of the three

complexes. Table 3.1 shows the most relevant angles and distances of the three complexes. The values of τ for all the complexes are also reported. These values indicate for the complex **salanFeCl 1** a structure closer to a square pyramidal geometry ($\tau = 0.31$), while the **salalenFeCl 3** is better described with a trigonal bipyramid geometry ($\tau = 0.78$) and, finally, the **salenFeCl 2** is between these two possible geometries ($\tau = 0.47$). Accordingly, the coordinative pocket in the position *trans* to the chloride would allocate the epoxide more easily in the order **salanFeCl 1** > **salenFeCl 2** > **salalenFeCl 3**. The coordination of the epoxide to the metal, activates it towards the attack of the nucleophile, which is the step which determines the rate in the formation of cyclic carbonates. Reasonably, more efficient coordination will result in better epoxide activation which implies faster product formation.

3.2.5. Study of the reactivity of Fe complexes in the polymerization of lactide and ϵ -caprolactone

There are some examples, reported in the literature, in which active complexes in the ROP of the lactide have been shown to be also active in the CO₂/epoxide coupling reactions.¹ For this reason we thought to verify the activity of Fe (III) complexes **1-3** as promoters of the ROP of L-lactide and ϵ -caprolactone, (Schemes 3.3 and 3.5).

Furthermore, it is known that the best initiator groups in the ROP of lactide are alkoxy groups,^{32,49} which mimic the growing chain, while metal chloride are not good initiators. According to different authors,^{49,50,51} if the polymerization is carried out in PO as solvent, it may act also as an initiator.

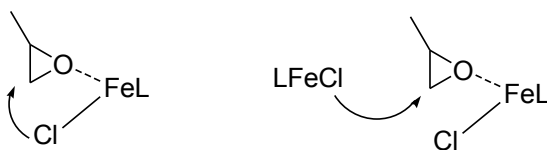


Scheme 3.3. Ring opening polymerization of L-LA.

Indeed, after the coordination of the PO to the metal and its opening by a nucleophile present in the reaction mixture, an alkoxide active species will be formed. Thus, the first step of the ROP would be the same described for the coupling of CO₂/ epoxide (i.e. the coordination of epoxide and its ring-opening by the nucleophile).

On the basis of these considerations, a preliminary experiment was carried out with the complex **2** in neat PO at 60 °C (entry 1 in Table 3.5). Under these conditions a conversion of L-lactide (100 equivalents) in PLA of 33% in four hours was found. The study of the polymer, by ¹H and ¹³C NMR analysis, (Figures 3.15 and 3.26 in Experimental Section) showed the presence of end groups indicative of ring-opening of PO by a chloride (-OCHCH₃CH₂Cl)³² and peaks corresponding to hydroxyl end groups (-OC = OCHCH₃OH), generated by the hydrolysis of the polylactyl growing chain. The chloride can derive from the

same iron complex that coordinated the epoxide, or from another complex (see Scheme 3.3).



Scheme 3.4. Opening mechanism of the PO by salenFeCl.

To facilitate the ring-opening of the coordinated PO, a cocatalyst was added in the reaction medium, that can provide chloride ions. For this purpose bis(triphenylphosphoranylidene)ammonium chloride (PPNCl) was used. As expected, conducting the polymerization of L-LA under the same conditions used for the previous reaction, but adding an equivalent of PPNCl, an activity about twice that of the previous experiment was obtained, achieving a conversion of 63% in four hours (entry 2 in Table 3.5). Also in this case, the ^1H and ^{13}C NMR spectra showed the presence of end groups that confirm the proposed mechanism. Subsequently, the L-LA polymerization reactions were conducted using complex **1** and **3**. Surprisingly, working under the same experimental conditions used for complex **2**, these complexes showed no activity.

Table 3.5. ROP of L-LA promoted by complexes **1-3** ^[a]

Entry	Cat	Co-Cat (eq)	Conversion (%)
1	2	-	33
2	2	PPNCI (1eq)	63
3	1	PPNCI (1eq)	0
4	3	PPNCI (1eq)	0

^[a] **General conditions:** Complexes: **1-3** = 17.2 μ mol, solvent: PO = 2 mL, L-LA= 1.7 mmol (100 equiv), temperature = 60°C, time = 4h.

The difference in the behaviour of complexes **1-3** in the ROP of L-LA, where only complex **2** showed some activity while complexes **1** and **3** were inactive, could be explained considering the order of Lewis acidity. This was deduced by the position of the LMCT transitions in the UV-vis spectra and by the Fe-N distances observed in the solid state structures of the three complexes, and resulted: salenFeCl **1** > salalenFeCl **3** > salenFeCl **2**. As reported in the literature,⁵² after the insertion of lactide into the iron alkoxide bond, an ester functionality adjacent to the growing polymer chain may form a five-membered ring chelate with the metal center (Figure 3.16). Higher acidity of the metal center would determine the formation of more stable bidentate lactate intermediate. Thus, a possible explanation of the observed behaviour could be the formation of a stable lactate intermediate for the more acidic

complexes **1** and **3** which hampers the insertion of other monomeric lactide units, *i.e.* the formation of the polymeric chain.

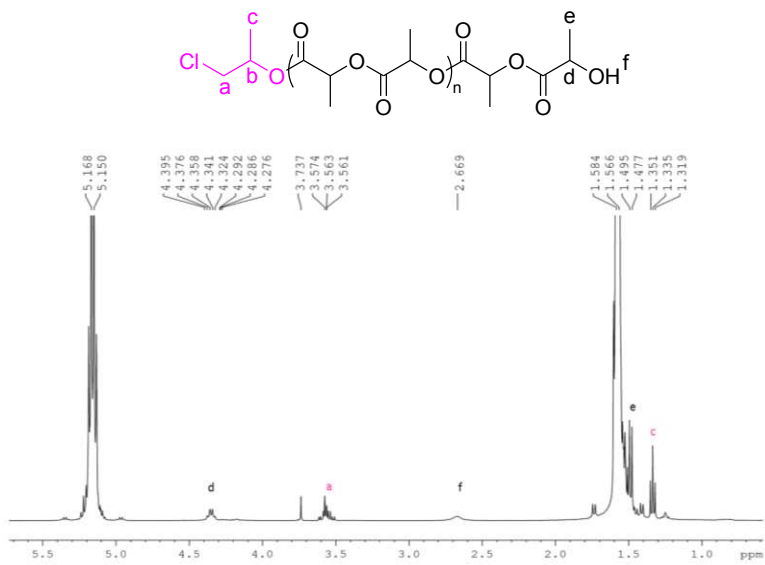


Figure 3.15. ^1H NMR spectrum (400 MHz, CDCl_3 , RT) of a PLA sample (entry 1 in Table 3).

On the other hand, in the case of the less acidic salenFeCl complex **2**, the less stable lactate intermediate will allow the insertion of subsequent lactide units and thus the growth of the polymeric chain.

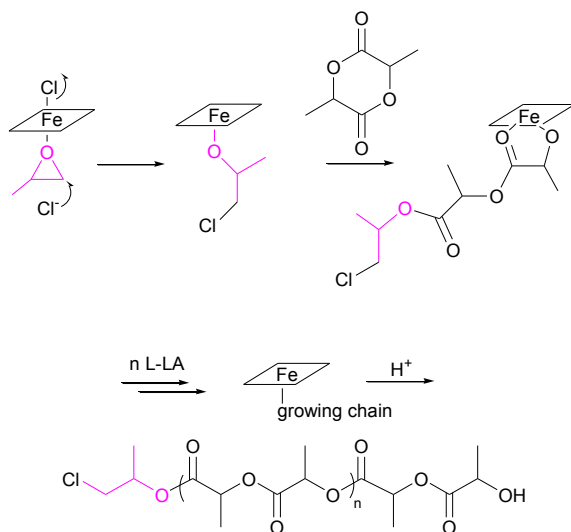
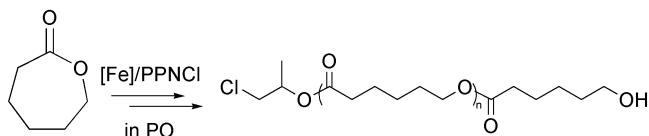


Fig. 3.16. Mechanism of the ring-opening polymerization of L-lactide

Subsequently, the behavior of the iron complexes **1-3** in the ROP of ϵ -caprolactone was explored. The ϵ -caprolactone is a cyclic ester showing some differences with respect to lactide, as it is generally more reactive, less sterically encumbered, and it cannot form bis-chelated intermediates. Thus complexes **1-3** were used as



Scheme 3.5. Ring opening polymerization of ϵ -caprolactone.

promoters of the ROP of the ϵ -caprolactone (Scheme 3.5). The experiments were carried out in PO as solvent, at room

temperature and either in the absence or in the presence of the cocatalyst.

The results are summarized in Table 3.6. Complex **1** gave a conversion of 78% in 8 hours, while complexes **2** and **3** did not show any activity after the same reaction time. By extending the reaction time to 30 hours and 24 hours for complex **2** and **3**, respectively, we were able to obtain an appreciable amount of polymer in both cases. Under these reaction conditions the order of reactivity found in the ROP of ϵ -caprolactone was: **salanFeCl 1** > **salalenFeCl 3** > **salenFeCl 2**. Thereafter, the polymerization reactions were carried out using complexes **1-3** in the presence of PPNCI as an exogenous source of chloride (see entries 4-6 in Table 3.6). In these conditions, after 8 hours, complexes **2** and **3** recorded higher conversions compared to the same polymerizations carried out in the absence of PPNCI (cf entry 5 and 6 vs 2 and 3, Table 3.6), while a not significant difference was found for complex **1** (cf entry 4 vs 1, Table 3.6). For longer reaction times, complex **2** showed an activity comparable to that in the absence of PPNCI (see entry 5 vs 2, Table 3.6), while complex **3** showed an improved activity (see entry 6 vs. 3, Table 3.6). Thus, even in the presence of PPNCI as a cocatalyst, the order of reactivity was: **salanFeCl 1** > **salalenFeCl 3** > **salenFeCl 2**. Finally, a polymerization experiment carried out with PPNCI alone showed that, under the same reaction conditions, this species did not show any activity (entry 7 in Table 3.6). The obtained polycaprolactones were examined by NMR spectroscopy and GPC analysis.

Table 3.6. ROP of ϵ -caprolactone promoted by complexes **1-3** and PPNCI. ^[a]

Entry	Cat/ Cocat	Time (h)	Conv (%)	M_n^{th} (KDa) ^a	M_n^{NMR} (KDa)	M_n^{GPC} (KDa) ^b	\bar{D} ^b
1	1/ -	8	78	8.8	10.2	12.1	1.07
2	2/ -	8	0	-	-	-	-
		24	32	-	-	-	-
		30	43	4.9	4.3	3.6	1.56
3	3/ -	8	0	-	-	-	-
		24	64	7.3	13.0	12.3	1.13
4	1/ PPNCI	8	83	9.4	8.3	10.9	1.12
5	2/ PPNCI	8 30	6 45	- 5.1	- 6.7	- 4.0	- 1.50
6	3/ PPNCI	8 24	34 90	- 10.3	- 14.3	- 15.5	- 1.19
7	-/ PPNCI	8	0	-	-	-	-

^[a] **General conditions:** Complexes: **1-3** = 17.2 μmol , 1 equiv of PPNCI, solvent: PO = 1 mL, ϵ -CL = 1.7 mmol (100 equiv), room temperature. Conversion of ϵ -CL as determined by ^1H NMR spectral data. ^a M_n^{th} (in g mol^{-1}) = $114.14 \times ([\epsilon\text{-CL}]_0/[I]) \times \text{conversion } \epsilon\text{-CL}$. ^b M_n^{GPC} (KDa) and \bar{D} values were determined by GPC in THF against polystyrene standards and corrected using the factor $0.56 M_n^{\text{GPC}}$.

^1H and ^{13}C NMR analysis (Figures. 3.17 and 3.27. in Experimental Section) revealed the presence of initiating groups generated by ring-opening of PO by chloride ($-\text{OCHCH}_3\text{CH}_2\text{Cl}$) and followed by insertion of the monomer unit into the so formed iron-oxygen bond with cleavage of the acyl-oxygen bond of the monomer, and hydroxyl end groups ($\text{CH}_2\text{CH}_2\text{OH}$; 3.62 ppm), generated by hydrolysis of the growing chain. The integration of the signal of the end group at 3.62 ppm with respect to the signal at 2.30 ppm of the repetitive unit, allowed us to calculate the molecular weight of the PCL sample (M_n^{NMR} in Table 3.6). Theoretical molecular weights (M_n^{th} in Table 3.6) were calculated assuming that a single PCL chain is produced per metal center through initiation of the polymerization by the opened propylene oxide group ($-\text{OCHCH}_3\text{CH}_2\text{Cl}$). Moreover, the samples were analyzed by GPC to determine the M_n^{GPC} and the dispersities (Đ). All the obtained PCLs possess quite narrow molecular weight distributions ($\text{Đ} = 1.07\text{--}1.56$) with unimodal characteristics. The good agreement between the M_n values determined both by GPC and by NMR with the theoretical molecular weights, indicated the occurrence of a controlled polymerization which proceeds exclusively by the mechanism detailed above. However, the PCL sample obtained by salalenFeCl complex **3** in the absence of PPNCI (entry 3) showed experimental molecular weights (M_n^{NMR} and M_n^{GPC}) almost twice those calculated by the converted monomer units (M_n^{th}) suggesting a low initiation efficiency.

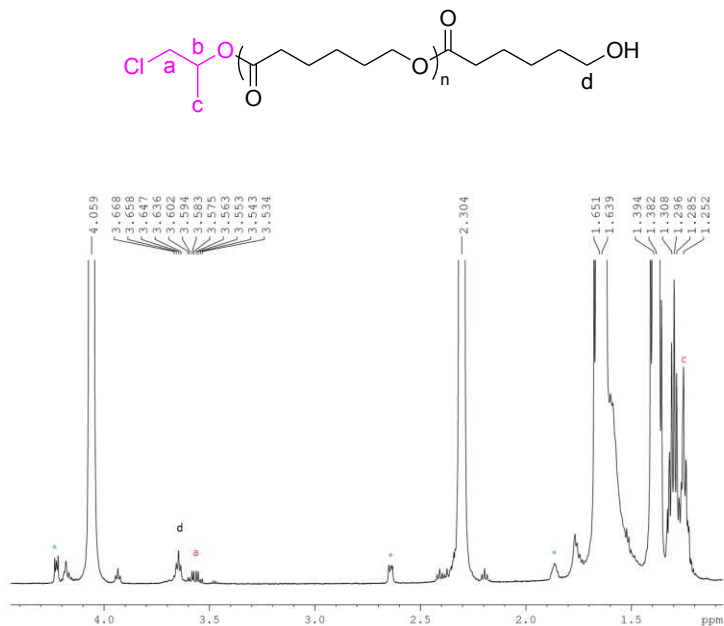


Figure 3.17. ^1H NMR spectrum (600 MHz, CDCl_3 , RT) of a PCL sample (entry 1 in Table 3). The peaks denoted with the blue star are related to residual ϵ -CL monomer.

In the case of ϵ -caprolactone, the difference in the activity of the three complexes would come from the difference in the rate of the propagating steps, i.e. the repeated insertions of the monomer in the iron-alkoxide bonds (Figure. 3.18). As reported in the literature,³² the activity of iron complexes in the ring-opening polymerization of ϵ -caprolactone, increases by increasing the acidity of the metal centre. Thus, the order of activity order observed in the ROP of ϵ -CL would be in agreement with the order of Lewis acidity ($\text{salanFeCl } \mathbf{1} > \text{salalenFeCl } \mathbf{3} > \text{salenFeCl } \mathbf{2}$). Moreover, the comparison of the polymerization experiments detailed in Table 3.6, after 8 hours, shows how the initiation

reaction is slower for complexes **2** and **3** than for complex **1** (and how it is accelerated by PPNCI) in agreement with what observed in the PO/CO₂ coupling reactions.

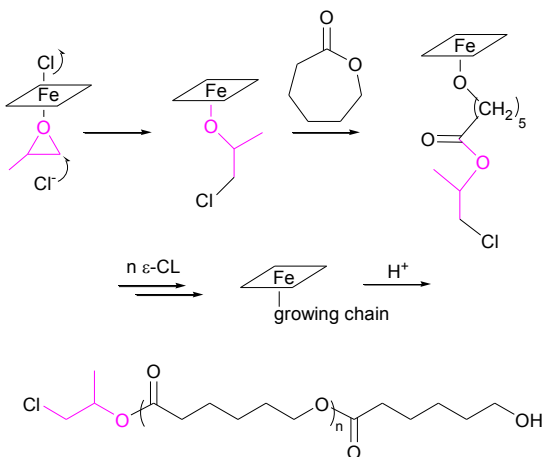


Figure 3.18. Mechanism of the ring-opening polymerization of ϵ -caprolactone.

3.3. Conclusions

In conclusion Fe (III) monometallic complexes with salan, salen, salalen ligands, with the same substituents on the aromatic rings were synthesized. These complexes were characterized by the following techniques: MALDI-ToF, UV-vis, IR and Evans NMR Method which showed the coordination of the ligands to the metal centers and the formation of d^5 high-spin Fe (III) complexes. Then, their behavior as promoters of the CO_2 /epoxide reaction and the ROP of L-LA and ϵ -CL was studied. For the coupling reactions, three different epoxides were used, representing three different classes of epoxides, namely: cyclohexeneoxide, CHO, (internal epoxide), propylene oxide, PO, (terminal epoxide) and styrene oxide, SO, (aromatic epoxide). The synthesized iron complexes were active and selective in CO_2 /epoxide reactions obtaining, in all cases, cyclic carbonates as exclusive products. In particular, in the coupling reactions of CO_2 with the three selected epoxides, the following order of reactivity was found: salanFeCl complex **1** > salenFeCl complex **2** > salalenFeCl complex **3**. Reasonably this was due to the different geometries of the three complexes. A possible explanation of the highest activity of the salanFeCl complex was related to its distorted square planar geometry which leaves enough room in the *trans* position to the chloride, to easily allocate the reacting epoxide. On the other hand, for the salalenFeCl, the chloride occupies an equatorial position of a distorted trigonal bipyramidal geometry thus leaving a reduced coordinative space for the incoming epoxide. The ROP of the ϵ -CL was carried out by using PO as initiator, to form, *in situ*, an active alkoxide species. As a consequence, the initial step of the

polymerization reaction is the same reaction occurring in the CO₂/epoxide coupling. However, for the ROP, this reaction is not the rate limiting step, thus it determines the rate of the initiation reactions but not the activities of the complexes. The order of activity observed in the ROP of ϵ -CL was **salanFeCl 1** > **salalenFeCl 3** > **salenFeCl 2** coinciding with the order of the acidity of the metal centers in the different complexes. Finally, in the ROP of L-LA, only the **salenFeCl complex 2** proved to be active. We propose that the more acidic complexes **1** and **3** form stable lactate intermediates which hamper the growth of polymer chain.

3.4. Experimental Section

3.4.1 General considerations

Materials and general methods

All manipulations of air- and/or moisture-sensitive compounds were carried out using standard Schlenk-line techniques under a dry nitrogen atmosphere or using a Braun Labmaster glovebox. All solvents and reagents were obtained from commercial sources (Sigma-Aldrich): anhydrous iron(III)chloride (FeCl_3 99.99% purity), tetrabutylammonium bromide (TBAB, 98% purity), tetrabutylammonium chloride (TBAC, 98% purity), and bis(triphenylphosphoranylidene)ammonium chloride (PPNCl) (98% purity). Methanol was distilled over sodium, propylene oxide ($\geq 99.5\%$; Sigma-Aldrich), styrene oxide (97%; Sigma-Aldrich), cyclohexene oxide (98%; Sigma-Aldrich) and ϵ -caprolactone were distilled under reduced pressure over calcium hydride and stored in a sealed flask in a glove-box; L-lactide was purified by recrystallization from toluene. Glassware and autoclave used in the reactions were dried in an oven at 120 °C overnight and exposed to vacuum–nitrogen cycles thrice. All other chemicals were commercially available and used as received unless otherwise stated.

Instruments and measurements

NMR spectra were collected on Bruker Avance spectrometers (600, 400, 300, or 250 MHz for ^1H NMR); the chemical shifts were referenced to tetramethylsilane (TMS) as an external reference, using the residual protio signal of the deuterated solvents. Deuterated solvents were purchased from Sigma–Aldrich and dried

over activated 3 Å molecular sieves prior to use. The molecular weights (M_n and M_w) and the dispersity ($\bar{D} = M_w/M_n$) of polymer samples were measured by gel permeation chromatography (GPC) at 30 °C, using THF as the solvent, an eluent flow rate of 1 mL min⁻¹, and narrow polystyrene standards as the reference. The measurements were performed on a Waters 1525 binary system equipped with a Waters 2414 RI detector using four Styragel columns (range: 1000–1000 000 Å). MALDI mass spectra were recorded using a Bruker solariX XR Fourier transform ion cyclotron resonance (FT-ICR) mass spectrometer (Bruker Daltonik GmbH, Bremen, Germany) equipped with a 7 T refrigerated actively shielded superconducting magnet (Bruker Biospin, Wissembourg, France). The samples were ionized in positive ion modes using the MALDI ion source. The mass range was set to m/z 150–2000. The laser power was 15% and 15 laser shots were used for each scan. The samples were prepared at a concentration of 1.0 mg mL⁻¹ in toluene. The matrix (anthracene) was mixed at a concentration of 10.0 mg mL⁻¹ to promote desorption and ionization. UV-Vis spectra were recorded on a Cary-50 Spectrophotometer, using a 1 cm quartz cuvette (Hellma Benelux bv, Rijswijk, Netherlands) and a slit-width equivalent to a bandwidth of 5 nm. Measurements were performed in CH₃CN at room temperature. FTIR spectra were obtained at a resolution of 2.0 cm⁻¹ with a FTIR (BRUKER Vertex70) spectrometer equipped with a deuterated triglycine sulfate (DTGS) detector and a KBr beam splitter, using KBr pellet disks. The frequency scale was internally calibrated to 0.01 cm⁻¹ using a He–Ne laser. 32 scans were signal-averaged to reduce the noise. Magnetic susceptibility measurements. According to Evans'

NMR method, 1 mL of a mixture of 95/5 v/v C6D6 and cyclohexane was prepared and a portion (0.5 mL) of this solution was transferred to an NMR tube. The other portion (0.5 mL) of this solution was used to dissolve a small amount of the iron complex (0.5 mg) and this was transferred in a capillary inserted into the tube. The difference in chemical shifts of the cyclohexane protons between the insert and the NMR tube solution at room temperature was used to calculate the molar susceptibility. The data were corrected for the diamagnetism of all atoms.⁵³

3.4.2. Synthesis and Characterization of Complexes 1-4

Synthesis of SalanFeCl complex 1

SalanFeCl complex **1** was prepared according to a published procedure¹. To a methanol solution (10 mL) of anhydrous iron chloride FeCl₃ (61.8 mg, $3.81 \cdot 10^{-4}$ mol) was added a methanol solution (15 mL) of the salanligand (200 mg, $3.81 \cdot 10^{-4}$ mol). Triethylamine (0.100 mL, $7.62 \cdot 10^{-4}$) was added to give a dark red solution. The resulting mixture was stirred for 2 h. Next, the solvent was removed under vacuum. The solid product was dissolved in acetone and filtered through Celite three times. Removal of solvent under vacuum yielded a violet powder (73%). Characterization of salanFeCl complex **1** was done by means of IR and UV-vis spectroscopy, MALDI-ToF mass spectrometry and Evans NMR technique. The results were in agreement with those reported in the literature.⁴²

IR (KBr, cm⁻¹): 2949, 2739, 2677, 2492, 1474, 1442, 1413, 1398, 1384, 1361, 1307, 1272, 1246, 1203, 1170, 1129, 1036, 928, 877, 837, 808, 746, 543 (Fe-N), 476 (Fe-O).

UV-vis (CH_3CN , 0.08 mM, 25 °C, $\epsilon = \text{L} \cdot \text{mol}^{-1} \cdot \text{cm}^{-1}$): 234 nm ($\epsilon = 9450$), 281 nm ($\epsilon = 8525$), 337 nm ($\epsilon = 5183$), 552 nm ($\epsilon = 3463$). MS (MALDI-ToF) m/z: 613.321 ($\text{FeCl}[\text{Salan}]^{+}$), 578,353 ($\text{Fe}[\text{Salan}]^{+}$).

Magnetic moment (298K) $\mu_{\text{eff}} = 5.32 \mu\text{B}$.

Synthesis of SalenFeCl complex 2

SalenFeCl complex **2** was prepared according to a published procedure². To a methanol solution (10 mL) of anhydrous iron chloride FeCl_3 (74.1 mg, $4.57 \cdot 10^{-4}$ mol) was added a methanol solution (8 mL) of the salen ligand (150 mg, $3.044 \cdot 10^{-4}$ mol). Triethylamine (0.100 mL, $7.62 \cdot 10^{-4}$) was added to give a dark violet solution. The resulting mixture was stirred for five hours at reflux and then overnight at room temperature. Next, the solvent was removed under vacuum. The solid product was dissolved in acetone and filtered through Celite three times. Removal of solvent under vacuum yielded a dark red powder (89%).

Characterization of salenFeCl complex **2** was done by means of IR and UV-vis spectroscopy, MALDI-ToF mass spectrometry and Evans NMR technique. The results were in agreement with those reported in the literature.^{32,44}

IR (KBr cm^{-1}): 2952, 2677, 1610 ($\text{C}=\text{N}$), 1535, 1438, 1385, 1362, 1330, 1301, 1270, 1252, 1198, 1172, 1044, 974, 837, 811, 779, 749, 547 (Fe-N), 480 (Fe-O).

UV-vis (CH_3CN , 0.08 mM, 25 °C, $\epsilon = \text{L} \cdot \text{mol}^{-1} \cdot \text{cm}^{-1}$): 230 nm ($\epsilon = 31588$), 265 nm ($\epsilon = 26950$), 327 nm ($\epsilon = 12338$), 504 nm ($\epsilon =$

3936). MS (MALDI-ToF) m/z : 581,258 ($\text{FeCl}[\text{Salen}]^{+}$), 546,289 ($\text{Fe}[\text{Salen}]^{+}$).

Magnetic moment (298 K) $\mu_{\text{eff}} = 5.99 \mu\text{B}$.

Synthesis of salalenFeCl complex 3.

To a methanol solution (10 mL) of anhydrous iron chloride FeCl_3 (63.8 mg, 3.93×10^{-4} mol) was added a methanol solution (10 mL) of the salalen ligand (200 mg, 3.93×10^{-4} mol). Triethylamine (0.109 mL, 7.86×10^{-4}) was added to obtain a dark violet solution. The resulting mixture was stirred for 2 h. Next, the solvent was removed under vacuum. The solid product was dissolved in acetone and filtered through a Celite three times. Removal of the solvent under vacuum yielded a violet powder, 88%. The characterization of salalenFeCl was done by means of IR- and UV-Vis-spectroscopy, MALDI-ToF mass spectrometry and Evans NMR technique.

IR (KBr, cm^{-1}): 2952 (C–H aromatic), 1614 (C=N), 1539, 1461, 1438, 1387, 1378, 1358, 1304, 1256, 1202, 1173, 1076, 1035, 963, 878, 838, 811, 784, 747, 609, 560, 537 (Fe–N), 479 (Fe–O).

UV–vis (CH_3CN , 0.08 mM, 25 °C, $\epsilon = \text{L mol}^{-1} \text{cm}^{-1}$): 240 nm ($\epsilon = 20\,575$), 270 nm ($\epsilon = 14\,300$), 329 nm ($\epsilon = 7769$), 524 nm ($\epsilon = 3853$).

MS (MALDI-ToF) $m/z(\text{ion})$: 597 289 ($\text{FeCl}[\text{salalen}]^{+}$), 562 321 ($\text{Fe}[\text{salalen}]^{+}$).

Magnetic moment (298 K) $\mu_{\text{eff}} = 5.31 \mu\text{B}$.

Synthesis of SalenC3FeCl complex 4

SalenC3FeCl complex **4** was prepared according to a published procedure². To a methanol solution (12 mL) of anhydrous iron chloride FeCl₃ (96.0 mg, $5.92 \cdot 10^{-4}$ mol) was added a methanol solution (12 mL) of the salenC3 ligand (200 mg, $3.95 \cdot 10^{-4}$ mol). Triethylamine (0.110 mL, $7.90 \cdot 10^{-4}$) was added to give a dark violet solution. The resulting mixture was stirred for three hours at reflux and then overnight at room temperature. Next, the solvent was removed under vacuum. The solid product was dissolved in acetone and filtered through Celite three times. Removal of solvent under vacuum yielded a dark red powder (89%).

Characterization of the salenC3FeCl complex **4** was done by means of IR and UV-vis spectroscopy, MALDI-ToF mass spectrometry and Evans NMR technique. The results were in agreement with those reported in the literature.^{32,44}

IR (KBr, cm⁻¹): 2948, 2677, 1713, 1609 (C=N), 1537, 1454, 1430, 1387, 1361, 1305, 1272, 1256, 1219, 1200, 1073, 1091, 970, 876, 838, 810, 780, 746, 540 (Fe-N), 482, 449(Fe-O).

UV-vis (CH₃CN, 0.08 mM, 25 °C, $\epsilon = \text{L} \cdot \text{mol}^{-1} \cdot \text{cm}^{-1}$): 242 nm ($\epsilon = 7135$), 273 nm ($\epsilon = 5186$), 332 nm ($\epsilon = 2475$), 524 nm ($\epsilon = 1022$).
MS (MALDI-ToF) m/z: 581,258 (FeClK[SalenC3]⁺), 546,289 (Fe[SalenC3Cl]⁺).

Magnetic moment (298 K) $\mu_{\text{eff}} = 5.82 \mu\text{B}$.

MALDI-ToF mass spectrometry

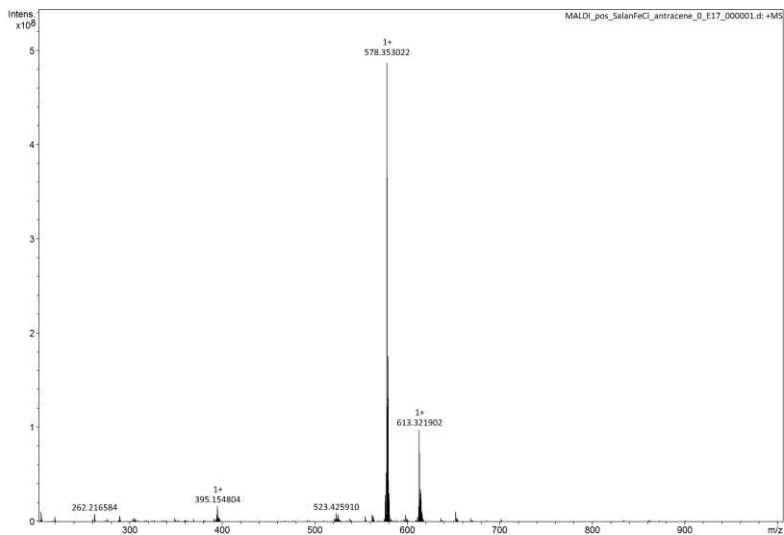


Figure 3.19. MALDI-TOF mass spectrum of **1**, peak at 613.3 m/z belongs to the species of complex **1**, 578.3 m/z belongs to the dechlorinated species of complex **1**

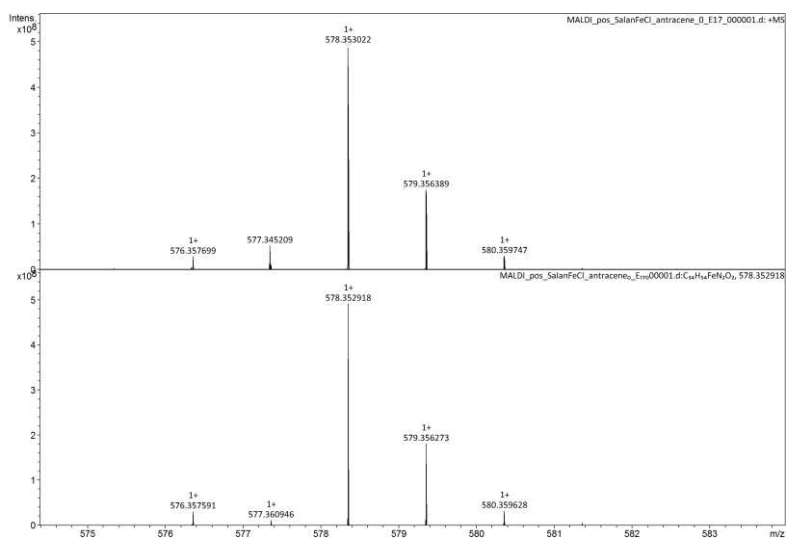


Figure 3.20. Experimental and Theoretical isotopic distribution pattern for **1**

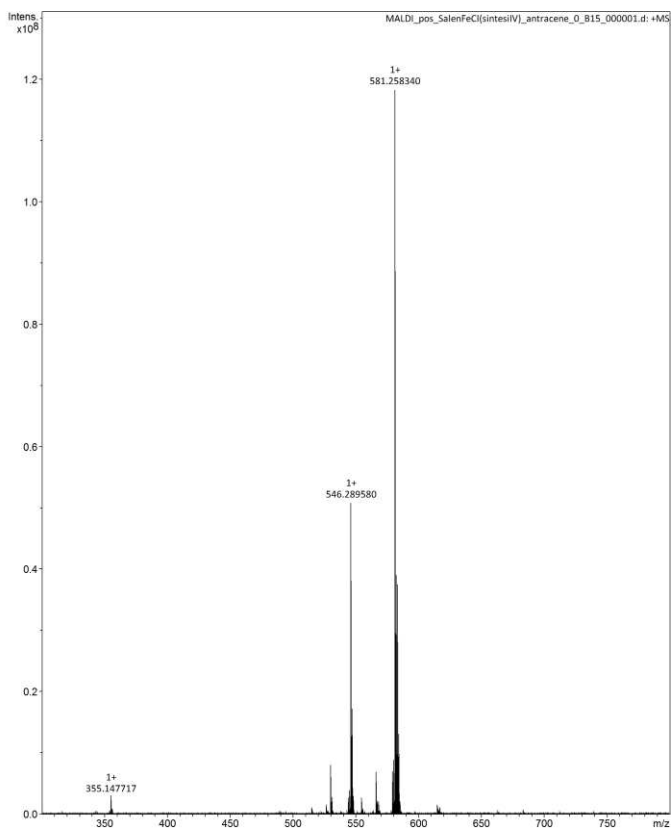


Figure 3.21. MALDI-TOF mass spectrum of **2**, peak at 581.2 m/z belongs to the species of complex **2**, 546.3 m/z belongs to the dechlorinated species of complex **2**

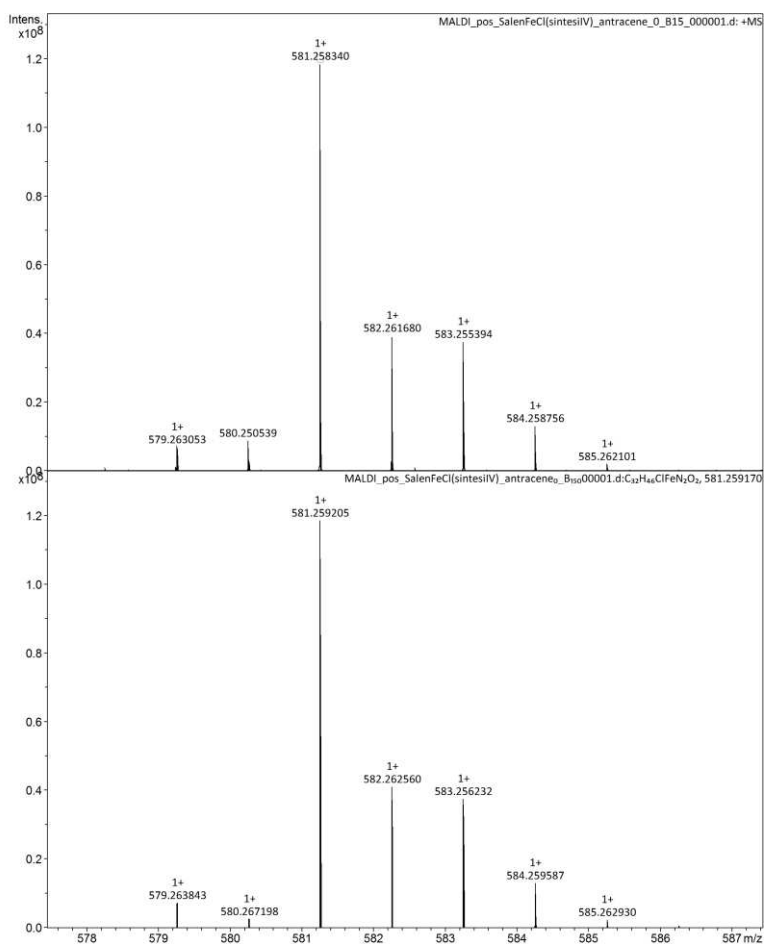


Figure 3.22. Experimental and Theoretical isotopic distribution pattern for complex **2**

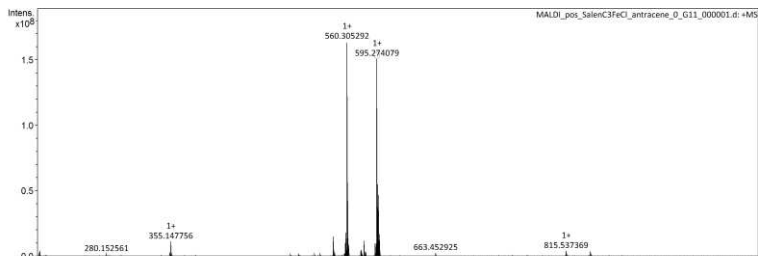


Figure 3.23. MALDI-TOF mass spectrum of **4**, peak at 595.3 m/z belongs to the species of complex **4**, 560.3 m/z belongs to the dechlorinated species of complex **4**

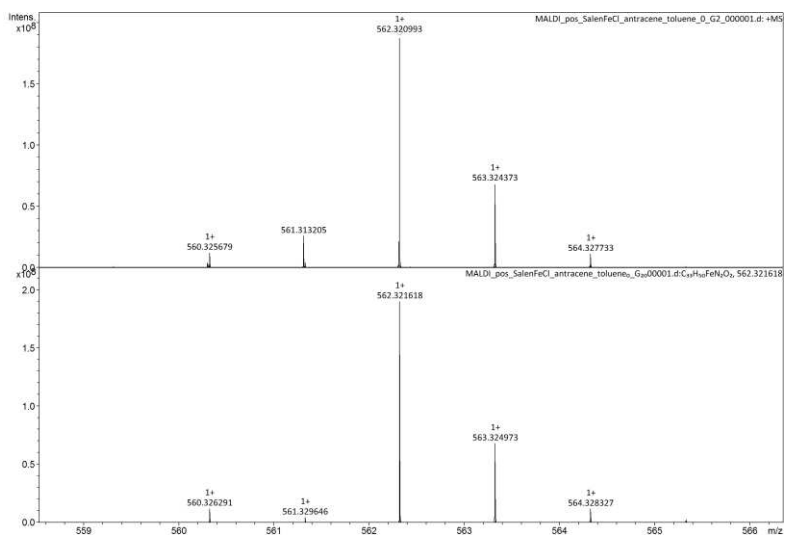


Figure 3.24. Experimental and Theoretical isotopic distribution pattern for complex **4**

FT-IR spectrum of SalenC3FeCl complex 4

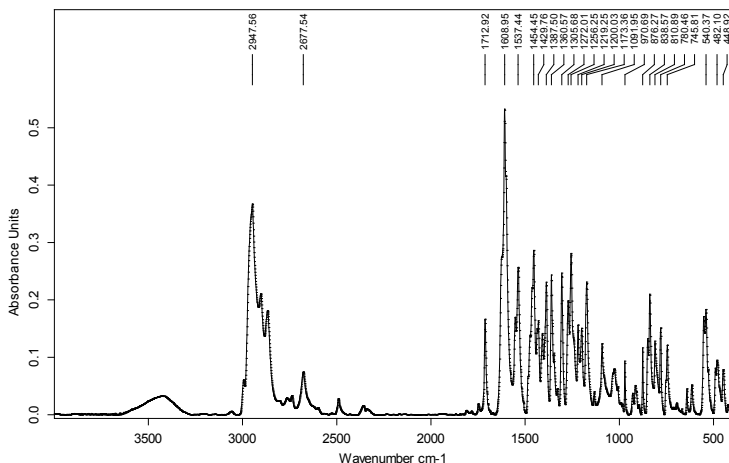


Figure 3.25. FT-IR spectrum of SalenC3FeCl complex 4

General procedure for the CO₂/epoxide reaction

A representative procedure for the CO₂/epoxide reaction is described as follows. The reaction was carried out using a ratio of epoxide/complexes of 4000 and TBAB/complex = 1 : 4. In a glove-box, the catalyst (0.0175 mmol) and the co-catalyst (TBAB) were dissolved in the epoxide (4000 equiv., 70 mmol) and then transferred into an autoclave. The autoclave was pressurized to the appropriate pressure of CO₂, and the mixture was allowed to stir at the desired temperature for the necessary reaction time. After the prescribed time, the reaction mixture was quenched by immersing the autoclave in an ice bath, opened in air and a small sample of the crude reaction mixture was used to calculate the conversion of epoxide into cyclic carbonate by ¹H NMR spectroscopy.

General procedure for L-lactide polymerization

In a typical experiment, in a glove-box, L-lactide (1.7 mmol, 0.248 g), the catalyst (0.017 mmol) and, when used, the cocatalyst (PPNCl, 0.017 mmol, 9.88×10^{-3} g) were dissolved in toluene or propylene oxide (2 mL) and then transferred into a tube. The tube was heated at 60 °C and stirred for the necessary reaction time. After the prescribed time, the tube was cooled to room temperature and a ^1H NMR spectrum of the crude reaction mixture was used to calculate the conversion. The polymer was isolated by precipitation in methanol. NMR spectroscopy (CDCl_3) was used to determine the molecular weights (M_n) of the polymers.

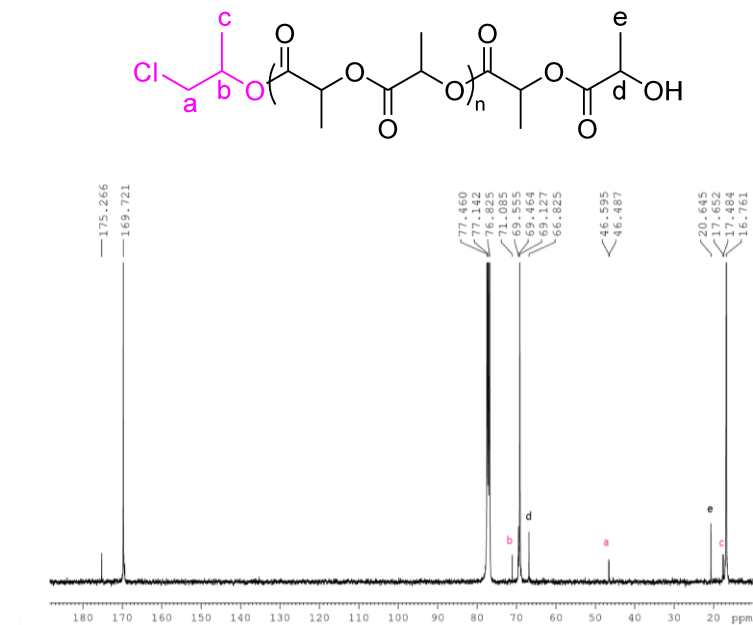


Figure3.26. ^{13}C NMR spectrum of PLA (400 MHz, CDCl_3 , RT)

General procedure for ϵ -caprolactone polymerization

In a typical experiment, in a glove-box, the monomer (1.7 mmol, 0.196 g), the catalyst (0.017 mmol) and the cocatalyst (PPNCl, 0.017 mmol, 9.88×10^{-3} g) were dissolved in PO (1 mL) and then transferred into a vial. The resulting mixture was stirred at room temperature for the necessary reaction time. After the prescribed time, the crude reaction mixture was used to calculate the conversion by ^1H NMR spectroscopy. The polymer was isolated by precipitation in hexane. NMR spectroscopy (CDCl_3) and GPC (THF) were used to determine the molecular weights of the obtained polymers.

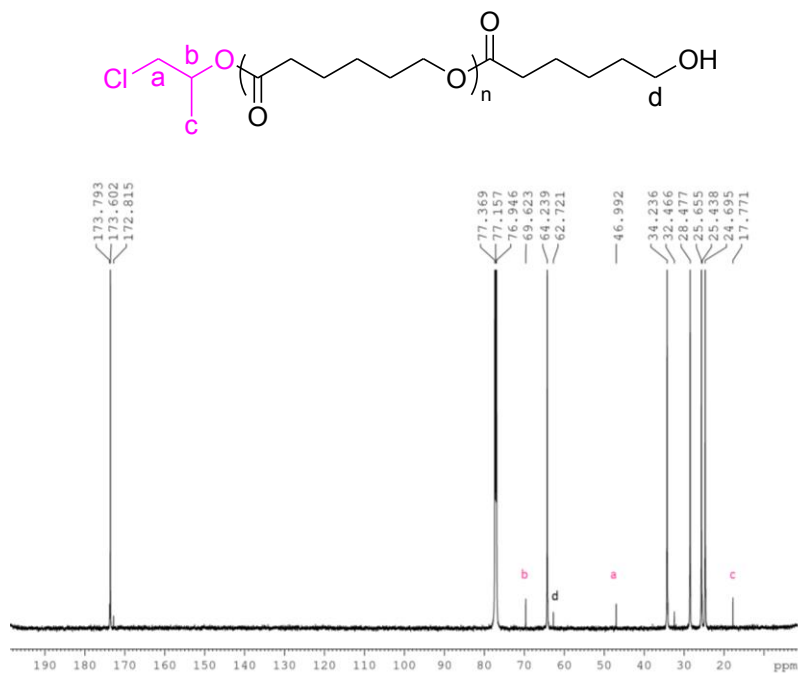


Figure 3.27. ¹³C NMR spectrum of PCL (400 MHz, CDCl₃, RT)

References

- 1 I. Bauer and H.-J. Knölker, *Chem. Rev.*, **2015**, 115, 3170–3387.
- 2 A. Buchard, M. R. Kember, K. G. Sandemanb, C. K. Williams, *Chem. Commun.*, **2011**, 47, 212–214.
- 3 J. Whiteoak, E. Martin, M. Martinez Belmonte, J. Benet- Buchholz and A. W. Kleij, *Adv. Synth. Catal.*, **2012**, 354, 469–476.
- 4 C. J. Whiteoak, B. Gjoka, E. Martin, M. M. Belmonte, E. C. Escudero-Adán, C. Zonta, G. Licini, A. W. Kleij, *Inorg. Chem.*, **2012**, 51, 10639–10649.
- 5 M. Taherimehr, S. M. Al-Amsyar, C. J. Whiteoak, A. W. Kleij and P. P. Pescarmona, *Green Chem.*, **2013**, 15, 3083–3090.
- 6 A. Buonerba, A. De Nisi, A. Grassi, S. Milione, C. Capacchione, S. Vagin and B. Rieger, *Catal. Sci. Technol.*, **2015**, 5, 118–123.
- 7 F. Della Monica, S. V. C. Vummaleti, A. Buonerba, A. De Nisi, M. Monari, S. Milione, A. Grassi, L. Cavallo and C. Capacchione, *Adv. Synth. Catal.*, **2016**, 358, 3231–3243.
- 8 F. A. Al-Qaisi, N. Genjang, M. Nieger and T. Repo, *Inorg. Chim. Acta*, **2016**, 442, 81–85.
- 9 M. Sunjuk, A. S. Abu-Surrah, E. Al-Ramahi, A. K. Qaroush and A. Saleh, *Transition Met. Chem.*, **2013**, 38, 253–257.
- 10 C. K. Karan and M. Bhattacharjee, *Inorg. Chem.*, **2018**, 57, 4649–4656.
- 11 O. Martínez-Ferraté, J. M. López-Valbuena, M. Martínez Belmonte, A. J. P. White, J. Benet-Buchholz, G. J. P. Britovsek, C. Claver and P. W. N. M. van Leeuwen, *Dalton Trans.*, **2016**, 45, 3564–3576.
- 12 F. Chen, N. Liu and B. Dai, *ACS Sustainable Chem. Eng.*, **2017**, 5, 9065–9075.
- 13 J. E. Dengler, M. W. Lehenmeier, S. Klaus, C. E. Anderson, E. Herdtweck and B. Rieger, *Eur. J. Inorg. Chem.*, **2011**, 2011, 336–343.
- 14 X. Sheng, L. Qiao, Y. Qin, X. Wang and F. Wang, *Polyhedron*, **2014**, 74, 129–133.
- 15 M. A. Fuchs, T. A. Zevaco, E. Ember, O. Walter, I. Held, E. Dinjus and M. Doring, *Dalton Trans.*, **2013**, 42, 5322–5329.

-
- 16 A. Södergård and M. Stolt, *Macromol. Symp.*, **1998**, 130, 393–402.
- 17 R. R. Gowda and D. Chakraborty, *J. Mol. Catal. A: Chem.*, **2009**, 301, 84–92.
- 18 C. S. Hege and S. M. Schiller, *Green Chem.*, **2014**, 16, 1410–1416.
- 19 M. Stolt and A. Södergård, *Macromolecules*, **1999**, 32, 6412–6417.
- 20 B. J. O’Keefe, S. M. Monnier, M. A. Hillmyer and W. B. Tolman, *J. Am. Chem. Soc.*, **2001**, 123, 339–340.
- 21 D. S. McGuinness, E. L. Marshall, V. C. Gibson and J. W. Steed, *J. Polym. Sci., Part A: Polym. Chem.*, **2003**, 41, 3798–3803.
- 22 X. Wang, K. Liao, D. Quan and Q. Wu, *Macromolecules*, **2005**, 38, 4611–4617.
- 23 H. R. Kricheldorf and D.-O. Damrau, *Macromol. Chem. Phys.*, **1997**, 198, 1767–1774.
- 24 B. J. O’Keefe, L. E. Breyfogle, M. A. Hillmyer and W. B. Tolman, *J. Am. Chem. Soc.*, 2002, 124, 4384–4393.
- 25 A. B. Biernesser, B. Li and J. A. Byers, *J. Am. Chem. Soc.*, **2013**, 135, 16553–16560.
- 26 C. Geng, Y. Peng, L. Wang, H. W. Roesky and K. Liu, *Dalton Trans.*, **2016**, 45, 15779–16782.
- 27 Y.-Y. Fang, W.-J. Gong, X.-J. Shang, H.-X. Li, J. Gao and J.-P. Lang, *Dalton Trans.*, **2014**, 43, 8282–8289.
- 28 V. C. Gibson, E. L. Marshall, D. Navarro-Llobet, A. J. P. White and D. J. Williams, *J. Chem. Soc., Dalton Trans.*, **2002**, 4321–4322.
- 29 A. Arbaoui, C. Redshaw, M. R. J. Elsegood, V. E. Wright, A. Yoshizawa and T. Yamato, *Chem. – Asian J.*, **2010**, 5, 621–633.
- 30 M. Z. Chen, H. M. Sun, W. F. Li, Z. G. Wang, Q. Shen and Y. Zhang, *J. Organomet. Chem.*, **2006**, 691, 2489–2494.
- 31A. S. Abu-Surrah, H. M. Abdel-Halim, H. A. N. Abu-Shehab and E. Al-Ramahi, *Transition Met. Chem.*, **2017**, 42, 117–122.
- 32 R. Duan, C. Hu, X. Li, X. Pang, Z. Sun, X. Chen and X. Wang, *Macromolecules*, **2017**, 50, 9188–9195.

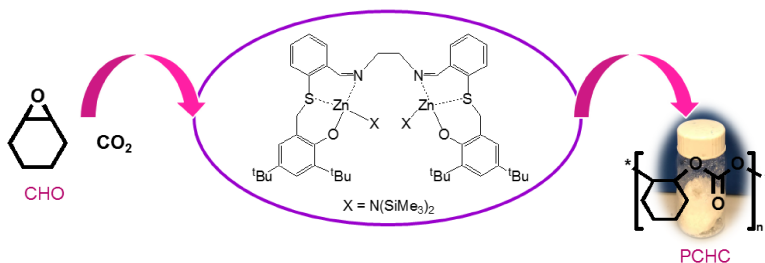
-
- 33 D. Alhashmialameer, J. Collins, K. Hattenhauera and F. M. Kerton, *Catal. Sci. Technol.*, **2016**, 6, 5364–5373.
- 34 M. Cozzolino, K. Press, M. Mazzeo and M. Lamberti, *ChemCatChem*, **2016**, 8, 455–460.
- 35 M. Cozzolino, T. Rosen, I. Goldberg, M. Mazzeo and M. Lamberti, *ChemSusChem*, **2017**, 10, 1217–1223.
- 36 J. M. Raquez, R. Mincheva, O. Coulembier and P. Dubois, 4.31 -Ring-Opening Polymerization of Cyclic Esters: Industrial Synthesis, Properties, Applications, and Perspectives A2 - Matyjaszewski, Krzysztof, in *Polymer Science: A Comprehensive Reference*, ed. M. Möller, Elsevier, Amsterdam, **2012**, pp. 761–778.
- 37 X. Zhang, M. Fevre, G. O. Jones and R. M. Waymouth, *Chem. Rev.*, **2018**, 118, 839–885.
- 38 A. Arbaoui and C. Redshaw, *Polym. Chem.*, **2010**, 1, 801–826.
- 39 R. H. Platel, L. M. Hodgson and C. K. Williams, *Polym. Rev.*, **2008**, 48, 11–63.
- 40 A. Pilone, N. De Maio, K. Press, V. Venditto, D. Pappalardo, M. Mazzeo, C. Pellicchia, M. Kol, M. Lamberti, *Dalton Trans.*, **2015**, 44, 2157–2165.
- 41 E. L. Whitelaw, G. Loraine, M. F. Mahon, M. D. Jones, *Dalton Trans.* **2011**, 40, 11469–11473.
- 42 K. Hasan, C. Fowler, P. Kwong, A. K. Crane, J. L. Collins and C. M. Kozak, *Dalton Trans.*, **2008**, 2991–2998.
- 43 J. B. H. Strautmann, S. DeBeer George, E. Bothe, E. Bill, T. Weyhermuller, A. Stammler, H. Bogge and T. Glaser, *Inorg. Chem.*, **2008**, 47, 6804–6824.
- 44 S. Liao and B. Lista, *Adv. Synth. Catal.*, **2012**, 354, 2363–2367.
- 45 A. M. Aslam, S. Rajagopal, M. Vairamani and M. Ravikumar, *Transition Met. Chem.*, **2011**, 36, 751–759.
- 46 D. D. Darensbourg, *Chem. Rev.*, **2007**, 107, 2388–2410.
- 47 S. Klaus, M. W. Lehenmeier, C. E. Anderson and B. Rieger, *Coord. Chem. Rev.*, **2011**, 255, 1460–1479.

-
- 48 A. Decortes, A. M. Castilla and A. W. Kleij, *Angew. Chem., Int. Ed.*, **2010**, 49, 9822–9837.
- 49 M. H. Chisholm, D. Navarro-Llobet and W. J. Simonsick, *Macromolecules*, **2001**, 34, 8851–8857.
- 50 S. Doherty, R. J. Errington, N. Housley and W. Clegg, *Organometallics*, **2004**, 23, 2382–2388.
- 51 M. Anker, C. Balasanthiran, V. Balasanthiran, M. H. Chisholm, S. Jayaraj, K. Mathieu, P. Piromjitpong, S. Praban, B. Raya and W. J. Simonsick Jr., *Dalton Trans.*, **2017**, 46, 5938–5945.
- 52 K. R. Delle Chiaie, A. B. Biernesser, M. A. Ortuño, B. Dereli, D. A. Iovan, M. J. T. Wilding, B. Li, C. J. Cramer and J. A. Byers, *Dalton Trans.*, **2017**, 46, 12971–12980.
- 53 G. A. Bain and J. F. Berry, *J. Chem. Educ.*, **2008**, 85, 532–536.

CHAPTER 4

Synthesis of a New Zinc Complex as Catalyst for ROCOP of CO₂ and Cyclohexeneoxide

In chapter 4 we describe the synthesis of a new class of hexadentate ligands, which presents two additional sulphur donors with respect to classic salen ligands, thus creating a coordinating environment able to allocate two metallic centers. This new class of ligands is very versatile, in fact they allow to vary the nature of nitrogen-donating atoms (amine and imine) and the substituents on aromatic rings allowing to modulate the properties of metal centers. They also allow to modulate the length of the bridge between the two nitrogen atoms in order to find the optimal distance between the metallic centers to promote their cooperation. The first ligand of this new class of ligands was synthesized and used for the preparation of the corresponding bimetallic zinc complex. This complex has been employed as catalyst for CO₂/CHO reactions. In particular, the effect of the reaction conditions (such as, temperature, CO₂ pressure and time) on the outcoming of this reaction was studied.



4.1. Introduction

Over the last decades a variety of catalytic systems have been proposed for CO₂/epoxides reactions. Generally for most of the applications the catalyst must be active, not expensive non-toxic, and colorless as it may remain in the resulting product. Under these aspects, the use of zinc (II) as the metal of the catalytically active species has tremendous advantages over other metals. It is an economic and ecofriendly metal providing ions that do not lead to colored polymer products.¹ Several zinc-based catalyst systems for the reaction of epoxides and CO₂ are already well-known in literature. Salen ligands show several advantageous hallmarks since they are easy to synthesize, cheap and may be sterically and electronically modified. Salen-type Zn complexes have been reported by some authors as active catalysts for the production of cyclic carbonates.² Shi *et al.* explored the catalytic performance of zinc(II) salen-type complexes derived from binaphthyldiamino Schiff bases in the chemical fixation of carbon dioxide. This type of complexes was found to efficiently catalyze the formation of cyclic carbonates from terminal epoxides, working at 100 °C and in the presence of an organic base, such as DMAP (4-dimethylaminopyridine).³ Kleij's group reported a mononuclear Zn(salphen) complex active towards CO₂ coupling with terminal epoxides under mild reaction condition (P_{CO2}= 0.2-1 MPa, T= 25-45 °C).⁴ The high activity of the Zn(salphen) complex was ascribed to its constrained geometry imposed by the ligand scaffold, which imparts increased Lewis acid character to the catalytically active zinc ion. A bifunctional Zn-salen complexes with multiple hydrogen bonding donors and protic ammonium bromides was reported by He

et al.⁵ This complex was active in the fixation of CO₂ in cyclic carbonate products with both terminal and internal epoxides under 0.1 MPa CO₂ pressure. TON and TOF values up to 49288 and 39473 h⁻¹, respectively, were obtained.

On the other hand, polycarbonate synthesis has been accomplished by employing dizinc complexes bearing different classes of ligands. These include β - diiminates and di-nuclear zinc phenoxides as well as bimetallic macrocyclic derivatives. Zinc β - diiminate, reported by Coates and co-workers showed high activity and excellent control in the CO₂ and CHO (cyclohexene oxide) reactions, producing PCHC (poly(cyclohexene carbonate)) under 7 atm CO₂ pressure and at 50°C.⁶ Rieger and coworkers reported a dizinc complex coordinated by two β -diiminate moieties that were linked by phenyl rings.⁷ This complex was one of the most active catalytic systems for the synthesis of PCHC under 30 bar of CO₂ pressure, at 100°C and at a catalyst loading of 0.0125 mol%. Xiao et al. reported a dizinc complex coordinated with the Trost phenolate ligand, which was moderately active for CO₂/CHO copolymerization, although the precise nature of the catalyst was not describe as it was prepared *in situ*.⁸ Williams et al. reported a series of bimetallic complexes coordinated by a novel reduced Robson's type macrocyclic ligand (Figure 1d), which were highly active with CHO under 1 atm CO₂ pressure and at 100°C giving a best TOF of 13 h⁻¹.⁹

As can be inferred from this short literature overview, monometallic zinc complexes employed in the CO₂/ epoxide reaction, generally lead to the formation of cyclic carbonates while bimetallic zinc complexes usually promote the formation of polycarbonates.

In order to obtain salalen-based bimetallic zinc complexes we tried the same strategy which worked with aluminum complexes, that is the increase of the length of the bridge between the two nitrogen atoms of the ligand skeleton which created enough space to allocate two metallic centers.¹⁰ However, in the case of the zinc complexes, the monometallic derivative was always obtained. Reasonably, this was due to the fact that zinc centers in the dimetallic complexes would be tricoordinate while the monometallic derivatives fix the zinc metal in a tetracoordinate environment. Starting from these considerations we designed a new class of hexadentate ligands which closely resembles on the salen ligands and preserve some of their advantages, while it shows two more additional sulphur neutral donors.

In this chapter we describe the synthetic strategy conceived for the preparation of these new hexadentate OSNNOS ligands, the synthesis and the characterization of the first ligand of this class and its corresponding dizinc complex and its use in the reaction of CO₂ with cyclohexene oxide under different reaction conditions.

4.2. Results and Discussion

4.2.1. Synthesis and characterization of salalen Zinc complexes

In a previous work, we described the synthesis of bimetallic aluminium complexes bearing salalen ligands, which presented propylenic bridge between the two nitrogen atoms (Figure 4.1.).¹⁰ Using the same synthetic strategy, we tried to synthesize bimetallic zinc complexes.

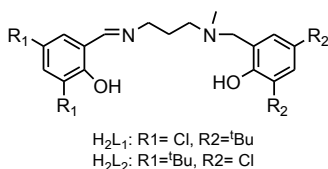
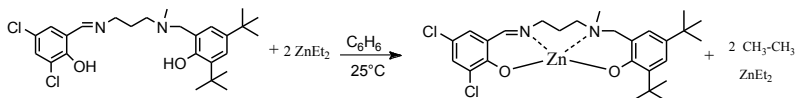


Figure 4.1. Structures of the salalen ligands.

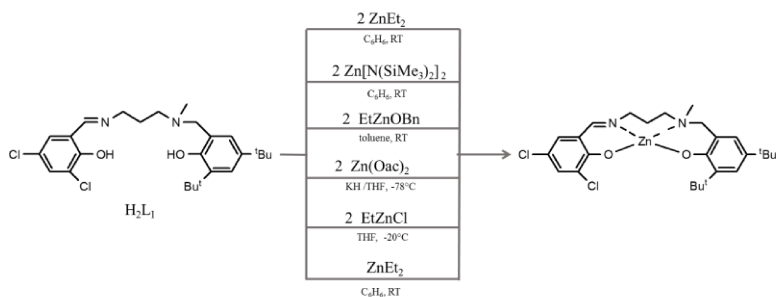
Conducting the direct reaction between H_2L_1 (see Figure 4.1.) and two equivalents of ZnEt_2 in C_6D_6 at room temperature, the formation of a different species with respect to the desired bimetallic complex was observed (Scheme 4.1).



Scheme 4.1. Reaction between salalen ligand (H_2L_1) and two equivalents of ZnEt_2

In particular, the high-field region of the ${}^1\text{H}$ NMR spectrum did not present signals attributable to ethyl groups coordinated to zinc, while the presence of signals of the unreacted ZnEt_2 was observed. These observations suggested the formation of a monometallic species, in which the zinc was coordinated to the four neutral

donors of the ligand, adopting a tetracoordination. The formation of the monometallic zinc species was confirmed by the mass analysis, which reveals an intense peak at 556 m/z attributable to the molecular ion. Probably the monometallic species is favored with respect to the bimetallic species, because tetracoordinate zinc is more stable than the tricoordinate metal. Subsequently, the reaction between the H_2L_1 ligand and other metallic precursors, such as $Zn[N(SiMe_3)_2]_2$, $Zn(OAc)_2$, $ClZnEt$ and $EtZnOBn$, was carried out.



Scheme 4.2. Reaction between salalen ligand (H_2L_1) and two equivalents of several zinc precursor.

The $Zn[N(SiMe_3)_2]_2$ was chosen because the presence of a encumbered labile ligand on the metal precursor could stabilize the tricoordination of zinc in the bimetallic species. Furthermore, mixed precursors such as $ClZnEt$ and $EtZnOBn$ were used because the bonds of $Zn-Cl$ and $Zn-OBn$ are stronger than the $Zn-Et$ bond, so they should remain unaltered during the reaction, allowing the formation of the desired bimetallic species. The reactions were conducted under different conditions and in some cases in the presence of a coordinating solvent, such as THF, which, by guaranteeing the tetracoordination of zinc also in the bimetallic complex, could facilitate its formation. However, the 1H NMR analysis indicated the formation of the monometallic zinc species in

all the performed syntheses. Thus, complexes **1** and **2** were intentionally synthesized by direct reaction of the ligands H₂L₁₋₂ and 1 equivalent of ZnEt₂ in dry benzene. The obtained complexes are powdery solids of yellow color.

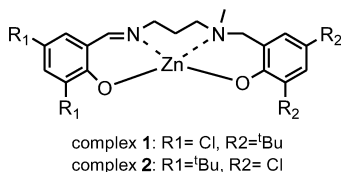


Figure 4.2. Structures of the salalen zinc complexes.

These complexes were characterized by ¹H NMR (Figure 4.3 and 4.11), ¹³C NMR (Figure 4.9 and 4.12), and 2D COSY NMR (Figure 4.10 and 4.13).

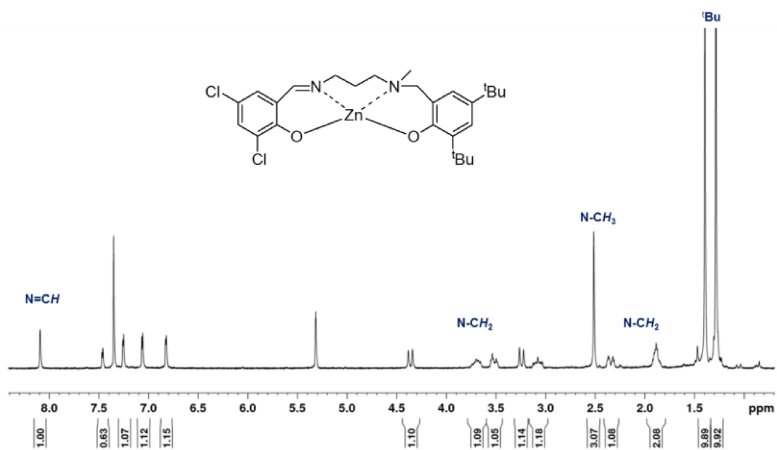
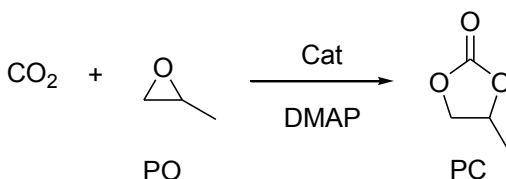


Figure 4.3. ¹H NMR spectrum (400 MHz, CD₂Cl₂, 298K) of complex **1**.

4.2.2. Cycloaddition of carbon dioxide with propylene oxide

We tested the catalytic activity and the product selectivity of complexes **1** and **2** in the reaction of CO₂ with PO. The complexes were active and selective in the cycloaddition reaction by furnishing propylene carbonate (PC) as an exclusive product. The experiments were carried out with complexes **1** and **2** in the presence of 4-dimethylaminopyridine (DMAP) as a cocatalyst (see entries 1 and 2 in Table 4.1), under the same reaction conditions used for a similar salen-type zinc complex reported by Shi *et al.*³



Scheme 4.3. CO₂/PO reaction promoted by complexes **1** and **2** in combination with DMAP

Table 4.1. CO₂/PO reaction promoted by complex **1** and **2** in presence of DMAP^[a]

Entry	Cat	Cocat	PO(eq)	% PC	TON	TOF(h ⁻¹)
1	1	DMAP	1000	41%	410	25.6
2	2	DMAP	1000	51%	510	31.9

^[a] **General conditions:** complexes **1**, **2** = 45 μmol, DMAP = 2 equiv., CH₂Cl₂ = 5 mL, Temperature = 100°C, P_{CO₂} = 30 bar, time = 16 h.

The results reported in Table 4.1 show that complex **1** has a slightly lower activity than complex **2** in the CO₂ / PO reaction. This small difference of reactivity was attributed to the different substituents on the aromatic rings of the skeleton of the ligands. In fact, complex **2** presents chloro substituents on the amine-side phenol and bulky

alkyl groups on the imineside phenol, while complex **1** has the opposite phenolate substitution pattern, viz., bulky alkyl substituents on the amine-side phenol and halo groups on the imine-side phenol.

The behavior of the zinc complexes **1** and **2** was compared with that of the salen zinc complexes reported in the literature (Figure 4.4).³ In particular, the comparison was made with the complexes having t-Bu groups or Cl atoms as substituents in the positions 3 and 5 of the phenolic rings. Our complexes were found to be more active (TONs = 410, 510) than that reported in the literature TONs= 53 and 132 respectively for complexes **a** and **b** (Figure 4.4).³

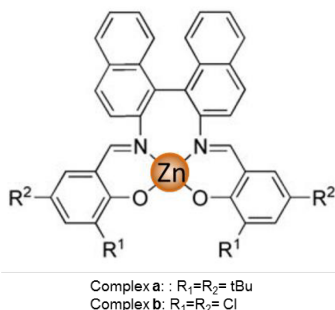


Figure 4.4. Structures of the salen-type zinc complex reported by Shi *et al.*

4.2.3. Synthesis of new hexadentate dianionic ligands

With the aim to synthesize a bimetallic zinc complex, we thought to increase the coordination number of each metal centres, modifying the ligand skeleton. Thus, we designed new hexadentate dianionic ligands resembling salen ligands although with two additional sulphur neutral donors and a methodology for the synthesis of this new class of hexadentate dianionic ligands has been developed.

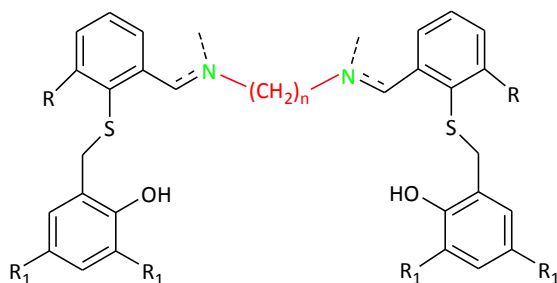
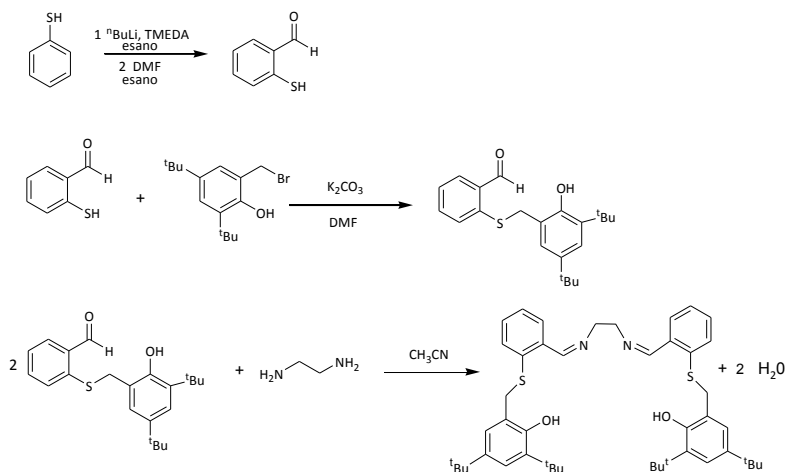


Figure 4.5. Structures of the new class of hexadentate dianionic ligands.

The first ligand of this class has been synthesized and characterized: it presents hydrogen atoms as R substituents, *t*-butyl groups as the R_1 substituents and an ethylene bridge between the two imino nitrogen donors.

The synthetic strategy, which allowed the preparation of this OSNNSO ligand, involves three steps. First, thiophenol, premixed with N,N,N',N'-tetramethylethylenediamine (TMEDA), reacted with *n*-butyl lithium giving the deprotonated product, this, by reaction with dry dimethyl formamide in hexane as solvent, gave the 2-mercaptobenzaldehyde.¹¹ The second step was the reaction of 2-mercaptobenzaldehyde with 2-(bromomethyl)-4,6-di-*tert*-butylphenol, purposely synthesized, using dry dimethyl formamide as the solvent.¹² Finally, the desired ligand was obtained by condensation of two equivalents of the 2-(3,5 di-*tert*butyl-2-hydroxybenzyl) sulfanyl benzaldehyde with ethylenediamine in dry acetonitrile.



Scheme 4.4. The synthetic strategy for preparation of OSNNSO ligand.

The ligand was characterized by ^1H and ^{13}C NMR and by MALDI-ToF spectrometry. In particular, the ^1H NMR spectrum showed: a singlet at 9.08 ppm for the acidic protons of the hydroxyl groups, a singlet due to the iminic protons at 8.17 ppm, six signals of different multiplicity between 7.45 and 6.43 ppm for the aromatic protons. The methylene groups bound to the sulphur (SCH_2Ar) and to the nitrogen ($\text{NCH}_2\text{CH}_2\text{N}$) gave two singlets, each integrating for 4 protons, respectively at 3.96 ppm and 3.40 ppm. Finally, two singlets, each integrating for 18 protons, were observed at 1.72 and 1.30 ppm for the protons of the t-butyl groups. The ^1H NMR spectrum clearly indicated a high symmetry for the described ligand. The number of the signals observed in the ^{13}C NMR spectrum was coherent with this observation. In fact, in the ^{13}C NMR spectrum (Figure 4.13) is observed a signal at 164.16 ppm relative to the carbons bound to the imino nitrogen atoms; the eleven signals between 151.9 and 123.9 ppm due to the aromatic

carbons. The methylene carbons bound to the sulphur (SCH_2Ar) and to the nitrogen ($\text{NCH}_2\text{CH}_2\text{N}$) were observed respectively at 61.95 ppm and 38.5 ppm. Finally, signals between 35.45 ppm and 30.16 ppm, are indicative of the carbons of the t-butyl groups, present on the aromatic rings.

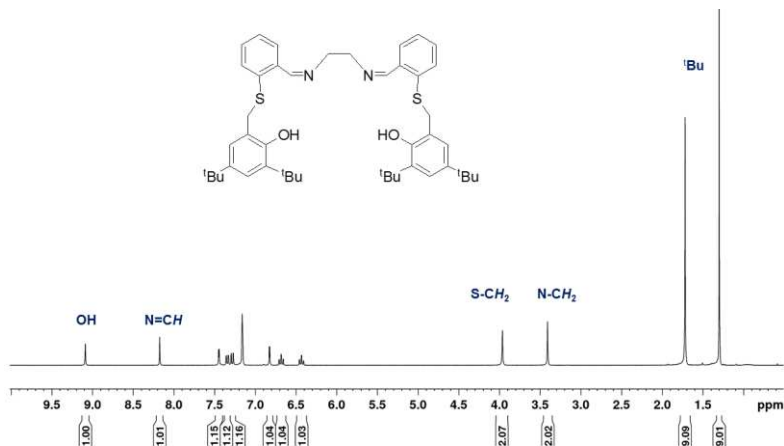


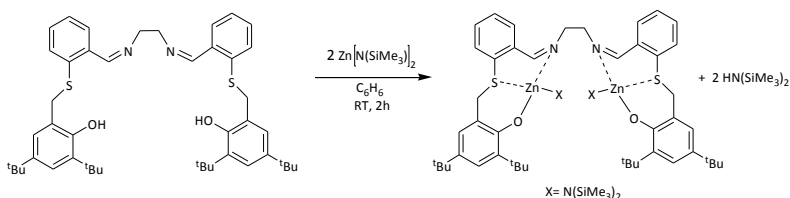
Figure 4.6. ¹H NMR spectrum (400 MHz, C₆D₆, 298K) of OSNNSO ligand.

The MALDI-ToF spectrum (Figure 4.15 in Experimental section) showed three signals: one at 737.417 m/z for the molecular ion, another one at 517,234 m/z indicating the fragment formed after the break of one of the S-CH₂ bond and, finally, a peak at 299.067 m/z indicating the fragment formed after the break of both the S-CH₂ bonds.

The synthetic method requires only three steps and the ligand was synthesized in 1 g scale without any chromatographic purification procedure.

4.2.4. Synthesis of the bimetallic zinc complex

The synthesis of the zinc complex **3** was accomplished by treating the ligand with 2 equivalents of the metal precursor, $\text{Zn}[\text{N}(\text{SiMe}_3)_2]_2$, in benzene (Scheme 4.5.). After two hours at room temperature the benzene was evaporated in vacuum and the product was washed with cold hexane to remove any impurities and the bis(trimethyl silyl) amine formed as a co-product. The dizinc complex appeared as a yellow powder (95 % yield).



Scheme 4.5. Synthesis of the bimetallic zinc complex **3**

^1H NMR spectrum showed the disappearance of the OH signal of the ligand and the appearance of two new broad peaks each integrating for 18 protons of the silylamido group at 0.145 and 0.041 ppm. Moreover, the narrow singlets observed for the methylene protons bound to the sulphur (SCH_2Ar) and to the nitrogen ($\text{NCH}_2\text{CH}_2\text{N}$) in the ligand spectrum, split in three broad signals at 4.98, 4.51 and 3.57 ppm, integrating, respectively, for two, four and two protons. All the other signals due to the protons of the ligand skeleton were shifted downfield with respect to the same signals in the spectrum of the free ligand (see Figure 4.7.).

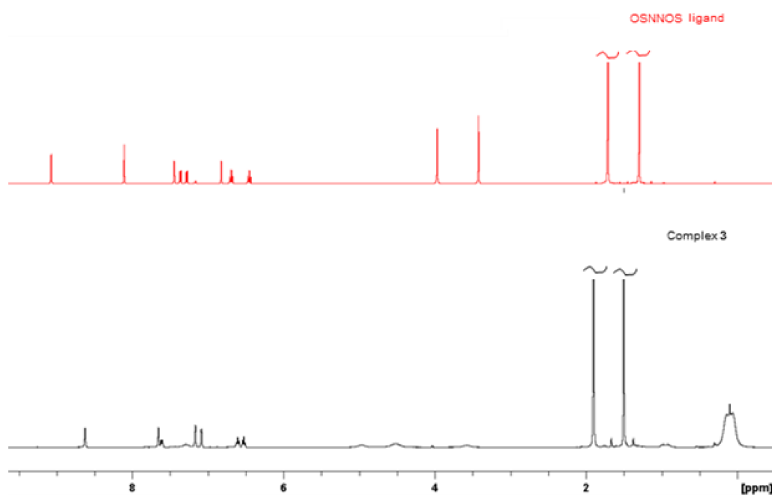


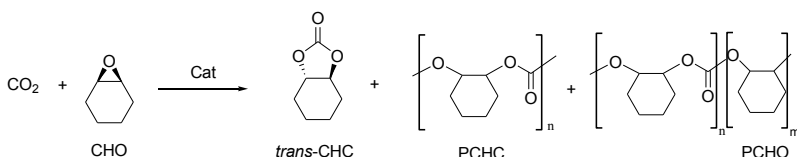
Figure 4.7. ^1H NMR spectrum (400 MHz, C_6D_6 , 298K) of ligand and complex **3**.

These observations supported the coordination of two zinc centers to the anionic and neutral donors of the ligand and revealed that the symmetry of the ligand was retained upon the complex formation, at least in solution. On the other hand, the broadened resonances observed for the methylene protons are consistent with the formation of a fluxional species.

4.2.5. Ring-opening copolymerization of carbon dioxide with cyclohexene-oxide

The dizinc complex was tested for the copolymerization of carbon dioxide and cyclohexene oxide under different reaction conditions and in the absence of cocatalyst (Table 4.2).

In all cases, we were delighted to observe that poly(cyclohexene carbonate) was obtained as the most abundant product. In addition, small percentages of ether linkages and *trans*-cyclohexene carbonate were found in the reaction mixture.



Scheme 4.6. CO_2/CHO reaction promoted by complex **3**.

At 80 °C and under 30 atmosphere of CO_2 pressure a conversion of 10% was obtained (Table 4.2, entry 1). By increasing the reaction temperature, the conversion increased (cf entries 1-3 with entry 1) although at 120 °C an increase in the *trans*-CHC product was also evaluated. *Trans*-CHC are usually generated by backbiting reaction which can occur at the end of the free or metal-bound copolymer, a process that is probably accelerated at a higher temperature.

Prolonging the reaction time the conversion increased showing that catalyst **3** is still active after 64 h of reaction (entry 4).

Two catalytic reactions were carried out under 10 and 20 bar of CO_2 pressure at 100 °C. In these conditions, the conversions decreased with respect to the reaction carried out at 30 bar at the same reaction temperature (cfr entries 5 and 6 vs entry 2).

Table 4.2. CO₂/CHO reaction promoted by complex **1**^[a]

Entry	T (°C)	P _{CO2} (bar)	Conv (%)	PCHC	<i>Trans</i> CHC	PCHO	M _n ^{GPC} (KDa)	Đ
1	80	30	10	93	3	4	5.6	8.9
2	100	30	28	89	4	7	14.6	6.0
3	120	30	29	85	11	4		
4 ^b	100	30	52	93	3	4	6.5	3.3
5	100	20	22	90	1	9		
6	100	10	7	89	8	3	1.3	2.6

^[a] **General conditions:** Complex **1**: = 19.8 μmol (0.05mol%), CHO = 40 mmol, (2000 equiv), time = 16 h. [b] time = 64 h.

The ¹H NMR spectra of the copolymers, in addition to the main signals due to the protons of the copolymer chains, showed two peaks at 3.60 and 4.45 ppm which have been assigned to the methine protons adjacent to the hydroxyl end groups (see Figure 4.8). No signals of other end groups were detectable. The formation of polymeric chain end-capped with hydroxyl groups on both side has been previously explained by other authors. According to Williams,¹³ the hydrolysis of CHO could generate the *in situ* formation of cyclohexane-1,2-diol, which, in turns, acting as a chain

transfer agent, generates a diol as a new initiating species that can propagate from both the two hydroxyl end groups (see Figure 4.8).

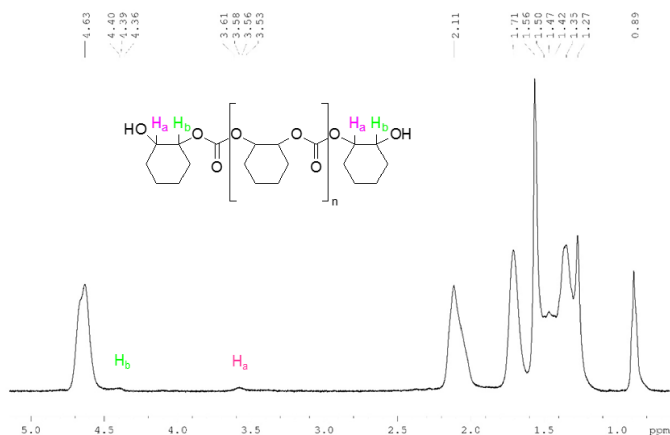


Figure 4.8. ^1H NMR spectrum (400 MHz, CDCl_3 , 298K) of PCHC.

GPC analysis of the polycarbonates showed, in all cases, broad molecular weight distributions ($\text{Đ} = 2.6 \div 8.9$) which could indicate either the formation of multiple active centers and/or the occurrence of post-copolymerization reactions such as hydrolysis, decarboxylation or other degradation.

4.3. Conclusions

With the aim to get dizinc complexes with salalen ligands, the reaction of salalen ligand, with a propylene bridge between two nitrogen donors, with same zinc precursor was carried out. In all cases, the monometallic species was obtained. Probably, the monometallic species is favored with respect to the bimetallic species because tetracoordinate zinc centers are more stable than

tricoordinate zinc centers. These new monometallic salalen zinc complexes were active in the CO₂/PO cycloaddition reaction. Subsequently, with the aim to increase the coordination number of each metal centre, we designed a new class of ligands with additional sulfur donors with respect to the salen ligands. In this work we developed a methodology for the synthesis of these new hexadentate dianionic OSNNSO ligands. In particular, we synthesized the first ligand of this class that present t-butyl groups as the substituents on the phenolate rings and ethylene bridge between the two imino nitrogen atoms. This ligand was characterized by using NMR and MALDI-ToF analysis. Then, the synthesis and the characterization of the corresponding dizinc complex has been performed. This bimetallic zinc complex, in the absence of cocatalyst, was able to produce polycyclohexene carbonate (PCHC) as the most abundant product, although showing low activity.

Worth of noting this new class of ligands offers the opportunity to easily introduce several modifications on the ligand skeleton and, as a consequence, to vary the features of the corresponding metal complexes. In fact, for this new designed class of ligands it is possible to vary both the nature of the nitrogen donor atoms (amine and imine) and the substituents on the aromatic rings in order to increase the activity of the catalyst. Moreover, it is also possible to change the nature of the bridge between the two nitrogen atoms both to vary its flexibility and to tune the distance between the two metallic centers (a crucial parameter for the cooperation mechanism in a bimetallic catalyst).

4.4. Experimental Section

4.4.1 General considerations

All manipulations of air- and/or water-sensitive compounds were performed under a dry N₂ atmosphere by using a Braun Labmaster glovebox or standard Schlenk techniques. The glassware and autoclave used in the polymerization were dried in an oven at 120°C overnight. Benzene and hexane were distilled over sodium benzophenone. Dichloromethane, cyclohexene oxide, and propylene oxide were distilled over calcium hydride. CD₂Cl₂ and C₆D₆ were dried with molecular sieves. All other chemicals were commercially available and used as received unless otherwise stated.

4.4.2. Synthesis of Salalen ligands

The ligands were prepared according to published procedures ¹⁴(rif 1,2) which involves the reaction of condensation of N-methyl- 1,2-diaminoethane with a substituted salicylaldehyde followed by nucleophilic substitution on a substituted bromomethylphenol. The identity of the compound was determined by ¹HNMR.

4.4.3. Synthesis and characterization of complex 1

The synthesis was carried out in a glove-box under a nitrogen atmosphere. In a 20 mL vial with a magnetic stirrer bar, 44.5 mg (3.60×10^{-4} mol) of ZnEt₂ were dissolved in 1 mL of dry benzene. In a 5 mL vial 172.8 mg (3.60×10^{-4} mol) of H₂L₁ were dissolved in 1.5 mL of dry benzene. The ligand solution was slowly added dropwise in the solution containing ZnEt₂, and other 0.5 mL of dry benzene

were used to wash the vial containing the ligand. The resulting mixture was stirred at room temperature for 1 hours. The solvent was then removed under vacuum and the solid residue was washed with Hexane. Complex **1** was obtained as a yellow powder. Yield: 98%.

^1H NMR (300 MHz, CD_2Cl_2 , 298 K): δ 1.285 (s, 9H, CCH_3), 1.396 (s, 9H, CCH_3), 1.887 (m, 2H, CH_2), 2.344 (m, 1H, CH_2), 2.515 (s, 3H, N-CH_3), 3.079 (m, 1H, CH_2), 3.243 (d, $J = 12.3$ Hz, 1H, CH_2), 3.523 (m, 1H, CH_2), 3.702 (m, 1H, CH_2), 4.360 (d, $J = 12.6$ Hz, 1H, CH_2), 6.825 (d, $J = 2.4$ Hz, 1H, Ar-H), 7.064 (d, $J = 2.7$ Hz, 1H, Ar-H), 7.256 (d, $J = 2.4$ Hz, 1H, Ar-H), 7.465 (d, $J = 2.7$ Hz, 1H, Ar-H). 8.092 (s, 1H, C=N)

^{13}C NMR (250 MHz, CD_2Cl_2 , 298 K): δ 27.91 (CH_2), 29.66 (CCH_3), 31.93 (CCH_3), 34.17 (CCH_3), 35.52 (CCH_3), 43.93 (N-CH_3), 57.27 (CH_2), 61.96 (CH_2), 65.30 (CH_2), 117.93 (Cq), 119.43 (Cq), 121.26 (Cq), 124.67 (CH), 126.47 (CH), 128.06 (Cq), 132.83 (CH), 134.13 (CH), 136.65 (Cq), 138.73 (Cq), 162.97 (Cq), 164.36 (Cq), 168.99 (CH=N).

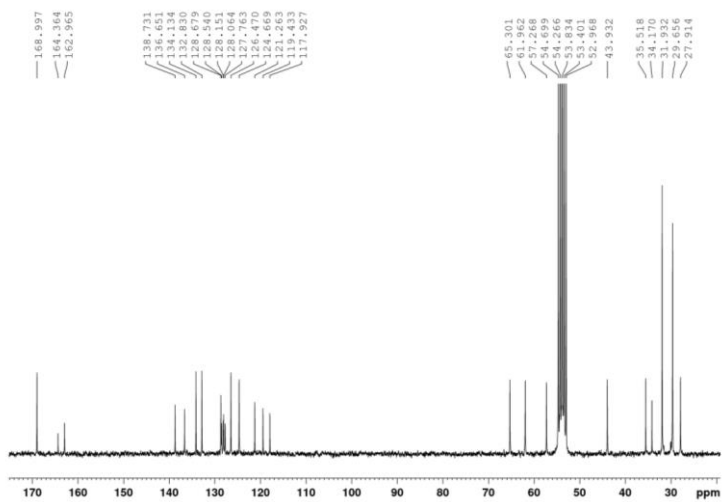


Figura 4.9. ^{13}C NMR spectrum (400 Hz, CD_2Cl_2 , 298K) of complex **1**.

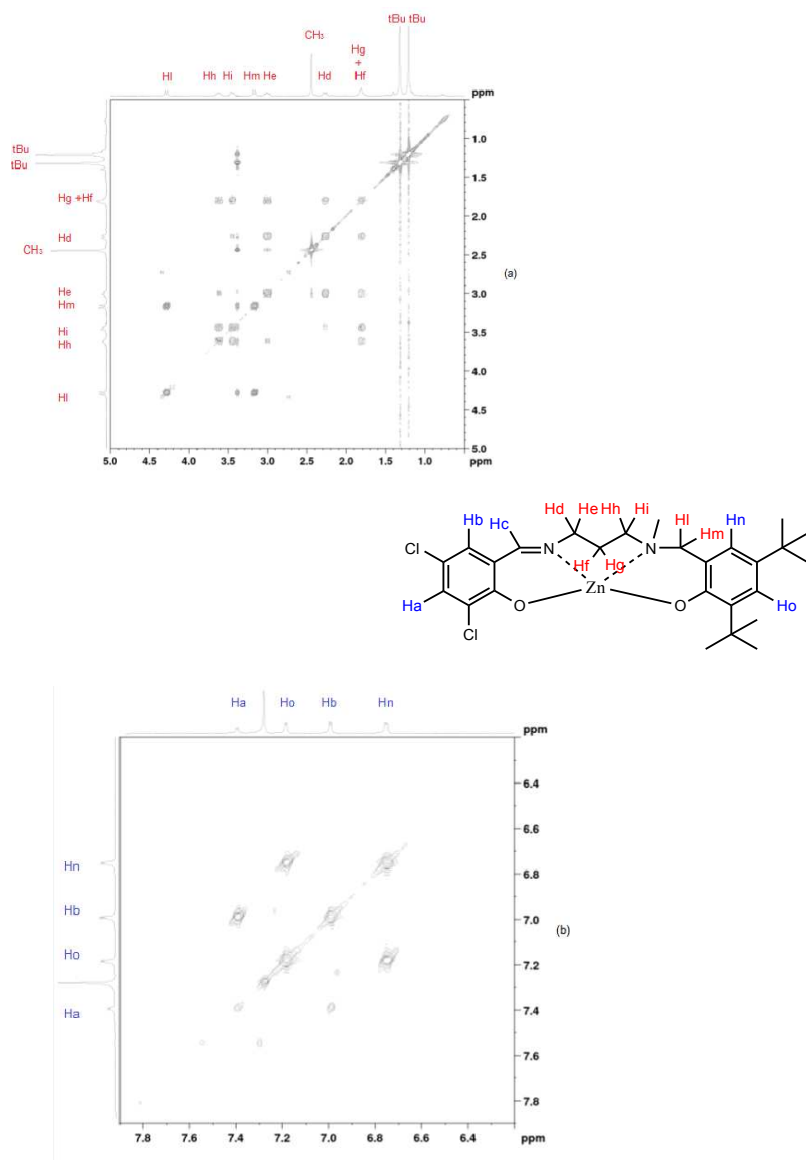


Figure 4.10. 2D COSY NMR spectrum (400 Hz, C_6D_6 , 298K) of complex 1.

4.4.4. Synthesis and characterization of complex 2

The synthesis was carried out in a glove-box under a nitrogen atmosphere. In a 20 mL vial with a magnetic stirrer bar, 32.5 mg (2.63×10^{-4} mol) of ZnEt_2 were dissolved in 1 mL of dry benzene. In a 5 mL vial 126.4 mg (2.63×10^{-4} mol) of H_2L_2 were dissolved in 1.5 mL of dry benzene. The ligand solution was slowly added dropwise in the solution containing ZnEt_2 , and other 0.5 mL of dry benzene were used to wash the vial containing the ligand. The resulting mixture was stirred at room temperature for 1 hours. The solvent was then removed under vacuum and the solid residue was washed with Hexane. Complex **2** was obtained as a yellow powder. Yield: 92%.

^1H NMR (400 MHz, C_6D_6 , 298 K): δ 0.983 (m, 1H, CH_2), 1.126 (m, 1H, CH_2), 1.348 (s, 9H, CCH_3), 1.502 (s, 3H, NCH_3), 1.542 (s, 9H, CCH_3), 1.816 (m, 1H, CH_2), 2.369 (d, $J = 10.4$ Hz, 1H, CH_2), 2.569 (m, 1H, CH_2), 2.725 (m, 1H, CH_2), 2.897 (m, 1H, CH_2), 4.048 (d, $J = 10.7$ Hz, 1H, CH_2), 6.831 (s, 1H, ArH), 6.944 (s, 1H, ArH), 7.365 (s, 1H, ArH), 7.548 (s, 1H, $\text{CH}=\text{N}$), 7.579 (s, 1H, ArH).

^{13}C NMR (400 MHz, C_6D_6 , 298 K): δ 29.02 (CH_2), 30.00 (CCH_3), 31.78 (CCH_3), 34.00 (CCH_3), 35.90 (CCH_3), 39.74 (N-CH_3), 60.68 (CH_2), 61.60 (CH_2), 64.66 (CH_2), 117.63 (CH), 121.03 (Cq), 126.55 (Cq), 127.55 (Cq), 128.81 (CH), 129.16 (CH), 130.52 (CH), 134.17 (Cq), 142.64 (Cq), 157.84 (Cq), 169.85 ($\text{CH}=\text{N}$), 170.43 (Cq).

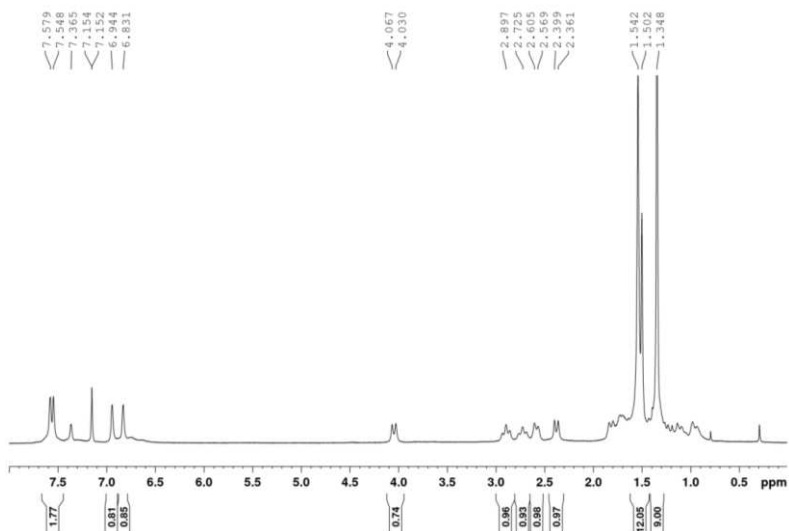


Figure 4.11. ¹H NMR spectrum (400 Hz, C₆D₆, 298K) of complex 2.

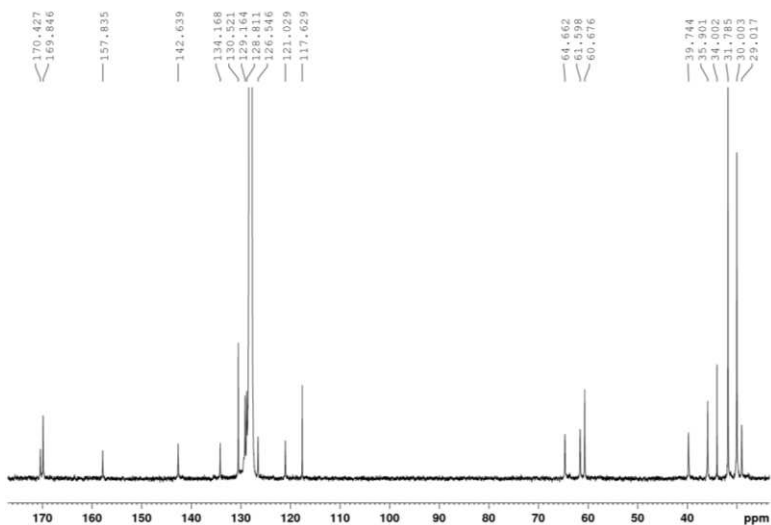


Figure 4.12. ¹³C NMR spectrum (400 Hz, C₆D₆, 298K) of complex 2.

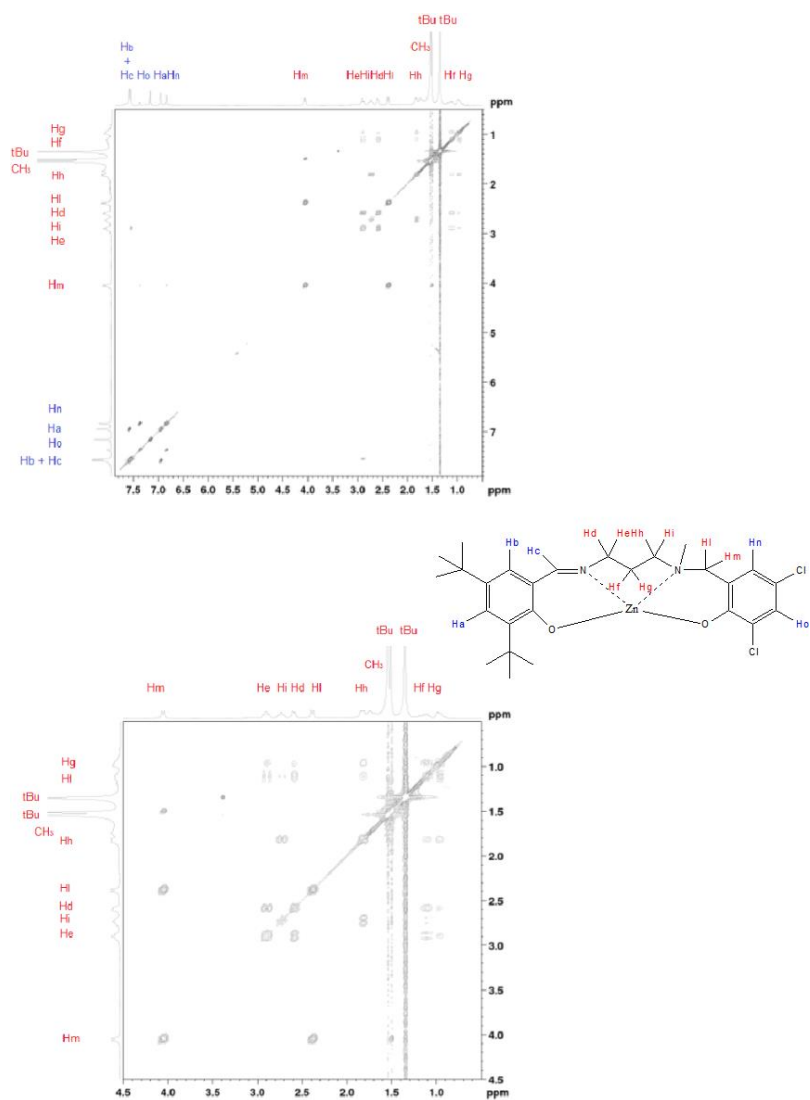


Figure 4.13. 2D COSY NMR spectrum (400 Hz, C₆D₆, 298K) of complex 2.

4.4.5. Synthesis and characterization of the OSNNSO ligand

I Step: Synthesis of 2-Mercaptobenzaldehyde

2-Mercaptobenzaldehyde was prepared according to the literature procedure.¹¹

In an oven-dried 100 mL round-bottom flask equipped with an nitrogen inlet, TMEDA (1.5 mL, 10 mmol; 2.2 equiv.) and thiophenol (0.46 mL, 4.54 mmol; 1.0 equiv.) was dissolved in 15 mL hexane. The resulting solution was cooled to 0 °C and a 1.8 M *n*BuLi solution in cyclohexane (5.5 mL, 10 mmol; 2.2 equiv.) was added dropwise over a few min. The resulting solution was allowed to attain r.t. and stir at r.t. for 16 h. DMF (0.9 mL, 11.35 mmol; 2.5 equiv.) was then added drop wise at r.t. and the resulting solution was allowed to stir at r.t. for 20 h. Et₂O (20 mL) was added and stirred for another 20 min. The reaction mixture was washed with 1 M HCl (50 mL) and the aqueous layer was back-extracted with Et₂O (2 × 20 mL). The combined organic layer was dried over anhydrous MgSO₄ and concentrated in vacuo to obtain orange oil.

II Step: Synthesis of 2-(3,5 ditertbutyl-2-hydroxybenzyl) sulfanyl benzaldehyde

2-(3,5 ditertbutyl-2-hydroxybenzyl) sulfanyl benzaldehyde was prepared according to the literature procedure¹²

To a stirred solution of 2-mercaptobenzaldehyde (1.041 g, 7.535 × 10⁻⁶) and K₂CO₃ (4.165 g, 30.1 mmol) in DMF (83 mL) at room temperature was added dropwise a solution of 2-(bromomethyl)-4,6-di-*tert*-phenol (2.255g, 7.535 × 10⁻⁶ mmol) in dry DMF (18 mL).

The flask was left to stir at room temperature for 3 h. 50 mL of water and 50 mL of diethyl ether were added. The organic layer was washed with water (3 x 30 mL) and brine (3 x 30 mL). The solution was dried over sodium sulfate and then filtered. The solvent was removed under vacuum yielding a white yellow solid that was recrystallized from pentane as a white solid, and collected by vacuum filtration.

III Step: Synthesis of OSNNSO ligand

To a stirred solution of 2-(3,5 ditertbutyl-2-hydroxybenzyl) sulfanyl benzaldehyde (1.628 g, 4.565×10^{-6} mmol) in dry acetonitrile (33 mL) at room temperature was added dropwise a solution of ethylenediamine (153 μ L, 2.289×10^{-6} mmol), in dry acetonitrile (24 mL). The flask was left to stir at room temperature for 2 h. After this time a white solid was precipitated. It was washed with cold pentane and dried using the trap-by-trap system. The formation of the desired species was confirmed by NMR analysis. Yield: 51%

^1H NMR (300 MHz, C_6D_6 , 298 K): δ 1.298 (s, 9H, tBu), 1.718 (s, 9H, tBu), 3.408 (s, 2H, N-CH₂-CH₂-N), 3.963 (s, 2H, ArC-CH₂-S), 6.430 (t, 1H, Ar-H), 6.654 (t, 1H, Ar-H), 6.820 (s, 1H, Ar-H), 7.294 (d, 1H, Ar-H), 7.328 (d, 1H, Ar-H), 7.451 (s, 1H, Ar-H), 8.174 (s, 1H, OH) 9.088 (s, 1H, CH=N).

^{13}C NMR (300 MHz, CD_2Cl_2 , 298 K): δ 30.16 (CCH_3)₃, 31.69 (CCH_3)₃, 34.49 (CCH_3)₃, 35.45 (CCH_3)₃, 38.56 (N-CH₂), 61.96 (S-CH₂), 123.96 (CH), 124.14 (CH), 128.79 (CH), 129.41 (CH), 130.90 (CH), 135.17 (Cq), 137.84 (Cq), 138.43 (Cq), 143.01 (Cq), 152.00 (Cq), 164.16 (CH=N).

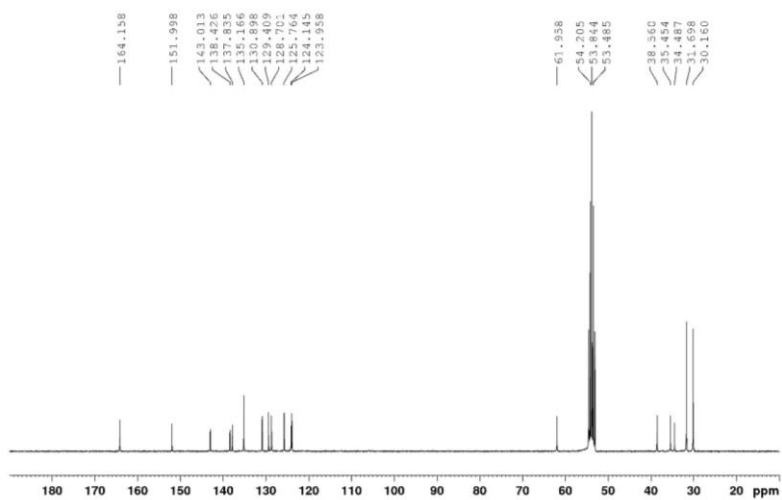


Figura 4.14. ^{13}C NMR spectrum (400 Hz, CD_2Cl_2 , 298K) of OSNNSO ligand.

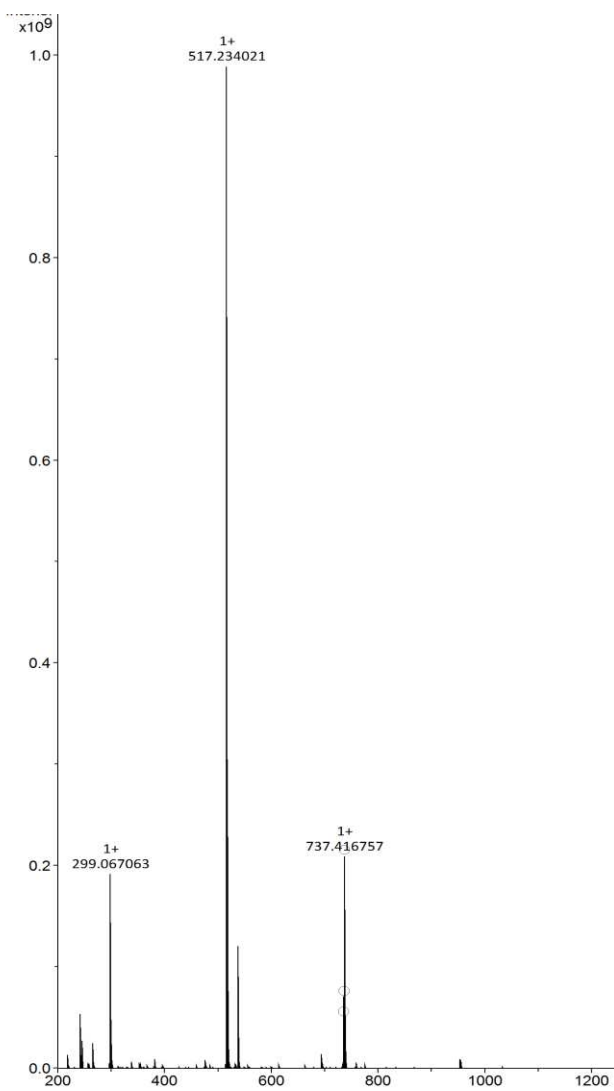


Figure 4.15. MALDI-TOF mass spectrum of OSNNSO ligand.

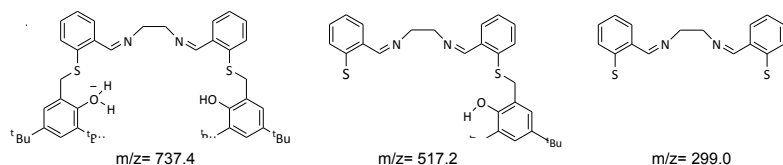


Figure 4.16. Fragmentations observed in the MALDI-ToF spectrum of the OSNNSO ligand.

4.4.6. Synthesis and characterization of complex 3

The synthesis was carried out in a glove-box under a nitrogen atmosphere. In a 20 mL vial with a magnetic stirrer bar, 157.2 mg (4.07×10^{-4} mol) of $\text{Zn}[\text{N}(\text{SiMe}_3)_2]_3$ were dissolved in 3 mL of dry benzene. In a 5 mL vial 150 mg (2.03×10^{-4} mol) of OSNNSO ligand were dissolved in 6 mL of dry benzene. The ligand solution was slowly added dropwise in the solution containing $\text{Zn}[\text{N}(\text{SiMe}_3)_2]_3$ and other 0.5 mL of dry benzene were used to wash the vial containing the ligand. The resulting mixture was stirred at room temperature for 2 hours. The solvent was then removed under vacuum and the solid residue was washed with Hexane. Complex **3** was obtained as a yellow powder. Yield: 95%.

^1H NMR (400 MHz, C_6D_6 , 298 K): δ 0.077 (br, 36H, $\text{Si}(\text{CH}_3)_3$), 1.507 (s, 18H, CCH_3), 1.902 (s, 18H, CCH_3), 3.569 (br, 2H, CH_2), 4.510 (br, 4H, CH_2), 4.972 (br, 2H, CH_2), 6.521 (t, 2H, Ar-H), 6.606 (t, 2H, Ar-H), 7.082 (s, 2H, Ar-H), 7.289 (br, 2H, Ar-H), 7.617 (d, $J = 8$ Hz, 2H, Ar-H), 7.653 (s, 2H, Ar-H), 8.626 (s, 2H, $\text{CH}=\text{N}$)

^{13}C NMR (400 MHz, C_6D_6 , 298 K): δ 1.611(2 $\text{Si}(\text{CH}_3)_3$), 30.437 (2 CCH_3), 32.330 (2 CCH_3), 34.322 (2 CCH_3), 35.709 (2 CCH_3), 53.311 (2 CH_2), 61.692 (2 CH_2), 122.344 (2 CH), 122.895 (2 Cq), 124.537 (2 CH), 128.218 (2 Cq), 131.393 (2 CH), 135.808 (2 CH),

136.470 (2 Cq), 137.791 (2 Cq), 138.939 (2 CH), 150.251 (2 Cq),
164.65 (2 Cq), 178.855 (2 CH=N),

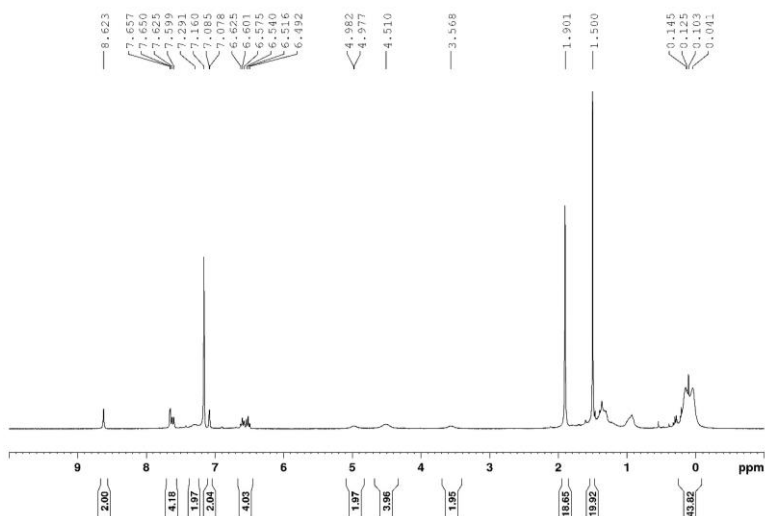


Figure 4.17. ^1H NMR spectrum (400 Hz, C_6D_6 , 298K) of complex **3**.

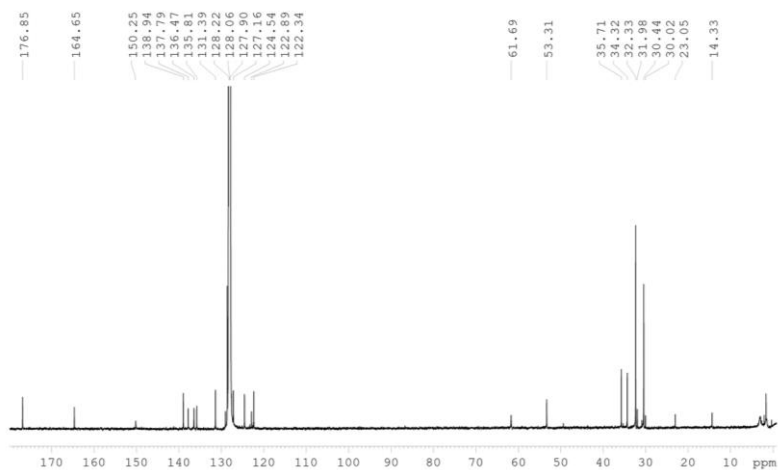


Figure 4.18. ^{13}C NMR spectrum (400 Hz, C_6D_6 , 298K) of complex **3**.

References

- 1 M. S. Holzwarth, B. Plietker, *ChemCatChem* **2013**, 5, 1650–1679.
- 2 A. Decortes, A. M. Castilla, A. W. Kleij *Angew. Chem. Int. Ed.* **2010**, 49, 9822–9837.
- 3 Y. M. Shen, W. L. Duan, M. Shi, *J. Org. Chem.*, **2003**, 60, 1559-1562.
- 4 A. Decores, M. M. Belmonte, J. B. Buchholz, A. W. Kleij *Chem. Commun.*, **2010**, 46, 4580-4582.
- 5 X. D. Lang, Y. C. Yu, L. N. He, *Journal of Molecular Catalysis A: Chemical*, **2016**, 420, 208-215.
- 6 M. Cheng, D. R. Moore, J. J. Reczek, B. M. Chamberlain, E. B. Lobkovsky and G. W. Coates, *J. Am. Chem. Soc.*, **2001**, 123, 8738-8749.
- 7 S. Kissling, M. W. Lehenmeier, P. T. Altenbuchner, A. Kronast, a M. Reiter, P. Deglmann, U. B. Seemann and B. Rieger, *Chem. Commun.*, **2015**, 51, 4579—4582.
- 8 Y. L. Xiao, Z. Wang, K. L. Ding, *Chem. Eur. J.*, 2005, 11, 3668-3678.
- 9 M. R. Kember, P. D. Knight, P. T. R. Reung, C. K. Williams, *Angew. Chem., Int. Ed.*, 2009, 48, 931-933.
- 10 M. Cozzolino, K. Press, M. Mazzeo, M. Lamberti, *ChemCatChem* **2016**, 8, 455-460.
- 11 A. R. Choudhury, S. Mukherjee, *Adv. Synth. Catal.* **2013**, 355, 1989 – 1995.
- 12 M. Lamberti, M. Mazzeo, C. Pellecchia, *Dalton Trans.*, **2009**, 41, 8831–8837
- 13 F. Jutz, A. Buchard, M. R. Kember, S. B. Fredriksen, C. K. Williams, *J. Am. Chem. Soc.* **2011**, 133, 17395–17405.
- 14 A. Yeorl, S. Gendler, S. Groysman, I. Goldberg, M. Kol, *Inorg. Chem. Commun.*, **2004**, 7, 280-282.

CHAPTER 5

Organocatalyzed Domino [3+2] Cycloaddition/Payne-Type Rearrangement using Carbon Dioxide and Epoxy Alcohols

During my third year of PhD, I spent a research period (October 2nd 2017- April 2nd 2018) at the laboratories of ICIQ, Institut Català d'Investigació Química, working under the supervision of Prof. Arjan W. Kleij. During this period I had the opportunity to take part to the research project: *“Organocatalyzed Domino [3+2] Cycloaddition/Payne-Type Rearrangement using Carbon Dioxide and Epoxy Alcohols”*.

In the chapter 5 is described an unprecedented organocatalytic approach towards the formation of highly substituted cyclic carbonates from the coupling reaction of tri- and tetra-substituted oxiranes and carbon dioxide.



5.1. Introduction

5.1.1. Synthesis of cyclic carbonates promoted by metal catalysis and organocatalysis

As mentioned in chapter 1, cyclic carbonates can be produced by CO₂ coupling reaction with epoxides. Cyclic carbonates show very interesting properties such as low evaporation rates, low toxicity and biodegradability.¹ These characteristics are industrially researched, in fact they find applications such as aprotic polar solvents with high boiling point, electrolytes for lithium-ion batteries, precursors of polymeric materials,² fine chemical intermediates, fuel additives, plastics.³ Furthermore, the use of CO₂ in their synthesis is a greener alternative to the use of phosgene^{3,4} typically used in combination with diols.

However, in the CO₂ molecule the carbon atom is in the most oxidized state and the activation barrier for the coupling reaction of CO₂ with epoxides was estimated to be between 50 and 70 kcal mol⁻¹.⁵ Considering that catalysis plays an important role to make this transformation possible, research has been focused on the development of a wide range of catalysts. Both catalysts based on metals and organocatalysts have been described in the literature, as promoters of the CO₂ coupling reaction with epoxides. It is known that metal-based catalysts which activate and/or stabilize the substrates/intermediates through coordination, are much more efficient than organ-based catalytic mediators.

On the other hand, the organocatalysts are non-toxic, economic molecules and are usually highly stable to air and humidity and, in some cases, they can have the advantage of being obtained from renewable sources.⁶ However, generally the organocatalysis

requires high energy, in fact, it is usually necessary to operate under high temperatures and pressures, for long reaction times and with large amounts of catalyst. Nevertheless, the organocatalysis is advantageous for the synthesis of products or to develop processes without metal, in fact, the absence of metals within its structure make these catalysts the first choice for application in process where metal toxicity issues are of great relevance, for example, in the pharmaceutical industry.

Several organocatalytic systems (Figure 5.1.) have been reported to be active in the synthesis of cyclic carbonates.^{6,7,8,9} These can be amines and organic bases,^{10,11,12,13} ionic liquids and organic salts (ammonium-, phosphonium-, imidazolium- and pyrrolidinium-based).^{14,15} N-heterocyclic carbenes (NHCs)^{16,17} and hydrogen bond donors (HBDs). This last class of organocatalysts (HBDs) is very interesting, because, they are able to assist the activation of the hydrogen bond epoxide, facilitating nucleophilic attack towards epoxide, during the ring-opening phase. As important limitation, they require to operate in combination with a nucleophilic source that, depending on its origin related to the catalyst structure (internal or external), lead to two types of systems: binary or bifunctional organocatalytic systems.

The most common hydrogen bonds donors are alcohols and diols,¹⁸ fluorinated alcohols,¹⁹ boronic acids,²⁰ silanols,²¹ carboxylic acids,²² amino alcohols,²³ amino acids,^{22,24} azaphosphatranes²⁵ and ureas.²⁶

Anions: Cl^- , Br^- , I^- , OH^- , H^- , AcO^- , HCO_3^- , HSO_4^- , BF_4^- , PF_6^-

Cations:

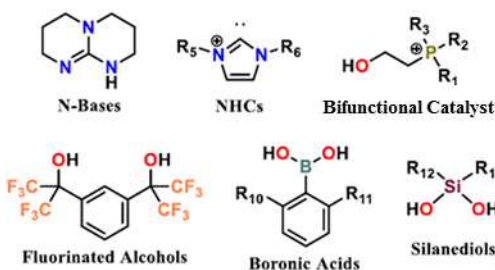


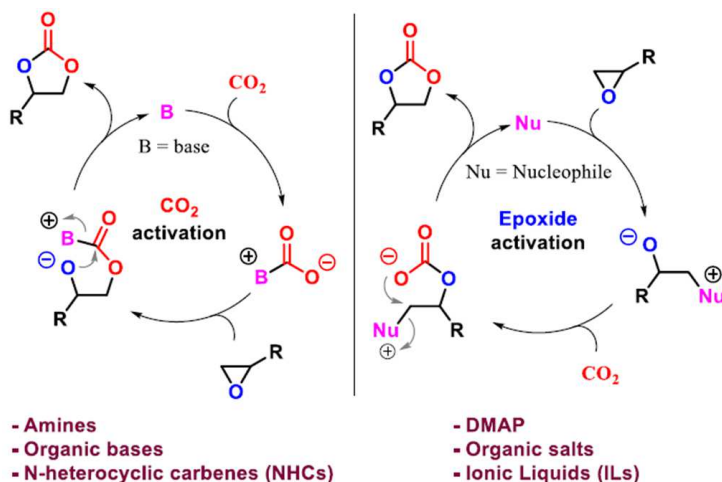
Figure 5.1. List of the most common organocatalysts applied to the synthesis of cyclic carbonates.

5.1.2. Mechanisms proposed for organocatalysts

For the organocatalyzed CO_2 /epoxide reaction, the proposed mechanism varies according to the selected catalyst and to the species involved in activation. Essentially, two mechanisms can be outlined:

1) “direct CO_2 activation pathway” or “halide free activation pathway”. In this case, the target molecule for activation is carbon dioxide (scheme 5.1. on the left). The catalyst coordinates the CO_2 molecule generating a stable catalyst- CO_2 adduct.²⁷ Then, the adduct ring-opens the epoxide and the resulting species evolves towards the formation of the cyclic carbonate product and the regeneration of the catalyst. This mechanism is generally promoted by nitrogen-based heterocycles (amines, organic bases or N-heterocyclic carbenes).

2) “direct epoxide activation pathway”. In this case the target molecule of activation is the epoxide (Scheme 5.1, on the right). First, the nucleophilic species ring opens the epoxide leading to the formation of the surrogated alkoxide. The enhanced nucleophilicity of this new intermediate makes possible the attack of the alkoxide to the carbon dioxide molecule, that, after carbonate ring closure and nucleophile regeneration, generates the desired cyclic carbonate.²⁸



Scheme 5.1. General proposed mechanisms for the coupling reaction of carbon dioxide and epoxides. Carbon dioxide activation mechanism (left) and epoxide activation mechanism (right).

5.1.3. The importance of highly substituted carbonates

The epoxide activation pathway is very efficient for the conversion of mono and disubstituted epoxides and the efficiency of the process can be improved by addition of hydrogen bond donors or under Lewis acid catalysis.^{29,30} Despite the considerable progress

made over the years in this field, the use of tri- and even tetrasubstituted epoxides as coupling partners, is still extremely challenging, due to the steric requirements of these substates.^{31,32} The importance of highly substituted carbonates is demonstrated by the presence in nature of different compounds such as, for example, triterpenoid carbonate Chukvelutin D and sesquiterpenoid Hololeucin carbonate which contain such substituted cyclic carbonates in their skeletons (Figure 5.2).³³ Up to now, no synthetic strategy has been reported for the production of tetra-substituted cyclic carbonates, although there are biosynthetic paths to these complex structures.

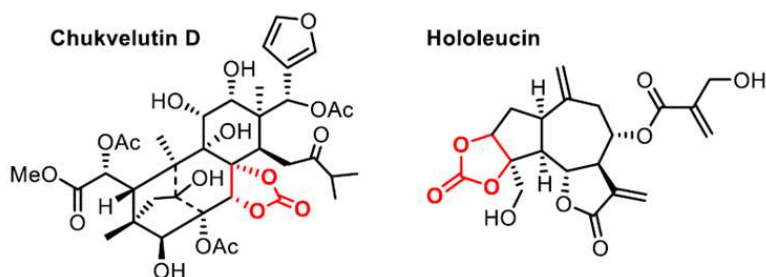
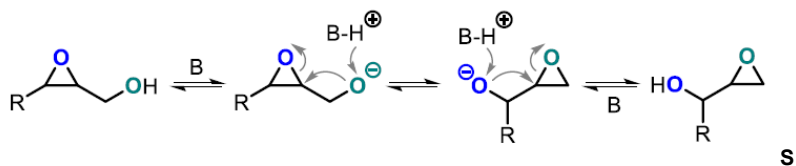


Figure 5.2. Natural products with cyclic carbonate functionalities within their structure.

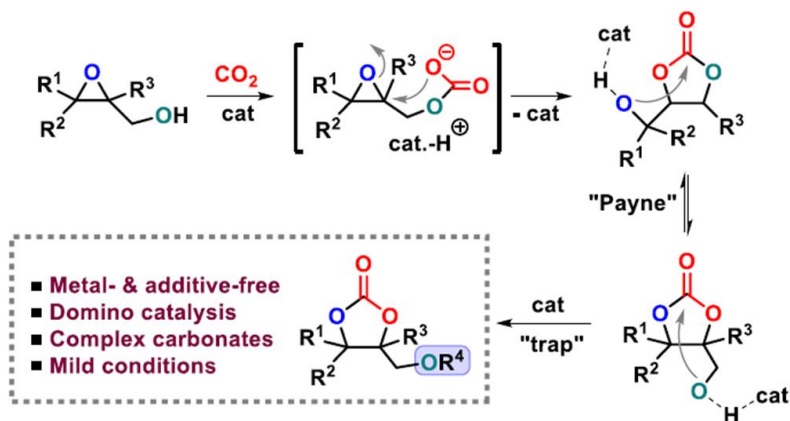
As known in the literature, epoxyalcohols undergo the transformation called Payne rearrangement (Scheme 5.2).³⁴ In the presence of a strong base, the epoxide undergo the corresponding alkoxide, followed by direct intramolecular attack at the epoxide. Then an isomeric alkoxide with inverted stereochemistry in C-2 is generated.



cheme 5.2. Payne rearrangement of 1,2-epoxy alcohols.

Kleij's group envisioned the possibility to induce a similar transformation in a previously generated cyclic carbonate allowing the access to new cyclic carbonate structures.^{32,35,36}

Recently, Kleij reported a substrate-controlled divergent synthesis of cyclic carbonates from epoxyalcohols under Al(III) catalysis. This work showed the potential of the Al-catalyst to act as a bifunctional entity with proton-relay capabilities and a crucial role for the alcohol unit of the substrate. Based on these considerations, Kleij reasoned that a proper organocatalyst could combine both potential of proton displacement, mediating the synthesis of cyclic carbonate from an epoxy alcohol and CO₂, and subsequently inducing an assisted base Payne rearrangement of hydroxymethyl-substituted cyclic carbonate. Selective trapping of the most reactive hydroxymethyl carbonate (Scheme 5.3), would allow a simple and conceptually new way to a structurally elusive formation of tetrasubstituted cyclic carbonates.



Scheme 5.3. New strategy for the synthesis of highly substituted cyclic carbonates.

Herein we present a new domino strategy, metal- and nucleophile-free, and generally applicable towards [3+2] cycloadditions involving highly substituted epoxy alcohols and CO₂ as substrates. As far as we are aware, this catalytic process is unprecedented in product scope and (in this respect) outcompetes all metal-based catalytic approaches reported to date.

5.2. Results and discussion

5.2.1 Monosubstituted epoxides

In the first moment, we focus our attention on the reaction of CO₂ with glycidol (**A**), as a benchmark substrate (Scheme 5.4).



Scheme 5.4. Reaction of glycidol (**A**) and CO₂ into its respective cyclic carbonate.

Different organocatalysts were used as catalysts in this reaction (figure 5.3). The reaction were carried out at 45°C, 10 bar of CO₂ pressure; the obtained results are summarized in the Table 5.1. It has been interesting to note that in the presence of DBU as catalyst, the cyclic carbonate **1** can easily be prepared with yield up to 95% (85% isolated) (Table 5.1, entry 7). Several N-bases have been tested, many of which have been shown to be active in the CO₂ / glycidol reaction producing the corresponding cyclic carbonate.

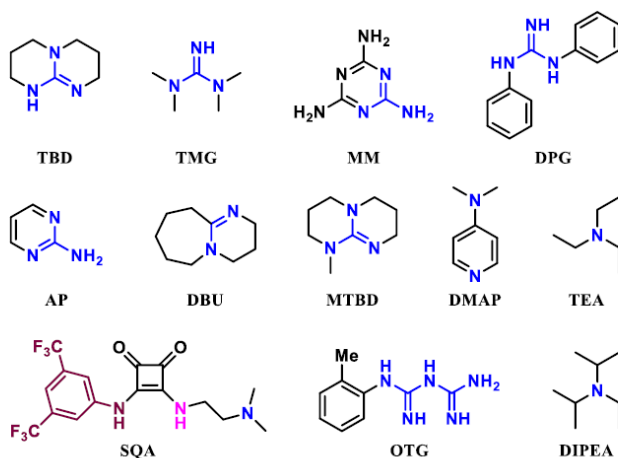
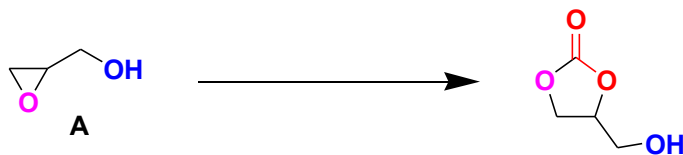


Figure 5.3. N-heterocyclic bases used in this study.

TBD (Table 5.1, entry 1, 91%), MTBD (Table 5.1, entry 8, 90%) and DMAP (Table 5.1, entry 10, 90%) produced glycidol carbonate with very high yields. As far as TMG is concerned despite the excellent NMR yield obtained (Table 5.1, entry 2, 95%), the NMR analysis of the raw product shows the presence of polyethers. Other organocatalysts such as OTG and TEA (Table 5.1, entries 5 and 9)

produced glycerol carbonate with moderate to good yields. While all the others N-containing bases investigated, including guanidine derivatives MM, DPG and AP (Table 5.1, entries 3, 4 and 6), tertiary amines DIPEA, (Table 5.1, entry 11) and a bifunctional squaramide with a tertiary amine pending group (Table 5.1, entry 12), gave very low yields.

Table 5.1. Screening of the catalytic activity of different organocatalysts in the conversion of glycidol **A** towards the corresponding cyclic carbonate.



Entry	Catalyst	Yield / %
1	TBD	91
2	TMG	95 ^a
3	MM	0
4	DPG	11
5	OTG	60
6	AP	3
7	DBU	95
8	MTBD	90
9	TEA	78
10	DMAP	90
11	DIPEA	-
12	SQ	26
13	No catalyst	1

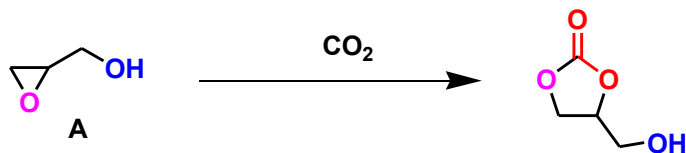
General conditions: Autoclave: glycidol (8.0 mmol), catalyst loading (5.0 mol%), mesitylene (10 mol%), MEK (5.0 mL), 45 °C, 18 h, P_{CO2} = 10 bar; ^a Polyether also formed (3%).

The coupling reaction of CO₂ with glycidol promoted by the DBU was studied by varying the reaction conditions, in particular the effect of the amount of catalyst, the concentration of glycidol, the

temperature and the pressure, on the progress of the reaction, was studied. The results obtained are summarized in Table 5.2.

As can be seen from entry 1 in Table 5.2 no improvement in yield was observed by increasing the catalyst loading up to 10% mol, while the reduction of the catalyst loading to 1% mol, showed a yield of 69% (Table 5.2, entry 3). With regard to the effect of glycidol concentration on the progress of the reaction (Table 5.2, entries 4-6), the best results were observed working with concentrated systems ($> 1\text{ M}$). Furthermore, it can also be noted that the presence of solvent is essential to decrease the viscosity of the system during the reaction (Table 5.2; entries 7 and 9). As expected, a decrease in the operating temperature reduces the yield (Table 5.2; entries 7 and 8) while an increase in pressure does not lead to any improvement in the amount of glycidol carbonate produced (Table 5.2; entries 3 and 8). Finally, only low yields were found when methyl glycidol was used as a substrate, pointing to a key role of the hydroxyl group in the epoxy substrate (Table 5.2, entry 10).

Table 5.2. Screening of reaction conditions in the DBU-mediated synthesis of carbonate 1.



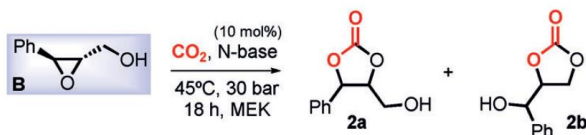
Entry	Glycidol / mmol	DBU. / mmol%	[M]	T / °C	P / bar	t / h	MEK / mL	Yield / %
1	8	10	1.6	45	10	18	5	92
2	8	5	1.6	45	10	18	5	95 ^a
3	8	1	1.6	45	10	18	5	69
4	2	5	0.4	45	10	18	5	69
5	2	5	1	45	10	18	2	>99
6	2	5	2	45	10	18	1	>99
7	8	5	1.6	rt	10	18	5	43
8	8	1	1.6	45	30	18	5	70
9	8	1	neat	rt	10	18	neat	34
10	8 ^b	5	1.6	45	10	18	5	9

General conditions: Autoclave, glycidol (amount indicated), DBU (amount indicated), MEK, 45 °C, P_{CO_2} = 10 bar, 18 h; ^aIsolated yield 85%;

^bMethyl glycidol used as substrate.

5.2.1. Disubstituted epoxides

Motivated by the excellent results obtained for glycidol, more stimulating substrates were tested (disubstituted epoxy alcohols) and (R, R) -phenyl glycidol (**B**) was selected as the reference substrate (Scheme 5.5)

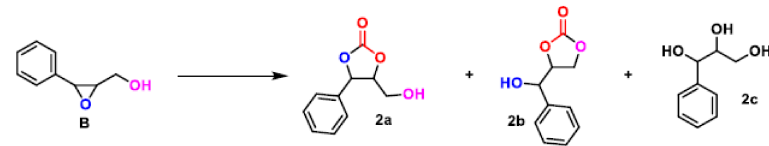


Scheme 5.5. Reaction phenyl glycidol (**B**) and CO_2 into its corresponding cyclic carbonates.

With this substrate, only the N-containing bases which gave the best results in previous screening reactions that involved glycidol, were tested (Table 5.1). The reactions were carried out under the previously optimized conditions (45°C , 30 bar and a catalyst loading of 10 mol%).

For this internal epoxide, TBD and DBU have shown the best catalytic characteristics, in fact we can see the best yields towards the production of carbonates **2a** and **2b**. Moreover, for these reactions, the formation of a triol product, was also detected by the NMR (Table 5.3, entries 1 and 2). The use of DMAP has shown moderate results in terms of overall yield, but greater selectivity for the production of mono-substituted cyclic carbonate **2a** and **2b** (Table 5.3, entry 3). DIPEA and TEA did not show any catalytic activity (Table 5.3, entries 4 and 5) while the TBAB nucleophile produced only a 7% yield for the cyclic carbonate mixture (ratio **2a** / **2b** = 55:45).

Table 5.3.: Screening of the catalytic activity of different organocatalysts in the conversion of phenylglycidol **B**



Entry	Catalyst	Conv / %	2a / %	2b / %	2c / %
1	TBD	>99	8	72	20
2	DBU	>99	25	62	13
3	DMAP	45	7	93	0
4	DIPEA	0	0	0	0
5	TEA	0	0	0	0
6	TBAB	7	55	45	0

General reaction conditions: HEL multi-reactor, phenyl glycidol (0.30 mmol), catalyst loading (10 mol%), 45 °C, P_{CO_2} = 30 bar, MEK (1.0 mL).

5.2.3. Trisubstituted epoxides

DBU and TBD showed similar activity in the CO_2 / (R, R) -phenyl glycidol (**B**) reaction both yielding complete conversions, however TBD showed greater selectivity as evidenced by the ratio between the produced cyclic carbonates (for TBD 2a: 2b = 1: 9 whereas for DBU 2a: 2b = 1: 2.5, see entries 1 and 2 Table 5.3).



Scheme 5.6. Reaction of a trisubstituted epoxide (**C**) and CO_2 into its respective cyclic carbonates.

For this reason, TBD was chosen as catalyst to optimize the reaction conditions in the CO_2 / trisubstituted epoxide (**C**) reaction. The results obtained are summarized in Table 5.4.

Surprisingly, working under conditions similar to those previously applied, (45 ° C, 10 bar of CO₂ and 10 mol% of TBD) the quantitative conversion of the trisubstituted epoxide **C** in the cyclic carbonates **3a** and **3b** with a ratio of the products 3a: 3b = 7: 3, was observed (Table 5.4, entry 2). As expected, both a reduction in the catalyst loading (Table 5.4, entry 3) and a reduction in the operating temperature (Table 5.4, entry 4) produced a drastic reduction in the reaction yield. Moreover, the reaction carried out in more drastic reaction conditions, *i.e.* 80 °C and at a CO₂ pressure of 30 bar, showed the same efficiency of the reaction carried out at 45 °C and 10 bar, generating the same mixture of cyclic carbonates but with increasing traces of triol (Table 5.4, entry 5).

Table 5.4. Screening of reaction conditions for the conversion of trisubstituted epoxy alcohol **C**.

Entry	TBD / mol%	Solvent	Conv / %	4.3b1 / %	4.3b2 / %
1	20	MEK	>99	70	30
2	10 ^a	MEK	>99	69	31
3	5	MEK	80	60	40
4	20	MEK	13 ^b	60	40
5	10	MEK	>99 ^{c, d, e}	63	29
6	10	MEK	>99 ^f	69	31
7	10	MEK	>99 ^g	68	32
8	10	EtAcO	25	80	20
9	10	HCCl ₃	47	64	36
10	10	DCM	92	63	32
11	10	THF	39	52	48
12	10	ACN	>99	70	30
13	10	MeOH	58	70	30

General reaction conditions: Autoclave, substrate (1.0 mmol), 45 °C, P_{CO_2} = 10 bar, 18 h, solvent (5.0 mL). ^aThe use of DBU gave the same results compared to TBD under similar conditions. ^bRoom temperature. ^cT = 80 °C. ^d P_{CO_2} = 30 bar. ^eAlso triol (8 %) was formed; ^f72 h. ^gMEK (1.0 mL).

As can be seen from Table 5.4, no significant variations in the selectivity of the examined reaction, were observed neither by varying the reaction time nor by varying the concentration of the system (Table 5.4, entries 6 and 7).

In addition, various solvents have been used, such as MEK, EtOAc, CHCl₃, DCM, THF, ACN and MeOH (Table 5.4, entries 7-13); the

best results were obtained with the MEK and the ACN. Finally, surprisingly, working under the optimized conditions, when TBD was replaced by DBU the same experimental results were achieved. The combined results of Table 5.4 strongly suggest that a thermodynamic mixture of carbonates is typically formed, with carbonate **3a** being the major component.

5.2.4. Selective protection of the primary alcohol

Since **3a** cannot be obtained through classical nucleophilic ring opening of the epoxide, its formation was ascribed to an equilibration between **3a** and **3b** under the experimental conditions, with the base (TBD or DBU) playing a key role.

Table 5.5. Study of the activity for different catalytic acetyl transfer reactions.

Entry	Catalyst	Time / [h]	Conversion / [%]
1	TBD	1	>99
2	DBU	4	>99
3	—	72	<1

General reaction conditions: Cyclic carbonate mixture (0.34 mmol; ratio **3a:3b** = 7:3), catalyst loading (20 mol%), MEK (1.7 mL), 1-acetylimidazole (1.5 equiv.), rt.

This hypothesis was confirmed as the isolated mixture of cyclic carbonates (ratio **3a:3b** = 7:3) was selectively and quantitatively

converted into the acetyl-protected trisubstituted carbonate **4** (see figure 5.4.), in the presence of 1-acetylimidazole and TBD or DBU (Table 5.5; entries 1 and 2), while in the absence of any catalyst, no conversion was observed.

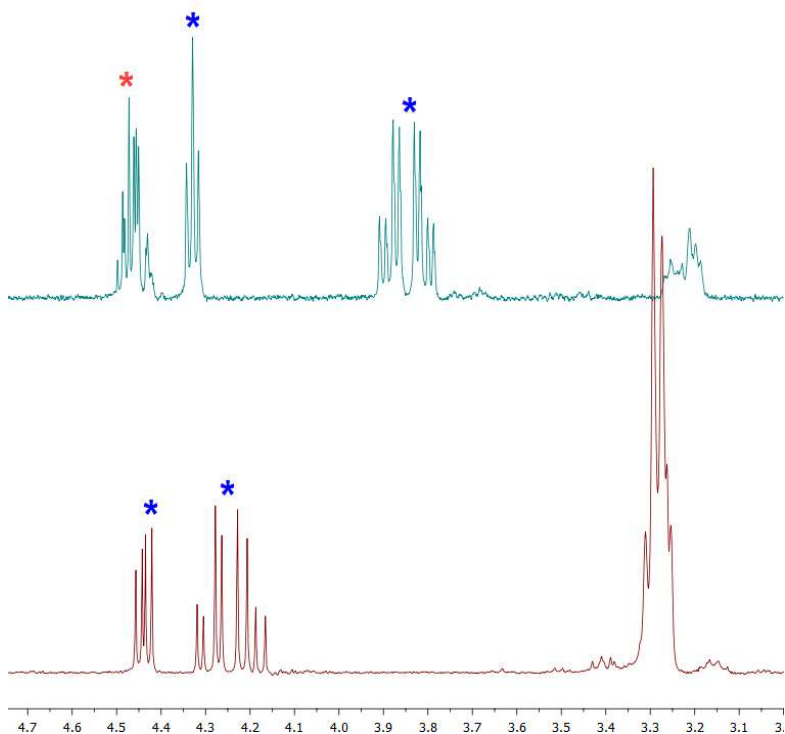
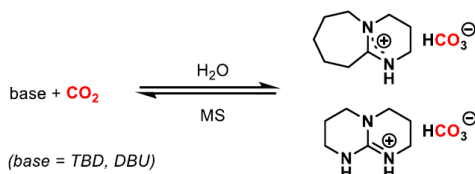


Figure 5.4. Selected ¹H-NMR region (3.0–4.7 ppm) of the carbonate product mixture (top; red and blue stars) and selective formation of product **4** (blue stars) after *in situ* acetylation (bottom).

5.2.5. One pot synthetic protocol

Next, we focused our attention on the development of an *in situ* protection protocol that avoids the isolation of the previously formed cyclic carbonate mixture. In the coupling reaction of CO₂ with tri-substituted epoxides to produce their corresponding cyclic carbonates, TBD and DBU have similar behaviors, in terms of cyclic carbonate formation and selective primary alcohol protection. DBU was selected as the preferred catalyst because it is cheaper, furthermore DBU should promote both the CO₂ and oxirane coupling reaction and the primary alcohol protection reaction. Thus an experiment was carried out by adding 1-acetylimidazole directly into the reaction mixture, this first attempt showed no conversion due to a known catalyst deactivation mechanism^{37,38} that operates when DBU reacts with CO₂ in the presence of water (Scheme 5.7).

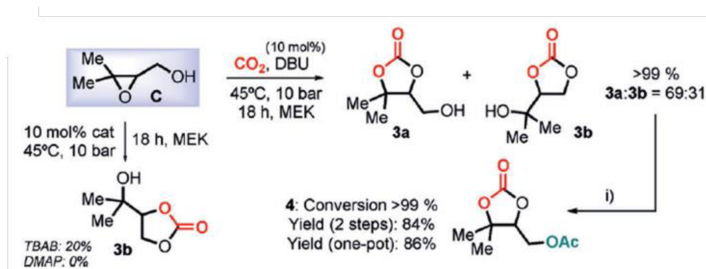


Scheme 5.7 Catalyst deactivation by reaction with CO₂ in the presence of water.

By adding the molecular sieves to the reaction solution, a small improvement in the reaction yield was observed, but a quantitative and selective conversion of the more substituted cyclic carbonate was obtained only by addition of a new batch of DBU (1 equiv.). Finally, the formation of **4** from **C** through a one-pot domino sequence (Scheme 5.8) was successfully tested and provided the trisubstituted cyclic carbonate **4** with a yield of 86% compared to

the yield of 84% obtained in the two phases synthetic route in the presence of DBU / AcIm.^{39,40}

These results imply that the more substituted carbonate product is favored and can be conveniently and selectively trapped *in situ* to provide elusive CO₂ derived heterocycles.



Scheme 5.8. DBU-catalyzed conversion of trisubstituted epoxide **C**. Details: i) DBU (1 equiv), acetyl imidazole (AcIm; 1.5 equiv), RT, 1.5 h; yields of isolated products are reported. MEK=methyl ethyl ketone.

5.2.6. Substrate scope

The encouraging results obtained in the synthesis of **4** led us to study the generality of this domino process using primarily tri- and tetra-substituted epoxides (figure 5.5). Thus, we probed the most functional epoxide precursors in the preparation of carbonates **5-8**, and we were pleased to find that, in all these cases, the trisubstituted acetate-protected carbonates could be formed selectively and with high isolated yields (75-90%). It was interesting to note that in the presence of a further double bond or epoxy group, the chemo-selectivity of these reactions did not change, since only the conversion of the epoxy alcohol fragment was observed. For **5** (as observed in the synthesis of **4**) a single-vessel

procedure was feasible and provided a higher yield of carbonate. For subsequent syntheses (**6-13**) we then used the onepot three-step sequence. Delightfully, the tetrasubstituted **9-13** carbonates could also be prepared with high yields (40-78%) and represent the first examples of [3 + 2] cycloadditions between tetrasubstituted epoxides and CO₂.^a Unlike the **9-11** spirocarbonates that were obtained under relatively mild reaction conditions, products **12** and **13** needed more drastic reaction conditions. The structure of **11b** was also confirmed by X-ray analysis.

^a For the one-pot reactions towards **9-13** we typically found 8:2 ratios for the desired tetrasubstituted carbonate and a disubstituted one, contrary to the syntheses of the trisubstituted carbonate products **4-8**. This observation indicates that the acetyl protection (third step in the one-pot synthesis) is more competitive because of a slower base-induced equilibration of both carbonates. For this reason, most of the unprotected trisubstituted carbonates were directly isolated.

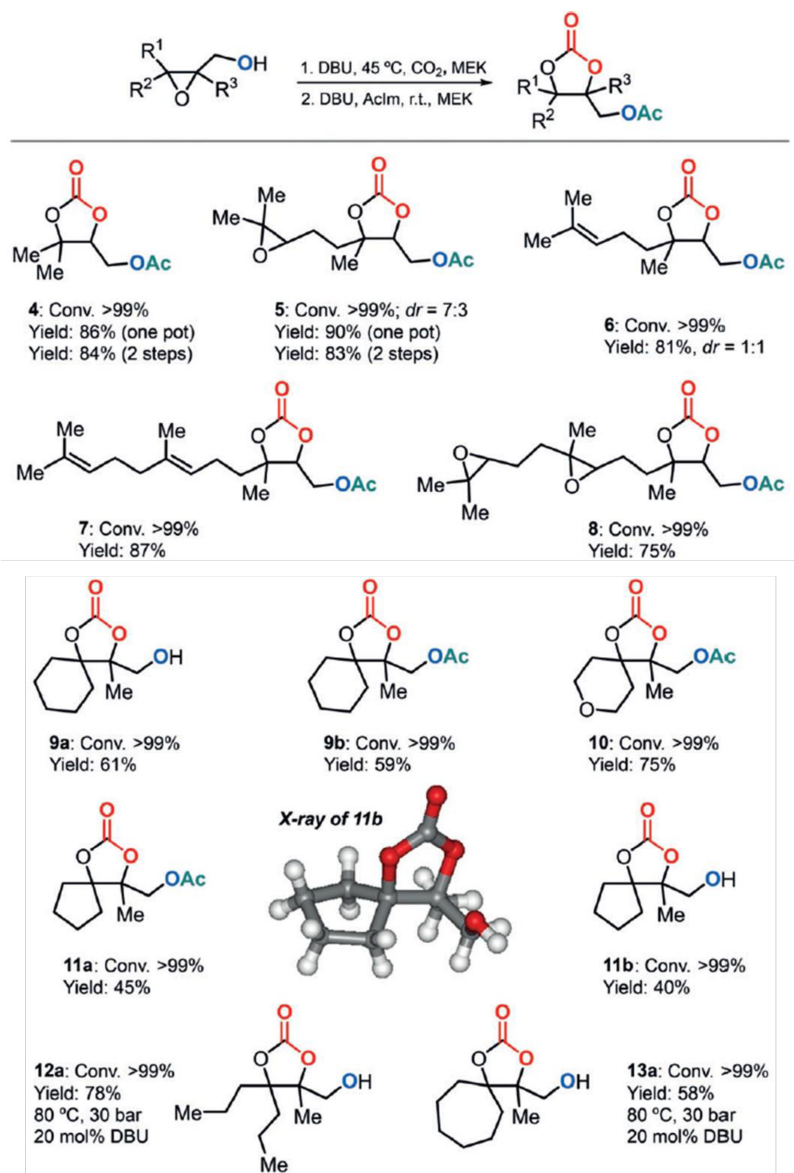
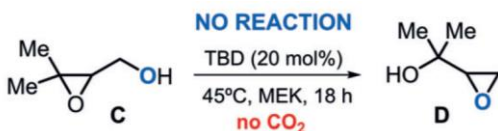


Figure 5.5. Scope with respect to the cyclic carbonates using a domino [3+2] cycloaddition/rearrangement sequence in the presence of DBU and Aclm.

5.2.7. Control experiments to support the mechanism proposal

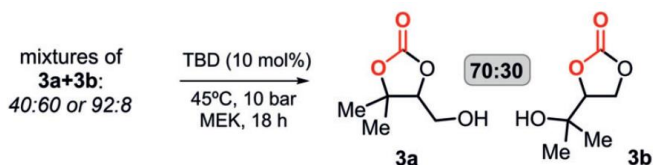
The operating mechanism was supposed to involve a Payne rearrangement placed between the carbonate products and that the desired substituted tri / tetra products can be trapped by selective protection. To support this mechanistic hypothesis various control experiments were performed.

First of all, to understand if the Payne rearrangement takes place before the carbonate formation, the reaction with the three-substituted epoxide **C** in the absence of CO₂ was carried out. After the reaction time, no conversion of the tri-substituted epoxide **C** into the monosubstituted epoxide **D** was observed (Scheme 5.9). This means that the presence of CO₂ is essential for the conversion into the trisubstituted carbonate product.



Scheme 5.9. Control experiments to support the rearrangement at the carbonate level.

Then reactions with two cyclic carbonate mixtures **3a** and **3b** were conducted (**3a:3b** = 40:60 and 92:8), operating under the same conditions of the previously described reaction. In both cases a rebalancing of the mixture in a ratio 70:30 of **3a** and **3b** was observed (Scheme 5.10). This observation supports the idea that the formation of the mixture of carbonates is base-mediated and follows initial formation of **3b** from **C**.

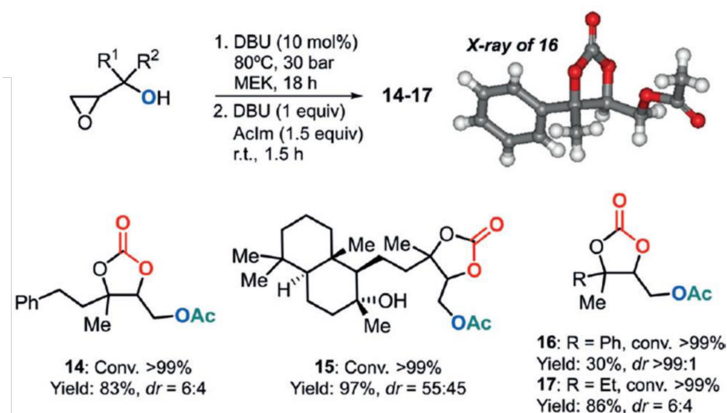


Scheme 5.10. Control experiments to support the rearrangement at the carbonate level.

Similar types of acetyl-protected tri-substituted carbonates (**14–17**; Scheme 5.11) were also conveniently and selectively derived from monosubstituted epoxides having a tertiary alcohol unit. The synthesis of these latter compounds further illustrates the value of this domino approach and its potential application as a general synthetic protocol for the formation of highly substituted cyclic carbonates from CO₂ and showed the intermediate presence of carbonate mixtures prior to protection. More importantly, it also shows, as in the case of trisubstituted epoxides, that the more substituted product can be trapped, as demonstrated in Table 5.5. The selective formation of **16** was compromised by the presence of an electronwithdrawing phenyl group, which enables a faster protection than isomerization of the intermediate mixture of carbonates. Consequently, a lower ratio (83:17) of the protected tri- and monosubstituted carbonate was formed.^b The X-ray structure

^b The pure trisubstituted carbonate **16** was isolated (30%) as a single diastereoisomer (d.r.>99:1) by chromatographic separation. Note, however, that initially quantitative formation of a mixture of both the tri- and monosubstituted carbonate occurred (ratio tri/mono=83:17, d.r.=57:43 for the trisubstituted product).

determined for **16** unequivocally revealed the trisubstituted nature of the cyclic carbonate product.



Scheme 5.11. Substrate scope for the conversion of mono-substituted epoxides.

To understand the differences between the organocatalytic approach and the metal-mediated approach for the synthesis of highly substituted cyclic carbonates, the coupling reaction of CO₂ with a bis-epoxide was studied (Scheme 5.12).

First we used a triphenolated aluminum complex as a promoter of this reaction.^{41,42} Working under the usual reaction conditions, we have witnessed the formation of a mixture of products in which both epoxides of the substrate have been transformed into cyclic carbonates.

the regioselective formation of monocarbonates with substrates based on bis- or tris-epoxy. This substrate-controlled conversion of carbon dioxide offers access to new, functional heterocyclic scaffolds with amplified potential in synthetic chemistry.

5.4. Experimental Section

5.4.1 General considerations

Methylethyl ketone (MEK) and carbon dioxide (purchased from PRAXAIR) were used as received without further purification or drying prior to use. Glycidol, methyl glycidyl ether and phenyl glycidol were purchased at Aldrich, Acros or TCI and used without further purification. ^1H NMR spectra were recorded on Bruker AV-300, AV-400 or AV-500 spectrometers and referenced to the residual deuterated solvent signals. FT-IR measurements were carried out on a Bruker Optics FTIR-ATR TR0 spectrometer. Exact mass analyses and X-ray diffraction studies were performed by the Research Support Area (RSA) at ICIQ.

5.4.2. General procedure for the catalytic experiments

Formation of the cyclic carbonate products mixture

All reactions were performed in a 30 mL stainless steel reactor. In a typical experiment, a solution of the TBD (10.0 – 20.0 mol%) and epoxide (2.0 mmol) in MEK (5.0 mL) was added to a stainless steel reactor. Three cycles of pressurization and depressurization of the reactor with 5 bar of CO_2 pressure were carried out before finally stabilizing the pressure at 10-30 bar. The reactor was then heated to the required temperature and left stirring for another 18 h. The reactor was cooled down, depressurized and an aliquot of the solution was analyzed by means of ^1H NMR spectroscopy using CDCl_3 as the solvent. For the reactions carried out in the substrate scope phase related the free OH-containing cyclic carbonate

products, the products were purified by flash chromatographic purification.

One-pot protection protocol

Upon targeting the protected cyclic carbonate product, the autoclave reactor was opened, and the reaction mixture was stirred for 15 min open to air. Then DBU (1 equiv) was directly added at room temperature to the reaction mixture, followed by the addition of 1-acetylimidazole (1.5 equiv). After 1.5 h, the reaction was transferred to a round-bottom flask, concentrated and purified by flash column chromatography using a mixture of acetate/hexane as eluent.

5.4.3. Spectroscopic data for all compounds

Compound 1; 4-(hydroxymethyl)-1,3-dioxolan-2-one

¹H NMR (400 MHz, DMSO, 298 K) δ 5.25 (t, ³J_{HH} = 5.6 Hz, 1H), 4.84 - 4.75 (m, 1H), 4.51 – 4.47 (m, 1H), 4.28 (dd, ²J_{HH} = 7.9 Hz, ³J_{HH} = 5.9 Hz, 1H), 3.66 (ddd, ²J_{HH} = 12.6 Hz, ³J_{HH} = 5.5 Hz, ³J_{HH} = 2.9, 1H), 3.50 (ddd, ²J_{HH} = 12.6 Hz, ³J_{HH} = 5.7 Hz, ³J_{HH} = 3.4 Hz, 1H);

¹³C NMR (101 MHz, CDCl₃, 298 K) δ 155.13, 76.99, 65.84, 60.57;

IR (neat, cm⁻¹) 3418 (OH), 1763 (C=O).

Compound 3a; 4-(2-hydroxypropan-2-yl)-1,3-dioxolan-2-one;

¹H NMR (500 MHz, CDCl₃, 298 K) δ 4.52 - 4.40 (m, 3H), 2.34 (bs, 1H), 1.34 (s, 3H), 1.18 (s, 3H);

¹³C NMR (126 MHz, CDCl₃, 298 K) δ 155.37, 81.95, 70.05, 65.68, 25.50, 24.38;

IR (neat, cm⁻¹) 3459 (OH), 2980 (C-H), 1775 (C=O).

Compound 3b; 4-(2-hydroxypropan-2-yl)-1,3-dioxolan-2-one;

¹H NMR (500 MHz, CDCl₃, 298 K) δ 4.52 - 4.40 (m, 3H), 2.34 (bs, 1H), 1.34 (s, 3H), 1.18 (s, 3H);

¹³C NMR (126 MHz, CDCl₃, 298 K) δ 155.37, 81.95, 70.05, 65.68, 25.50, 24.38;

IR (neat, cm⁻¹) 3459 (OH), 2980 (C-H), 1775 (C=O).

Compound 4; (5,5-dimethyl-2-oxo-1,3-dioxolan-4-yl)methyl acetate;

¹H NMR (500 MHz, CDCl₃, 298 K) δ 4.46 (dd, ³J_{HH} = 6.6 Hz, ³J_{HH} = 4.3 Hz, 1H), 4.32 (dd, ²J_{HH} = 12.3 Hz, ³J_{HH} = 4.3 Hz, 1H), 4.23 (dd, ²J_{HH} = 12.3 Hz, ³J_{HH} = 6.6 Hz, 1H), 2.12 (s, 3H), 1.56 (s, 3H), 1.45 (s, 3H);

¹³C NMR (126 MHz, CDCl₃, 298 K) δ 170.27, 153.43, 83.00, 81.50, 61.20, 26.93, 21.13, 20.63;

IR (neat, cm⁻¹) 2985 (C-H), 1791 (C=O), 1742 (C=O);

HRMS (ESI+; MeOH): m/z calcd. (C₈H₁₂NaO₅) 211.0577 (M+Na)⁺; found: 211.0576.

Compound 5; (5-(2-(3,3-dimethyloxiran-2-yl)ethyl)-5-methyl-2-oxo-1,3-dioxolan-4-yl)methyl acetate; dr: (69:31)

¹H NMR (400 MHz, CDCl₃, 298 K) δ 4.53 - 4.45 (m, 1H), 4.41 - 4.22 (m, 2H), 2.77 - 2.69 (m, 1H), 2.12 (s, 3H), 2.08 - 1.59 (m, 4H), 1.58 - 1.49 (m, 3H), 1.34 - 1.26 (m, 6H);

¹³C NMR (101 MHz, CDCl₃, 298 K) δ 170.39, 170.33, 153.32, 153.28, 84.68, 84.43, 82.50, 82.45, 63.75, 63.35, 60.94, 60.87, 59.07, 58.83, 31.04, 31.00, 24.91, 24.89, 24.08, 23.63, 23.29, 23.25, 20.78, 18.90, 18.85;

IR (neat, cm⁻¹) 2977 (C-H), 1794 (C=O), 1744 (C=O);

HRMS (ESI+; MeOH): m/z calcd. (C₁₃H₂₀NaO₆) 295.1152 (M+Na)⁺; found: 295.1156.

Compound 6; (5-methyl-5-(4-methylpent-3-en-1-yl)-2-oxo-1,3-dioxolan-4-yl)methyl acetate; dr (51:49);

¹H NMR (400 MHz, CDCl₃, 298 K) δ 5.13 - 5.02 (m, 1H), 4.44 (dd, ³J_{HH} = 6.9 Hz, ³J_{HH} = 4 Hz, 1H), 4.33 (dd, ³J_{HH} = 12.3 Hz, ³J_{HH} = 4 Hz, 1H), 4.23 (dd, ³J_{HH} = 12.3 Hz, ³J_{HH} = 6.9 Hz, 1H), 2.24 - 2.13 (m, 1H), 2.11 (s, 3H), 1.83 - 1.73 (m, 1H), 1.58 - 1.51 (m, 8H);

¹³C NMR (101 MHz, CDCl₃, 298 K) δ 170.45, 153.58, 133.55, 122.38, 84.98, 82.58, 61.11, 34.20, 25.79, 23.87, 22.13, 20.79, 17.85;

IR (neat, cm⁻¹) 2973 - 2928 (C-H), 1795 and 1745 (C=O);

HRMS (ESI⁺; MeOH): *m/z* calcd. (C₁₁H₁₅NaO₅) 279.1203 (M+Na)⁺; found: 279.1192.

Compound 7; (E)-(5-(4,8-dimethylnona-3,7-dien-1-yl)-5-methyl-2-oxo-1,3-dioxolan-4-yl)methyl acetate; dr (>99:1)

¹H NMR (300 MHz, CDCl₃, 298 K) δ 5.11 - 5.03 (m, 2H), 4.47 (dd, ³J_{HH} = 7.0 Hz, ³J_{HH} = 4.0 Hz, 1H), 4.36 (dd, ²J_{HH} = 12.0 Hz, ³J_{HH} = 4.0 Hz, 1H), 4.25 (dd, 2J_{HH} = 12.0 Hz, ³J_{HH} = 7.0 Hz, 1H), 2.22 - 2.14 (m, 1H), 2.12 (s, 3H), 2.09 - 1.95 (m, 3H), 1.87 - 1.73 (m, 1H), 1.68 (s, 3H), 1.61 (s, 3H), 1.60 (s, 3H), 1.54 (s, 3H), 1.53 (s, 3H);

¹³C NMR (101 MHz, CDCl₃, 298 K) δ 170.44, 153.57, 137.16, 131.72, 124.19, 122.24, 84.99, 82.58, 61.11, 39.72, 34.16, 26.70, 25.83, 23.85, 22.01, 20.77, 17.83, 16.20;

IR (neat, cm⁻¹) 2922 (C-H), 1797 (C=O), 1747 (C=O).

HRMS (ESI⁺; MeOH): *m/z* calcd. (C₁₈H₂₈NaO₅) 347.1829 (M+Na)⁺; found: 347.1830.

Compound 8; (5-(2-(3-(2-(3,3-dimethyl oxiran-2-yl) ethyl)-3-methyloxiran-2-yl) ethyl) -5-methyl-2-oxo- 1,3-dioxolan-4-yl) methyl acetate;

¹H NMR (400 MHz, CDCl₃, 298 K) δ 4.52 - 4.47 (m, 1H), 4.41 - 4.32 (m, 1H), 4.31 - 4.22 (m, 1H), 2.80 - 2.65 (m, 2H), 2.12 (s, 3H), 2.06 - 1.60 (m, 7H), 1.56 - 1.51 (m, 3H) 1.35 - 1.21 (m, 10H);

¹³C NMR (101 MHz, CDCl₃, 298 K) δ 170.39, 170.33, 153.32, 153.28, 84.68, 84.43, 82.50, 82.45, 63.75, 63.35, 60.94, 60.87, 59.07, 58.83, 31.04, 31.00, 24.91, 24.89, 24.08, 23.63, 23.29, 23.25, 20.78, 18.90, 18.85;

IR (neat, cm⁻¹) 2967 (C-H), 1798 (C=O), 1745 (C=O);

HRMS (ESI⁺; MeOH): *m/z* calcd. (C₁₈H₂₈NaO₇) 379.1727 (M+Na)⁺; found: 379.1733.

Compound 9a; 4-(hydroxymethyl)-4-methyl-1,3-dioxaspiro [4.5]decan-2-one;

¹H NMR (300 MHz, CDCl₃, 298 K) δ 3.81 (dd, ²J_{HH} = 12.0 Hz, ³J_{HH} = 5.1 Hz, 1H), 3.68 (dd, ²J_{HH} = 12.0 Hz, ³J_{HH} = 7.2 Hz 1H), 2.27 - 2.17 (m, 1H), 2.15 - 1.89 (m, 2H), 1.80 - 1.56 (m, 5H), 1.53 - 1.39 (m, 2H), 1.37 (s, 3H), 1.30 - 1.14 (m, 1H);

¹³C NMR (126 MHz, CDCl₃, 298 K) δ 154.15, 87.31, 86.98, 65.09, 32.16, 29.72, 25.00, 22.11, 21.79, 16.84;

IR (neat, cm⁻¹) 3298 (O-H), 2934 - 2860 (C-H), 1765 (C=O);

HRMS (ESI⁺; MeOH): *m/z* calcd. (C₁₀H₁₆NaO₄) 223.0941 (M+Na)⁺; found: 223.0935.

Compound 9b; (4-methyl-2-oxo-1,3-dioxaspiro[4.5]decan-4-yl) methyl acetate;

¹H NMR (400 MHz, CDCl₃, 298 K) δ 4.24 - 4.15 (m, 2H), 2.11 (s, 3H), 2.01 - 1.93 (m, 2H), 1.81 - 1.64 (m, 5H), 1.46 - 1.35 (m, 5H), 1.27 - 1.14 (m, 1H);

¹³C NMR (126 MHz, CDCl₃, 298 K) δ 170.30, 153.48, 86.55, 85.35, 65.32, 31.91, 30.02, 24.95, 22.06, 21.78, 20.84, 17.47;

IR (neat, cm⁻¹) 2937 - 2864 (C-H), 1792 (C=O), 1744 (C=O);

HRMS (ESI⁺; MeOH): *m/z* calcd. (C₁₂H₁₈NaO₅) 265.1046 (M+Na)⁺; found: 265.1044.

Compound 10; (4-methyl-2-oxo-1,3,8-trioxaspiro[4.5]decan-4-yl)methyl acetate;

¹H NMR (400 MHz, CDCl₃, 298 K) δ 4.25 (d, ²J_{HH} = 12.1 Hz, 1H), 4.15 (d, ²J_{HH} = 12.1 Hz, 1H), 4.01 - 3.92 m, 2H), 3.81 - 3.70 (m, 2H), 2.12 (s, 3H), 1.86 - 1.78 (m, 4H), 1.42 (s, 3H);

¹³C NMR (101 MHz, CDCl₃, 298 K) δ 169.92, 152.69, 84.75, 83.86, 64.89, 63.57, 63.50, 32.11, 30.44, 20.65, 17.40;

IR (neat, cm⁻¹) 2966 - 2868 (C-H), 1798 (C=O), 1744 (C=O);

HRMS (ESI⁺; MeOH): *m/z* calcd. (C₁₁H₁₆NaO₆) 267.0839 (M+Na)⁺; found: 267.0827.

Compound 11b; (4-methyl-2-oxo-1,3-dioxaspiro[4.4]nonan-4-yl) methyl acetate;

¹H NMR (400 MHz, CDCl₃, 298 K) δ 3.80 (d, ²J_{HH} = 12.0 Hz, 1H), 3.70 (d, ²J_{HH} = 12.0 Hz, 1H), 2.17 - 2.07 (m, 1H), 2.06 - 1.96 (m, 2H), 1.92 - 1.71 (m, 6H), 1.43 (m, 3H);

¹³C NMR (101 MHz, CDCl₃, 298 K) δ 153.93, 97.08, 85.84, 66.04, 34.58, 31.96, 22.68, 22.16, 18.24;

IR (neat, cm⁻¹) 3399 (OH), 2955 - 2878 (C-H), 1768 (C=O).

Compound 11a; (4-methyl-2-oxo-1,3-dioxaspiro[4.4]nonan-4-yl) methyl acetate;

¹H NMR (400 MHz, CDCl₃, 298 K) δ 4.21 (s, 2H), 2.12 (s, 3H), 2.07 - 1.96 (m, 2H), 1.94 - 1.67 (m, 6H), 1.45 (s, 3H);

¹³C NMR (101 MHz, CDCl₃, 298 K) δ 170.16, 96.40, 83.62, 66.16, 34.44, 31.93, 22.48, 22.16, 20.69, 18.55;

IR (neat, cm⁻¹) 2959 - 2879 (C-H), 1791 (C=O), 1744 (C=O);

HRMS (ESI⁺; MeOH): *m/z* calcd. (C₁₁H₁₆NaO₅) 251.0890 (M+Na)⁺; found: 251.0878.

Compound 12 a; 4-(hydroxymethyl)-4-methyl-5,5-dipropyl-1,3-dioxolan-2-one:

¹H NMR (500 MHz, CDCl₃, 298 K) δ 3.88 (dd, J_{HH} = 12.2 Hz, J_{HH} = 4.9 Hz, 1H), 3.63 (dd, J_{HH} = 12.1 Hz, J_{HH} = 7.9 Hz, 1H), 2.11

(bs, 1H), 1.88 - 1.66 (m, 4H), 1.51 - 1.20 (m, 7H), 0.97 (t, JHH = 7.3 Hz, 3H), 0.96 (t, JHH = 7.3 Hz, 3H);

¹³C NMR (126 MHz, CDCl₃, 298 K) δ 154.07, 89.66, 87.83, 65.48, 35.38, 33.23, 17.44, 17.41, 16.45, 14.60, 14.50;

IR (neat, cm⁻¹): 3463 (OH), 2963 - 2876 (C-H), 1767 (C=O);

HRMS (ESI⁺; MeOH): *m/z* calcd. (C₁₁H₂₀NaO₄) 239.1254; (M-Na)⁺ found: 239.1265.

Compound 13a 4-(hydroxymethyl)-4-methyl-1,3-dioxaspiro[4.6]undecan-2-one (13):

¹H NMR (400 MHz, CDCl₃, 298 K) δ 3.86 (dd, JHH = 12.1 Hz, JHH = 4.8 Hz, 1H), 3.71 (dd, JHH = 12.1 Hz, JHH = 7.7 Hz, 1H), 2.20 (dd, JHH = 14.4 Hz, JHH = 8.6 Hz, 1H), 2.07 - 1.91 (m, 3H), 1.80-1.67 (m, 4H), 1.66 - 1.57 (m, 3H), 1.48 - 1.38 (m, 5H);

¹³C NMR (101 MHz, CDCl₃, 298 K) δ 154.19, 91.10, 88.08, 65.20, 34.93, 32.97, 29.73, 29.50, 22.28, 16.74;

IR (neat, cm⁻¹): 3311 (O-H), 2928 - 2855 (C-H), 1766 (C=O);

HRMS (ESI⁺; MeOH): *m/z* calcd. (C₉H₁₃N₆O₂) 237.1095; (M-Na)⁺ found: 237.1095.

Compound 14; (5-methyl-2-oxo-5-phenethyl-1,3-dioxolan-4-yl)methyl acetate; dr (61:39)

¹H NMR (400 MHz, CDCl₃, 298 K) δ 7.36 - 7.11 (m, 5H), 4.57 - 4.47 (m, 1H), 4.39 - 4.19 (m, 2H), 2.93 - 2.66 (m, 2H), 2.18 - 1.79 (m, 5H), 1.64 - 1.43 (m, 3H);

¹³C NMR (126 MHz, CDCl₃, 298 K) δ 170.41, 153.44, 140.45, 140.10, 128.90, 128.35, 126.66, 84.70, 82.62, 80.51, 61.60, 60.97, 42.02, 36.29, 29.75, 29.50, 23.93, 20.79, 20.76, 19.42, 17.71;

IR (neat, cm⁻¹) 3028 - 2942 (C-H), 1793 (C=O), 1742 (C=O);

HRMS (ESI⁺; MeOH): *m/z* calcd. (C₁₅H₁₈NaO₅) 301.1046 (M+Na)⁺; found: 301.1048.

Compound 15; sclareol trisubstituted cyclic carbonate; dr (55:45)

¹H NMR (400 MHz, CDCl₃, 298 K) δ 4.62 - 4.41 (m, 1H), 4.38 - 4.17 (m, 2H), 2.15 - 2.08 (m, 3H), 2.06 - 1.93 (m, 1H), 1.90 - 1.77 (m, 1H), 1.69 - 1.57 (m, 3H), 1.56 (s, 3H), 1.48 - 1.36 (m, 6H), 1.31 - 1.23 (m, 3H), 1.20 - 1.13 (m, 3H), 1.11 - 1.01 (m, 1H), 0.96 - 0.85 (m, 5H), 0.82 - 0.76 (m, 6H);

¹³C NMR (126 MHz, CDCl₃, 298 K) δ 170.55, 153.80, 153.78, 85.39, 85.38, 82.81, 79.82, 74.51, 74.38, 61.78, 61.57, 61.40, 61.29, 56.26, 56.22, 44.86, 44.69, 43.10, 42.02, 42.01, 39.91, 39.28, 39.21, 37.74, 33.51, 33.37, 29.83, 27.05, 24.64, 24.51, 24.47, 21.58, 20.82, 20.81, 20.63, 20.60, 19.95, 19.07, 18.55, 15.58.

IR (neat, cm⁻¹) 3519 (OH) 2927 – 2850 (C-H), 1793 (C=O), 1747 (C=O). **HRMS (ESI⁺; MeOH):** *m/z* calcd. (C₂₃H₃₈NaO₆) 433.2561 (M+Na)⁺; found: 433.2559.

Compound 16; (5-methyl-2-oxo-5-phenyl-1,3-dioxolan-4-yl) methyl acetate; dr (>99:1)

¹H NMR (400 MHz, CDCl₃, 298 K) δ 7.49 - 7.33 (m, 5H), 4.79 (dd, ³J_{HH} = 6.9 Hz, ³J_{HH} = 4.1 Hz, 1H), 4.51 (dd, 2J_{HH} = 12.3 Hz, ³J_{HH} = 4.0 Hz, 1H), 4.39 (dd, 2J_{HH} = 12.4 Hz, ³J_{HH} = 6.8 Hz, 1H), 2.12 (s, 3H), 1.76 (s, 3H);

¹³C NMR (101 MHz, CDCl₃, 298 K) δ 170.40, 153.25, 141.29, 129.31, 129.04, 124.04, 85.51, 82.68, 61.49, 22.27, 20.76;

IR (neat, cm⁻¹) 3041 - 2957 (C-H), 1792 (C=O), 1731 (C=O);

HRMS (ESI⁺; MeOH): *m/z* calcd. (C₁₃H₁₄NaO₅) 273.0733 (M+Na)⁺; found: 273.0730.

Compound 17; (5-ethyl-5-methyl-2-oxo-1,3-dioxolan-4-yl) methyl acetate; dr (58:42)

¹H NMR (400 MHz, CDCl₃, 298 K) δ 4.55 - 4.47 (m, 1H), 4.40 - 4.32 (m, 1H), 4.29 - 4.20 (m, 1H), 2.16 - 2.12 (m, 3H), 1.93 - 1.80 (m, 1H), 1.68 - 1.57 (m, 1H), 1.55 - 1.41 (m, 3H), 1.12 - 1.02 (m, 1H);

¹³C NMR (126 MHz, CDCl₃, 298 K) δ 170.46, 153.62, 85.38, 85.28, 82.44, 80.12, 61.79, 61.04, 33.12, 27.03, 23.36, 20.78, 18.95, 7.89, 7.53;

IR (neat, cm⁻¹) 2980 (C-H), 1790 (C=O), 1742 (C=O);

HRMS (ESI⁺; MeOH): *m/z* calcd. (C₉H₁₄NaO₅) 225.0733
(M+Na)⁺; found: 225.0733.

References

- 1 M. Yoshida, M. Ihara, *Chem. Eur. J.* **2004**, *10*, 2886–2893.
- 2 P. P. Pescarmona, M. Taherimehr, *Catal. Sci. Technol.* **2012**, *2*, 2169–2187.
- 3 T. Sakakura, K. Kohno, *Chem. Commun.* **2009**, 1312–1330.
- 4 F. Shi, Y. Deng, T. SiMa, J. Peng, Y. Gu, B. Qiao, *Angew. Chem. Int. Ed.* **2003**, *42*, 3257–3260.
- 5 C. J. Whiteoak, A. Nova, F. Maseras, A. W. Kleij, *ChemSusChem* **2012**, *5*, 2032–2038.
- 6 R. R. Shaikh, S. Pornpraprom, V. D'Elia, *ACS Catal.* **2018**, *8*, 419–450.
- 7 H. Büttner, L. Longwitz, J. Steinbauer, C. Wulf, T. Werner, *Top. Curr. Chem.* **2017**, *375*, 50.
- 8 M. Alves, B. Grignard, R. Mereau, C. Jerome, T. Tassaing, C. Detrembleur, *Catal. Sci. Technol.* **2017**, *7*, 2651–2684.
- 9 G. Fiorani, W. Guo, A. W. Kleij, *Green Chem.* **2014**, *17*, 1375–1389.
- 10 R. A. Shiels, C. W. Jones, *J. Mol. Catal. A Chem.* **2007**, *261*, 160–166.
- 11 B. Wang, Z. Luo, E. H. M. Elageed, S. Wu, Y. Zhang, X. Wu, F. Xia, G. Zhang, G. Gao, *ChemCatChem* **2016**, *8*, 830–838.
- 12 K. K. and T. H. Lin Wang, *Catal. Sci. Technol.* **2016**, *6*, 3872–3877.
- 13 A. Barbarini, R. Maggi, A. Mazzacani, G. Mori, G. Sartori, R. Sartorio, *Tetrahedron Lett.* **2003**, *44*, 2931–2934.
- 14 A. R. Hajipour, Y. Heidari, G. Kozehgary, *RSC Adv.* **2015**, *5*, 61179–61183.
- 15 B.-H. Xu, J.-Q. Wang, J. Sun, Y. Huang, J.-P. Zhang, X.-P. Zhang, S.-J. Zhang, *Green Chem.* **2015**, *17*, 108–122.
- 16 Y.-B. Wang, D.-S. Sun, H. Zhou, W.-Z. Zhang, X.-B. Lu, *Green Chem.* **2015**, *17*, 4009–4015.
- 17 W. Desens, T. Werner, *Adv. Synth. Catal.* **2016**, *358*, 622–630.

-
- 18 F. Della Monica, A. Buonerba, A. Grassi, C. Capacchione, S. Milione *ChemSusChem* **2016**, 3457–3464.
- 19 M. Alves, B. Grignard, S. Gennen, R. Méreau, C. Detrembleur, C. Jérôme, T. Tassaing, *Catal. Sci. Technol.* **2015**, 5, 4636–4643.
- 20 J. Wang, Y. Zhang, *ACS Catal.* **2016**, 6, 4871–4876.
- 21 A. M. Hardman-Baldwin, A. E. Mattson, *ChemSusChem* **2014**, 7, 3275–3278.
- 22 X. F. Liu, Q. W. Song, S. Zhang, L. N. He, *Catal. Today* **2016**, 263, 69–74.
- 23 L. Wang, G. Zhang, K. Kodama, T. Hirose, *Green Chem.* **2016**, 18, 1229–1233.
- 24 V. B. Saptal, B. M. Bhanage, *ChemSusChem* **2017**, 10, 1145–1151.
- 25 B. Chatelet, L. Joucla, J. P. Dutasta, A. Martinez, V. Dufaud, *Chem. Eur. J.* **2014**, 20, 8571–8574.
- 26 M. Liu, L. Liang, X. Li, X. Gao, J. Sun, *Green Chem.* **2016**, 18, 2851–2863.
- 27 C. Villiers, J. P. Dognon, R. Pollet, P. Thuéry, M. Ephritikhine, *Angew. Chem. Int. Ed.* **2010**, 49, 3465–3468.
- 28 V. Caló, A. Nacci, A. Monopoli, A. Fanizzi, *Org. Lett.* **2002**, 4, 2561–2563.
- 29 A. Decortes, A. M. Castilla, A. W. Kleij, *Angew. Chem. Int. Ed.* **2010**, 49, 9822–9837.
- 30 M. North, R. Pasquale, C. Young, *Green Chem.* **2010**, 12, 1514–1539.
- 31 V. Laserna, E. Martin, E. C. Escudero-Adán, A. W. Kleij, *ACS Catal.* **2017**, 7, 5478–5482.
- 32 G. Fiorani, M. Stuck, C. Martín, M. M. Belmonte, E. Martin, E. C. Escudero-Adán, A. W. Kleij, *ChemSusChem* **2016**, 9, 1304–1311.
- 33 H. Zhang, H. B. Liu, J. M. Yue, *Chem. Rev.* **2014**, 114, 883–898.
- 34 G. B. Payne, *J. Org. Chem.* **1962**, 27, 3819 – 3822.
- 35 V. Laserna, G. Fiorani, C. J. Whiteoak, E. Martin, E. Escudero-Ad_n, A.W. Kleij, *Angew. Chem. Int. Ed.* **2014**, 53, 10416 – 10419.

-
- 36 C. J. Whiteoak, E. Martin, E. C. Escudero-Adan, A.W. Kleij, *Adv. Synth. Catal.* **2013**, 355, 2233 – 2239.
- 37 C. Villiers, J. P. Dognon, R. Pollet, P. Thuéry, M. Ephritikhine, *Angew. Chem. Int. Ed.* **2010**, 49, 3465–3468.
- 38 B. A. Vara, T. J. Struble, W. Wang, M. C. Dobish, J. N. Johnston, *J. Am. Chem. Soc.* **2015**, 137, 7302–7305.
- 39 H. Hagiwara, K. Morohashi, T. Suzuki, M. Ando, I. Yamamoto, M. Kato, *Synth. Commun.* **1998**, 28, 2001–2006.
- 40 R. C. Pratt, B. G. G. Lohmeijer, D. A. Long, R. M. Waymouth, J. L. Hedrick, *J. Am. Chem. Soc.* **2006**, 128, 4556–4557.
- 41 J. Rintjema, R. Epping, G. Fiorani, E. Mart_n, E. C. Escudero- Adan, A.W. Kleij, *Angew. Chem. Int. Ed.* **2016**, 55, 3972 – 3976.
- 42 J. Rintjema, R. Epping, G. Fiorani, E. Mart_n, E. C. Escudero- Adan, A.W. Kleij,; *Angew. Chem.* **2016**, 128, 4040 – 4044.

Course Activity Summary

Candidate: Mariachiara Cozzolino

Tutor: Prof.ssa Marina Lamberti

Co-Tutor: Prof.ssa Mina Mazzeo

Attended Courses

- *Physical methods of organic chemistry* - Prof. Carmine Gaeta.
- *Laboratory characterization of polymeric materials* - Prof. Paola Rizzo
- *Theoretical and practical course for the use of DSC and TGA* - Marco Coletti (TA instruments)
- *Introductory course about statistics with R* - Prof. Emmanuelle Becker
- *Uses and Applications of Crystallographic Data in Structural Chemistry and Drug Discovery* - The Cambridge Crystallographic Data Centre.

Visiting Periods

Settember 2017 – April 2018 Institut Català d'Investigació Química Tarragona, (Spagna) under the supervision of Prof. Arjan W. Kleij

Publications

“Salen, salan and salalen iron(III) complexes as catalysts for CO₂/epoxide reactions and ROP of cyclic esters”

Mariachiara Cozzolino, Vincenza Leo, Consiglia Tedesco, Mina Mazzeo, Marina Lamberti.

Dalton Trans., 2018, **47**, 13229-13238.

“Organocatalyzed Domino [3+2] Cycloaddition/Payne-TypeRearrangement using Carbon Dioxide and Epoxy Alcohols”

Sergio Sopeña, **Mariachiara Cozzolino**, Cristina Maquilón, Eduardo C. Escudero-Adàn, Marta Martínez Belmonte, Arjan W. Kleij
Angew. Chem. Int. Ed., 2018, **57**, 11203-11207.

“Selective Synthesis of Cyclic Carbonate by Salalen Aluminum Complexes and Mechanistic Studies”

Mariachiara Cozzolino, Tomer Rosen, Israel Goldberg, Mina Mazzeo, Marina Lamberti.
ChemSusChem, 2017, **10**, 1217-1223.

“CO₂/Epoxide Reactions Catalyzed by Bimetallic Salalen Aluminum Complexes”

Mariachiara Cozzolino, Konstantin Press, Mina Mazzeo, Marina Lamberti.
ChemCatChem, 2016, **8**, 455-460.

“Phenoxy-based Aluminum Complexes: Simple and Efficient Catalysts for the Ring-Opening Copolymerization of Epoxides and Anhydrides”

Florence Isnard, Federica Santulli, Mariachiara Cozzolino, Marina Lamberti, Mina Mazzeo
Submitted.

Scientific Contributions

- Paestum, 10-14th September 2017; XXVI National Congress of Italian Chemistry Society (SCI)
Best Poster Award

Poster contribution entitled: **“Fixation of Carbon Dioxide in Organic Carbonates Catalyzed by Bimetallic Complexes”**

- Salerno, 16th February 2017; NanoMeetsBio@Nanomates - 3rd Workshop on research at interface between bio-medical and nano-science.

Poster contribution entitled: **“Salalen Aluminum Catalysts for CO₂/epoxide coupling and Mechanistic Studies”**

- Rimini, 25-27th October 2016; Young Chemists Symposium, an event by Italian Chemistry Society (SCI)

Poster contribution entitled: **“CO₂ Fixation in Cyclic Carbonates by Salalen Aluminum Complexes”**

Special Thanks

Alla fine di questa esperienza sono tante le persone che desidero ringraziare perché tutte, in un modo o nell'altro, hanno contribuito al raggiungimento di questo mio traguardo.

Ringrazio il Prof. Claudio Pelecchia, punto di riferimento durante il mio percorso accademico, per avermi dato l'opportunità di lavorare nel suo gruppo di ricerca, dove grazie alle fantastiche persone, mi sono sentita parte di una grande famiglia.

Un ringraziamento particolare va alla mia tutor Marina per i preziosi insegnamenti durante tutti questi anni, che mi hanno formata e mi hanno permesso di arrivare fin qui; inoltre, desidero ringraziarla per essermi stata sempre vicina, supportandomi e sopportandomi in ogni circostanza.

Un ringraziamento speciale a Mina che ha la capacità di prendere la vita sempre con un sorriso e che con la sua grinta e voglia di fare ha contribuito a darmi la giusta carica anche nei momenti difficili.

Grazie a Mariella, per la sua gentilezza e disponibilità, sempre pronta ad ascoltarmi e darmi un suo prezioso consiglio.

Grazie a Ilaria, per avermi sempre sostenuta e guidata, incoraggiandomi a fare di più e meglio.

Grazie alla piccola Flo, con la quale ho condiviso dal primo all'ultimo giorno di questa avventura, alle "nostre" pause caffè/sigaretta alle nostre chiacchierate ai nostri aperitivi in inglese, durati troppo poco, ma soprattutto grazie perché oltre a una collega ho trovato una vera amica.

Grazie a Marco che tra una canzone stonata e un gossip televisivo ha reso i giorni di lavoro più leggeri e piacevoli. Grazie a tutti i componenti del Lab 3 e a tutti i miei colleghi di corso per aver condiviso con me questa meravigliosa esperienza.

Inoltre vorrei ringraziare la fondazione Cariplo (progetto Apollo 2016) per aver finanziato parte del mio progetto di dottorato.

Non potrei non ringraziare tutte le mie amiche, a quelle di sempre, a quelle perse e poi ritrovate, a quelle nuove; grazie a tutte voi perché nel vostro piccolo mi siete state di grande aiuto.

Un ringraziamento alla mia numerosa e splendida famiglia che con il suo dolce e immutevole sostegno mi ha resa una persona migliore.

Il ringraziamento più importante va a mio padre, ad ilia e ad Antonio; voi ci siete da sempre e più di tutti mi avete sopportata, comprendendomi sempre e dimostrando di credere in me; ma soprattutto grazie per avermi sostenuta in qualsiasi mia scelta, giusta o sbagliata che fosse. Grazie, grazie, grazie, perché a voi devo tutto!